Paulo Jorge Miranda da Silva Gaspar

Impact of LIMP-2 deficiency on lysosome composition and function

Tese de Candidatura ao grau de Doutor em Ciências Biomédicas submetida ao Instituto de Ciências Biomédicas Abel Salazar da Universidade do Porto

Orientadora – Doutora Maria Clara Pereira de Sá-Miranda

Categoria – Investigadora do Instituto de Biologia Celular e Molecular

Afiliação – Instituto de Biologia Celular e Molecular

Co-Orientador – Doutor Johannes Maria Franciscus Geradus Aerts

Categoria – Professor

Afiliação – Leiden Institute of Chemistry, University of Leiden

Tutor – Doutor Jorge Eduardo da Silva Azevedo

Categoria – Professor Catedrático

Afiliação – Instituto de Ciências Biomédicas Abel Salazar da Universidade do Porto

TABLE OF CONTENTS

PRECEITOS LEGAIS

O autor desta tese declara que interveio na concepção e execução do trabalho experimental, na interpretação e redacção dos resultados que, além de incluídos nesta tese, culminaram nas publicações internacionais (artigos abaixo indicados), sob o nome de "**Gaspar P.**".

The author of this thesis declares to have participated in the planning and execution of the experimental work, in the interpretation and preparation of the data which, besides being included in this thesis, were published in international journals, under the name "**Gaspar P.**".

Rothaug M, Zunke F, Mazzulli JR, Schweizer M, Altmeppen H, Lüllmann-Rauch R, Kallemeijn WW, **Gaspar P**, Aerts JM, Glatzel M, Saftig P, Krainc D, Schwake M, Blanz J. LIMP-2 expression is critical for β-GCase activity and α-synuclein clearance. Proc Natl Acad Sci USA. 2014 Oct 28; **111** (43): 15573-8. doi:10.1073/pnas.1405700111

Gaspar P, Kallemeijn WW, Strijland A, Scheij S, Van Eijk M, Aten J, Overkleeft HS, Balreira A, Zunke F, Schwake M, Sá Miranda C, Aerts JM. Action myoclonus-renal failure syndrome: diagnostic applications of activity-based probes and lipid analysis. J Lipid Res. 2014 Jan; **55** (1): 138-45. doi:10.1194/jlr.M043802

This work was supported by Fundação para a Ciência e Tecnologia through a Phd fellowship (SFRH/BD/72862/2010) and by FEDER funds through the Operational Competitiveness Programme – COMPETE and by National Funds through FCT – Fundação para a Ciência e a Tecnologia under the projects FCOMP-01-0124-FEDER-011135 (PTDC/SAU-GMG/105344/2008), FCOMP-01-0124-FEDER-022718 (PEst-C/SAU/LA0002/2011) and FCOMP-01-0124-FEDER-037277 (PEst-C/SAU/LA0002/2013)

Este trabalho foi financiado pela Fundação para a Ciência e Tecnologia através de uma bolsa de doutoramento (SFRH/BD/72862/2010) e por fundos FEDER através do Programa Operacional de Competição – COMPETE e por fundos nacionais através da Fundação para a Ciência e Tecnologia através dos projectos FCOMP-01-0124-FEDER-011135 (PTDC/SAU-GMG/105344/2008), FCOMP-01-0124-FEDER-022718 (PEst-C/SAU/LA0002/2011) e FCOMP-01-0124-FEDER-037277 (PEst-C/SAU/LA0002/2013).

ACKNOWLEDGMENTS /AGRADECIMENTOS

E assim acabou!!! Mas acima de tudo tive o privilégio de ter trabalhado e conhecido pessoas únicas. Gostaria de agradecer a todas as pessoas que me acompanharam, apoiaram e ajudaram ao longo destes 4 anos.

Gostaria de agradecer à Doutora Clara que me permitiu o concretizar de um sonho e sempre se mostrou disponível e interessada nesta caminhada. Muito obrigado por me ter incutido a busca constante pelo porquê e fazer-me voltar à idade dos “Porquês”.

To Professor Hans, an enourmous thanks. I will always be grateful to you. I will miss our talks and discussions, your lessons of history. The meetings of Thorn were unique. You were able to motivate us to conquer the world. In the end of those meetings we were able to discover anything. I will miss that feeling. Although being a very busy person, you always manage to do everything. Thank you very much, Hans.

Ao Professor Jorge, um agradecimento especial. Pelos conselhos sábios e por ter sido aquela pessoa, que nos momento mais difíceis conseguiu que o barco se mantivessse a tona e no rumo certo. Obrigado, Comandante.

À Fundação para a Ciência e Tecnologia (FCT) pela bolsa de Doutoramento (SFRH/BD/72862/2010) que me foi atribuída para a realização deste trabalho.

Agradeço a todos os membros que fizeram ou fazem parte da UniLipe, Lorena, Fátima, João, Marisa, Rui, Daniel, Cátia. Em particular, ao Daniel que sempre se mostrou pronto a ajudar e pela camaradagem. À Cátia, pelo companheirismo a todos os níveis. Amizade, alegrias e dissabores, quer futebolísticos, quer científicos, e por não me deixar sozinho na minha insanidade laboratorial. Afinal Cátia, “Não estou farto de te aturar”. Ao Rui, pelas nossas discussões filosóficas e científicas e acima de tudo pela amizade.

À OBF, muito obrigado pelo apoio e amizade. Claudete Mariette, muito obrigado pela disponibilidade constante, pela preocupação e atenção. Manel, meu companheiro futebolístico, obrigado pelas aulas bioquímicas e de cultura geral. Ao Tony, pela descontração e boa disposição contagiante. Às meninas Cátia Macieira, Ana Noites, Marisa Cruz, Martinha e Mendes, obrigado pelo acolhimento e

fraternidade. A amigos que aqui ganhei e que já voaram para outras paragens, Jotinha, Marge, Ricardo e Claúdia, obrigado pela entreajuda sempre presente.

À “Tia Julia” e aos meus “primos” me por me darem todos os dias o doping necessário para ter um razoável funcionamento mental.

Às pessoas que me mostram que para além de laboratório existe uma vida cá fora, a eles, um muito obrigado. Paula e Luísa, minhas amigas de longa data, muito obrigado pela vossa amizade, carinho e disponibilidade. Vocês são únicas e isto tem um bocadinho de vocês. Aos meus amigos Pedro, Rui e Mário, companheiros de luta, vocês deram-me a energia para fazer isto. Aos meus amigos Carlos, Catarina, Ricardo e Sandra, obrigado pelo apoio e presença constante.

To my dutch and non dutch friends. This was only possible due to you too, because you received me in Amsterdam like I was an old friend. A special thanks to Maria for all the support in the academic life, as well as in my personal life. Without you, this would have been much more difficult, for sure. André, my friend, thank you for the support, friendship and for helping me a lot in the dutch land. Dear Jessica, it was a privilegie to live with you. It was an amazing experience. Duco, Matthias and Vincenzo my enourmous thanks to you for making me feel at home. To my collegues at MBIOC departement, Babu, Wouter, Marc, Daniela, Tanit, Mina, Anke, Alessandra, Teja, Emma, Rossela, little Saskia, Sandhya, thank for all the good moments. Rolf, thank you for the expert advices, support and for being always willing to help. Marco, my dutch-portuguese friend, I will miss our football talks. Professor Jan Aten, thank you for being always willing to help and to chase the knowledge with beautiful pictures. Wouter, thank you for the constant transfer of knowledge. Marc, my Dynasore friend, I will miss the insane moments in the culture room that converted science into funny things. Cindy and Roelof, I don´t have words to thank all the effort that you did so that I could finish all the work on time. Thank you. Anneke, for sure, without you, I was not able to accomplish all these goals. You make things evolve with your dedication and friendship. You make results appear. Thank you. Big Saskia and Marri, thank for being always worry if I was ok and if I needed something. Às minhas amigas “dutch” Ana Santos e Inês, obrigado pelo conforto e carinho.

À minha família, quer à de sangue ou emprestada, o meu obrigado por me darem conselhos sábios e conforto.

Aos meus Pais. Por fazerem tudo por mim e pelos meus sonhos. À minha mãe, por ter sido, não agora mas sempre, o meu ombro amigo e reconfortante. Ao meu pai, pelos seus conselhos sábios e me ajudar sempre que eu preciso. Ao meu irmão, por me ensinar a relativizar as coisas, pois tudo se resolve.

Ao Nuno e a Teresinha, por não só nestes últimos quatro anos, mas por sempre, terem estado ao meu lado e terem sido como uns segundos pais para mim.

Aos meus avós. Pelos ensinamentos de justiça, bondade, sacrifício e de ajuda que me transmitiram. Tenho pena que, avó e avô, vocês não estejam cá. Sinto falta do vosso beijo, abraço e carinho.

E sim, se alguém que merece um agradecimento és tu, Francisca. Tu celebraste comigo as minhas vitórias e descobertas, mas acima de tudo sofreste comigo as minhas derrotas e sempre me ajudaste a superá-las. Foste, e és, aquela pessoa que me alegrava e motivava todos os dias, mesmo que tivesses o coração apertadinho. Muito obrigado minha amiga e companheira. Isto custou, mas juntos ultrapassámos. Obrigado por tudo.

SUMMARY/RESUMO

SUMMARY

As one of the main lysosomal membrane proteins, lysosomal integral membrane protein, type 2 (LIMP-2) contributes to the biogenesis and maintenance of the endosomal/lysosomal system. Besides this general role, LIMP-2 takes specifically care of the transport to lysosomes of newly formed glucocerebrosidase (GCase), the enzyme responsible for lysosomal degradation of glucosylceramide (GlcCer). In humans, inherited defects in the LIMP-2 protein lead to Action Myoclonus Renal Failure syndrome (AMRF). AMRF patients show a marked decrease in cellular GCase activity. This reduction seems however cell-type specific, being almost complete in fibroblasts but relatively small in leucocytes. This thesis reports the research done on the impact of LIMP-2 deficiency on GCase in human and mice.

The availability of fluorescent activity-based probes (ABPs), which sensitively label GCase molecules, allowed a detailed investigation of the residual GCase activity in AMRF samples. It was re-confirmed with ABP labelling that leukocytes of AMRF patients contain relatively high residual GCase, contrary to fibroblasts. It was observed that a substantial amount of GCase was incorrectly secreted by AMRF fibroblasts into the medium. In accordance, inspection of AMRF plasma revealed increased GCase activity. Since GCase rapidly loses its enzymatic activity at neutral pH condition, as in plasma, it is not recommended to use plasma GCase measurement for laboratory diagnosis of AMRF. A close examination of glycosphingolipids in AMRF fibroblasts using LC-MS/MS analyses pointed to increased levels of glucosylsphingosine (GlcSph), likely formed by de-acylation of accumulating GlcCer. GlcSph was also increased in the plasma of AMRF patients and *LIMP-2 Knock-out* mice. Since AMRF patients lack the chitotriosidase, seen in Gaucher disease (GD), detection of increased plasma GlcSph in the absence of elevated chitotriosidase in an individual is an indication for AMRF. Demonstration of markedly reduced GCase activity in fibroblasts points to the diagnosis AMRF, which can be further, substantiated with the sequencing of the *SCARB2* gene.

Next, the lysosomal proteome of hepatocytes from *LIMP-2 KO* mice was analyzed. It was found that only GCase is absent among the soluble matrix lysosomal

proteins detected. Next, in various tissues of WT and *LIMP-2 KO* mice, GCase was studied by measurement of enzymatic activity as well as by labelling with selective fluorescent ABPs. Deficiency of GCase protein and activity was noted in almost all organs. Recapitulating findings for AMRF patients, it was observed that *LIMP-2 KO* mice show a marked tissue dependence regarding GCase reduction. Whereas liver and pancreas contain very little residual GCase, enzyme levels are relatively high in brain and leukocytes. Subsequent investigation of sphingolipids in tissues of WT and *LIMP-2 KO* mice showed no significant elevations in GlcCer. However, a correlation was noted between increased GlcSph levels and the extent of GCase reduction in various tissues. It seems that cellular deficiency of GCase caused by LIMP-2 defects is compensated by deacylation of GlcCer to GlcSph. The lipid abnormalities develope rapidly in *LIMP-2 KO* mice: already at 2 months of age animals show an extreme increase in GlcSph in various tissues and its levels do not increase further with age. The observed ability of *LIMP-2 KO* mice to avoid prominent GlcCer storage in tissues likely explains the lack of prominent pathological abnormalities in the animals. Analysis of tissues of *LIMP-2 KO* mice revealed the presence of increased amounts of cholesterol-glucoside (GlcChol), a recently discovered metabolite, suggesting that GCase normally largely degrades glucosylated sterol.

The marked differences in clinical symptoms of AMRF and GD patients are likely due to the absence of “Gaucher cells” in AMRF patients and their prominent presence in GD patients. The cause for this prominent difference was further investigated. It was observed a considerable uptake through (dynamin-dependent) endocytosis of GCase from the medium by AMRF lymphoblasts, but not fibroblasts. Based on this observation, it seems likely that in AMRF patients the re-uptake of secreted GCase from plasma by leukocytes and macrophages may render sufficient GCase activity in these cells to prevent formation of “Gaucher cells” and accompanying visceral symptoms.

At present, there is still no treatment available for AMRF. Since LIMP-2 deficiency in AMRF causes a secondary GCase deficiency, present therapies for GD were examined for potential use in AMRF patients. For GD enzyme replacement therapy (ERT) and substrate reduction therapy (SRT) are registered treatments.

AMRF fibroblasts and mannose-receptor expressing LIMP-2 deficient HEK293T cells were exposed to recombinant GCase, to mimic ERT. After uptake of GCase into LIMP-2 deficient lysosomes, the stability of the enzyme was strongly reduced as compared to normal cells. This difference disappeared upon inhibition of lysosomal cathepsins with leupeptin. This suggests that LIMP-2 stabilizes the fold of GCase inside lysosomes by transient interactions, and consequently protects it against proteolytic breakdown. Thus, LIMP-2 has a dual action as transporter and as intralysosomal chaperone of GCase. For this reason, recombinant GCase cannot be used to treat LIMP-2 deficiency. However, one of the new recently developed brain-permeable and potent GCS inhibitors, biphenyl-pentoxy-ido-deoxynojirimycins, was given to *LIMP-2 KO* mice to analyze their feasibility as a treatment. The applied amount of compound was too small to render prominent reduction of glycosphingolipids in the animals. Higher doses will have to be tested to establish therapeutic efficacy in *LIMP-2 KO* mice.

In conclusion, the work here presented has rendered several new insights regarding LIMP-2 and its deficiency causing AMRF. It has resulted in a novel procedure for differential laboratory diagnosis of AMRF, it has offered an explanation for the different clinical outcome of secondary GCase deficiency in AMRF as compared to primary GCase deficiency in GD, it has rendered indications for an important stabilizing interaction of LIMP-2 and GCase inside lysosomes, and finally it has generated a rational basis for future development of a substrate reduction based treatment of AMRF.

RESUMO

Uma das mais abundantes proteínas da membrana do lisossoma, a proteina integral da membrana do lisossoma, tipo 2 (LIMP-2) contribui para a biogénese e manutenção do sistema endossoma/lisossoma. Para além desta função, a LIMP-2 é responsável pelo transporte específico da recém formada glucocerebrosidase (GCase) para o lisossoma, que por sua vez é responsável pela degradação da glucosilceramida (GlcCer). Em humanos, deficiências heriditárias na proteína LIMP-2 estão na origem da doença Mioclonia de Acção com Falência Renal (AMRF). Os doentes com AMRF apresentam uma redução dos níveis celulares de GCase. No entanto, esta redução célula-dependente, sendo praticamente total em fibroblastos e relativamente baixa em leucócitos. Nesta tese é apresentado o estudo sobre o impacto que a deficiência em LIMP-2 tem na GCase, em humanos e em ratinho.

O recente desenvolvimento de sondas específicas de actividade (ABP), bastante sensíveis, que detectam GCase activa, permitiram um estudo detalhado sobre a actividade residual de GCase em doentes de AMRF. Confirmou-se, através do uso das ABPs, que os leucócitos destes doentes têm uma actividade remanescente bastante alta quando comparada com a obtida em fibroblastos. Foi observado que níveis significativos de GCase eram secretados para o meio de cultura de fibroblastos. Em concordância, foi verificado que os os doentes de AMRF apresentam um aumento da actividade de GCase no plasma. No entanto, como esta actividade decresce rapidamente devido ao pH neutro, a sua medição no plasma não é recomendada para efeitos de diagnóstico da doença AMRF.

O estudo de glicosesfingolipidos em fibroblastos de doentes de AMRF demonstrou que existe um aumento de glucosilesfingosina (GlcSph), provavelmente formada pela de-acilação da glucosilceramida acumulada. A glucosilesfingosina também se encontra acumulada no plasma de doentes de AMRF assim como no ratinho *LIMP-2 KO.* Uma vez que os doentes de AMRF não apresentam aumento de quitotriosidase como os doentes da doença de Gaucher (GD), o aumento de glucosilesfingosina detectado na ausência do aumento de quitotriosidase aponta para um diagnóstico de AMRF. O diagnóstico pode ser confirmado pela actividade

reduzida de GCase em fibroblastos, acompanhado da sequenciação do gene *SCARB2.*

O subsequente estudo do proteoma lisossomal de hepatócitos revelou que, entre as enzimas lisossomais solúveis identificadas, apenas a proteína GCase está ausente no ratinho *LIMP-2 KO*. Foi analisada a actividade da GCase através da medição actividade e do uso de ABP em vários tecidos de ratinho WT e *LIMP-2 KO*, o que revelou que esta se encontra reduzida em quase todos os tecidos de ratinho de *LIMP-2 KO* analisados. O ratinho *LIMP-2 KO* parece recapitular os resultados previamente obsercados, ao apresenta uma deficiência em GCase dependente do tipo celular. A deficiência em GCase pode ser correlacionada com os níveis de acumulação de GlcSph, mas não com a acumulação de GlcCer. Tal sugere que a redução da actividade de GCase, resultante da deficiência em LIMP-2, é compensada pela de-acilação de GlcCer para GlcSph. Estas alterações lipídicas são desenvolvidas rapidamente no ratinho LIMP-2 KO, uma vez que aos 2 meses os níveis máximos são atingidos. A análise dos tecidos provenientes do ratinho LIMP-2 KO revelou um aumento, comparativamente com o ratinho WT, de colesterol-glucosídeo (GlcChol), um metabolito recentemente descoberto, sugerindo que a GCase é responsável pela degradação de esterois glucosilados.

A diferença fenotípica entre doentes de AMRF e de GD deve-se essencialmente à ausência de “células de Gaucher” nos doentes de AMRF e à sua abundante presença nos doentes de GD. A causa para tal diferença foi investigada e foi observado que GCase é endocitada do meio de cultura no caso dos linfoblastos e não no caso dos fibroblastos, por um processo dependente de dinamina. Este resultado, sugere que os leucócitos e os macrófagos re-absorvem a GCase que foi secretada, o que providencia actividade enzimática suficiente para prevenir o aparecimento das “células de gaucher” e os sintomas viscerais que as acompanham. Presentemente não existe qualquer tratamento para a doença AMRF. No entanto, como a deficiência em LIMP-2 origina uma depleção secundária de GCase, os tratamentos disponivéis para a GD, foram avaliados para o tratamento da doença AMRF. Para a GD estão disponíveis dois tratamentos: o tratamento de substituição enzimática (ERT) e o de redução de substrato (SRT). Fibroblastos e células

HEK293T deficientes em LIMP-2, transfectadas com com receptores manose, foram cultivadas na presença de GCase recombinante para simular a ERT. Verificou-se que após a absorção de GCase recombinante, esta apresenta uma menor estabilidade nas células deficientes em LIMP-2 comparativamente com as células controlo. Esta diferença desaparece quando as células são tratadas com um inibidor de catepsinas, a leupeptina. Tal sugere que a LIMP-2 tem uma dupla função: transporta a GCase para o lisossoma e funciona como chaperone intralisossomal, estabilizando a GCase dentro do lisossoma, evitando a sua degradação proteolítica. Assim, a ERT não é uma opção válida para tratar doentes com AMRF. Um dos recém desenvolvidos inibidores da glucosilceramida sintetase, da classe dos bifenil-pentoxi-ido-deoxinojirimicinas, que consegue atravessar a barreira hemato encefálica, foi administrado ao ratinho LIMP-2 KO, para testar a sua eficácia como tratamento. Contudo, a concentração usada não foi a mais adequada, não conduzindo a reduções significativas nos níveis glicosesfingolipidos nos animais tratados. Para testar a sua eficácia como tratamento aplicável a doença de AMRF, concentrações maiores terão que ser testadas.

Em conclusão, o trabalho aqui apresentado demonstra novos detalhes sobre a proteína LIMP-2 e a sua deficiência que origina a doença AMRF. Descreve uma nova metodologia de diagnóstico diferencial para a doença AMRF, fornecendo uma explicação para as diferenças clínicas observadas entre a deficiência secundária em GCase observada na doença AMRF e a deficiência primária em GCase na doença de GD. É igualmente descrito o papel importante da LIMP-2 na estabilização da GCase na matriz lisossomal e finalmente apresenta as bases científicas para um futuro tratamento da doença AMRF com base na redução de substrato.

ABBREVIATIONS

4-MU-TCT – 4-methylumbelliferyl β-DNN'N''-triacetylchitotrioside
4-MU-β-D-Glc – 4-methylumbelliferyl-β-D-glucopyranoside
aa – amino acid
ABP – Activity based probe
AF – Abdominal fat
AG – Adrenal gland
AMRF – Action myoclonus renal failure
AP – Adaptor protein
BAT – Brown adipose tissue
BBB – Blood brain barrier
BM – Bone marrow
BSA – Bovine serum albumin
CBE – conduritol β-epoxide
CD36 – Cluster of differentiation 36
DMEM – Dulbecco's modified Eagle's medium
EBV – Epstein-Barr virus
EF – Epidydimal fat
EP – Epidydimis
ER – Endoplasmic reticulum
ERAD –Endoplasmic reticulum associated degradation
ERT – Enzyme replacement therapy
EV71 – Enterovirus 71
FACS – Fluorescence-activated cell sorting
FBS – Fetal bovine serum
FDG – Fluorescein di-β-D-glucopyranoside
FSGS – Focal and segmental glomerular sclerosis
Gb3 – Globotriaosylceramide
GCase – Glucocerebrosidase
GCS – Glucosylceramide synthase

GD – Gaucher Disease

GlcCer – Glucosylceramide

GlcChol – Cholesterol-glucoside

GlcSph – Glucosylsphingosine

GM2 – Ganglioside monosialic 2

HEK293T – Human embryonic kidney 293 (HEK293) cells (ATCC CRL 1573)

hrGBA – Human recombinante GBA (Cerezyme®)

IF – Inguinal fat

LAMP-2 – Lysosome associated membrane protein 2

LIMP- 2 – Lysosomal integral membrane protein, type 2

LIMP-2 KO mice – LIMP-2 *knock-out* mice

LMP – Lysosomal membrane protein

LN – Lymph node

LSD – Lysosomal storage disorder

M6P – Mannose-6-phosphate

M6PR – Mannose-6-phosphate receptor

MBP – Myelin basic protein

MPS – Mucopolysaccharidoses

NPC – Niemann Pick disease, type C

OF – Omental fat

OPA – o-phthaldialdehyde

PBMC – Peripheral blood mononuclear cells/Leukocytes/White blood cells

PBS – Phosphate buffered saline

PD – Parkinson disease

PI4K – Phosphatidylinositol 4 kinases

PME – Progressive myoclonic epilepsy

PMP – Peripheral myelin protein

RPMI – Roswell park memorial institute medium

SCARB2 – Scanvenger receptor class B, member 2

SDS-PAGE – Sodium dodecyl sulfate polyacrylamide gel electrophoresis

SG – Salivary gland

SN – Sciatic nerve

SPE – Solid phase extraction

SRT – Substrate reduction therapy

TBS – Tris-buffered saline

TE – Testis

TGN – Trans golgi network

THP-1 – Human acute monocytic leukemia cell line

WT – Wild type

1. INTRODUCTION

1.1. Lysosomes

Lysosomes were firstly described in 1955 by Christian De Duve [1]. They are ubiquitous, single membrane bound, organelles specialized in the degradation of macromolecules. Lysosomes are viewed as the terminal station of the endosomal/lysosomal system of cells. They are distinguished from endosomes by their lack of recycling mannose-6-phosphate receptors (M6PR) [2] and by their heavily glycosylated membrane containing glycan-rich integral membrane proteins [3, 4].

Macromolecular substrates for degradation reach the lysosome either by autophagy or endocytotic events like pinocytosis, phagocytosis or receptor-mediated endocytosis involving clathrin-coated vesicles or by early endosomes and late endosomes [5–7]. Intralysosomal digestion is accomplished by the sequential and coordinated, action of individual hydrolases, each one with a unique specificity towards a particular chemical linkage. Lysosomes constitute 0.5 - 5% of the total cell volume and are located close to the microtubule centers. Lysosomes normally present a mean size of 1 μm diameter but they can reach several μm, depending on their content and the stage of the lysosomal degradation process [6, 8]. They are important in supplying the cell with building blocks released from macromolecule degradation, like amino acids (aa), nucleotides, fatty acids and sugars that are re-used in biosynthesis [9–11]. Their lumen is characterized by presenting a very low pH, ranging from 4.0 to 5.0, which is maintained by the vacuolar membrane proton pump. This V-type H^+-ATPase actively translocates protons against the gradient from the cytosol into the lysosome [12–14]. The acid intralysosomal pH provides an optimal environment for the action of more than 50 distinct lysosomal hydrolases (phosphatases, nucleases, glycosidases, proteases, sulfatases, and lipases) [15]. Moreover, it promotes denaturation of protein substrates, thus increasing the efficiency of their proteolytic breakdown.

The protein constituents of the lysosomal membrane are integral membrane glycoproteins that prevent leakage and protect the cell from toxic release of protons and lysosomal hydrolases [16, 17]. The physiological importance of lysosomes is

illustrated by the existence of several inherited metabolic disorders that result from the malfunction of the lysosome in general or specific catabolic hydrolases. More than 50 inherited lysosomal storage disorders (LSDs) are presently known. Most are the result of an impairment of a catabolic enzyme, leading to the accumulation of the corresponding specific substrate or substrates and subsequent pathology [18]. Besides their role in macromolecule turnover, lysosomes are also essential for other processes like degradation of phagocytosed microorganisms, cholesterol homeostasis, cell death regulation by cathepsins and repair of plasma membrane [19–21].

Recently, it is has been recognized that lysosomes also play a key role in metabolism. Lysosomes act as an important cellular sensor of the cellular nutrient status. Attached to the surface of lysosomes is a key regulator of cellular metabolism, the mechanistic/mammalian target of rapamycin (mTOR) [22]. This is crucially involved in cellular responses to nutrient availability. Amongst others, mTOR regulates the nuclear location of the transcription factor EB (TFEB), the transcription factor that controls the rate of lysosome biogenesis and autophagy [23]. Another recently identified crucial role of lysosomes is the efflux of Ca^{2+} to the cytosol [13, 24].

1.2. Lysosomal biogenesis

Lysosomal proteins are synthesized at the endoplasmic reticulum (ER). Correct trafficking of newly formed lysosomal proteins from ER via the Golgi apparatus is an essential step in lysosomal biogenesis and crucial to the maintenance of the lysosomal function [15, 25, 26]. Soluble lysosomal matrix proteins are all synthesized at the ER. They are imported co-translationally into the lumen of the ER and their N-terminal signal sequence (20-25 aa) is cleaved after termination of translation by a ER resident signal peptidase [27, 28]. Inside the ER, the newly formed proteins fold into their correct conformation. Misfolded proteins are usually removed by the ER associated protein degradation (ERAD) machinery and targeted to degradation in the cytosolic proteasomes [29, 30]. Correctly folded soluble lysosomal proteins leave the ER to traverse the Golgi apparatus from *cis* to *trans*

cisternae. Already co-translationally in the ER, lysosomal proteins acquire N-linked glycans which are covalently attached to specific asparagine residues. This co-translational glycan modification is crucial for correct folding of the newly formed protein in the ER, and its subsequent receptor-mediated sorting and transport to the lysosome (see section below for the recognition mechanism and receptors involved) [31, 32]. After passing through the Golgi apparatus, newly formed soluble lysosomal proteins reach the Trans Golgi Network (TGN). From this sorting location, receptor-bound lysosomal proteins reach the endosomal/lysosomal system by different routes [7]. In acid pre-lysosomal (endosomal) structures, dissociation of soluble lysosomal proteins from their transport receptors occurs, the latter returning to the TGN to bind a new round of newly formed lysosomal proteins [33].

1.2.1. Mannose-6-phosphate recognition signal-mediated transport of newly synthesized acid hydrolases to lysosomes

In mammalian cells, targeting of most soluble lysosomal matrix proteins, like the acid hydrolases, is mediated by the presence of a specific recognition signal in their N-linked glycans, the mannose-6-phosphate (M6P) moieties, recognized by M6PR. The attachment of one or more M6P residues on N-linked glycans of soluble lysosomal proteins occurs shortly after entry in the *cis* Golgi apparatus [4]. The addition of M6P groups in glycans is a multi-step process. The enzyme N-acetylglucosamine-1-phosphotransferase first generates a N-acetylglucosamine-phosphate group, followed by N-acetylglucosamine-1-phosphodiesterase, which removes the capping N-acetylglucosamine, generating M6P [34–36]. The exposed M6P groups of soluble lysosomal proteins are then recognized in the TGN by M6P receptors. Following binding, the receptor-ligand complex is targeted to pre-lysosomal compartments [37]. M6PR are type 1 transmembrane proteins, containing a dileucine signal [DXXLL] in their cytosolic domain [15, 38]. In mammalian cells, two M6PR occur in the late TGN [39]. One is the M6PR46 dimer (46 kDa), which is cation dependent (also named CD-MPR) and it has only one M6P binding site. M6PR300

(300 kDa), is cation independent (also named CI-MPR) and has two M6P binding sites [6, 40].

After the binding of lysosomal proteins to M6PR, these complexes are packed into clathrin-coated vesicles. These structures then traffic to the endo-lysosomal system, directly or via plasma membrane. After exposure to the relatively low pH of late endosomes, dissociation of lysosomal proteins from the recycling M6PR takes place [41]. In late endosomes and lysosomes, phosphate residues are removed from M6P groups by the lysosomal acid phosphatase [4, 42, 43]. A small proportion of both M6PR are also present at the plasma membrane, but only the M6PR300 seems to be involved in endocytosis of extracellular lysosomal enzymes.

An important role in sorting to lysosomes is played by the so-called adapter proteins (AP), in particular AP-1 and AP-2. The AP-1 and GGAs (Golgi localized, γ-ear-containing, Arf-binding family of proteins) mediate transport from the TGN to the endo/lysosomal system [44]. The AP-1 complex interacts with the cytoplasmic tail of M6PR [45, 46]. Four binding motifs were identified in the cytoplasmic tail: a tyrosine-based motif (^{26}YSKV^{29}), an internal dileucine-based motif (^{39}ETEWLM^{44}), and two casein kinase 2 (CK2) sites (^{84}DSEDE^{88}) and (^{154}DDSDED^{159}). The YSKV motif mediats the strongest interaction with AP-1, and the two CK2 motifs bound AP-1 only when they are phosphorylated. The C-terminal dileucines are not required for interaction with AP-1 [47]. The AP-2 complex, on the other hand, mediates endocytotic trafficking of M6PR from the cell surface via clathrin-coated vesicles. AP-2 interacts with tyrosine sorting signals in the cytoplasmic tail of M6PR [15].

1.2.2. Mannose-6-phosphate independent transport

In several cell types (e.g. fibroblasts), most soluble lysosomal proteins are targeted to the lysosome in M6P dependent manner. However, it is also clear that many proteins may reach lysosomes in a M6P independent manner. For example, lysosomal membrane proteins (LMP) do not acquire M6P moieties. Their features and transport to lysosomes is discussed in section 1.4.1. Specific proteins such as lysosomal acid phosphatase and glucocerebrosidase (GCase) use a unique

mechanism to reach lysosomes as it is discussed below. Finally, in some cell types like hepatocytes, many soluble lysosomal proteins manage to reach lysosomes independently of the M6P sorting mechanism [48].

The first indications for sorting mechanisms of newly formed lysosomal proteins were provided by the LSD Mucolipidosis type II (ML II) (I-cell disease, OMIM 252500) [49]. This disease is caused by mutations in the gene encoding N-acetylglucosamine-1-phosphotransferase (*GNPTG*, EC 2.7.8.17) that is important for the addition of M6P groups [50, 51]. While total loss of N-acetylglucosamine-1-phosphotransferase activity results in ML II, a partial reduction in its activity causes ML III, also known as pseudo-Hurler polydystrophy (OMIM 252600). In both cases, the lack of M6P in lysosomal enzymes causes faulty intracellular sorting and secretion from cells [52]. The generalized lack of hydrolases in lysosomes in certain cells, like fibroblasts of ML II and ML III patients, causes massive storage of multiple non-degraded substrates, the so-called inclusion bodies [53]. The same phenomenon occurs in the mouse model of ML II disease deficient in *GPNTG* [54]. However, both in ML II and III patients and in ML II mice, some soluble lysosomal proteins are correctly sorted to lysosomes of hepatocytes and other cell types despite the lack of M6P moieties in lysosomal proteins. The molecular basis for this alternative transport has not yet been established. Several examples of M6P independent transport of lysosomal matrix proteins are known in fibroblasts. As mentioned above, one example is the lysosomal acid phosphatase. This initially membrane bound enzyme is targeted as such to the plasma membrane and thereafter transported to lysosomes through endocytosis, via its tyrosine-based motif YRHV present in its cytosolic domain [55]. Inside the lysosome, the enzyme is partly released as a soluble protein through proteolytic cleavage. Another example is GCase, the lysosomal acid β-glucoside (GCase, E.C.3.2.1.45), encoded by the *GBA* gene. Its levels are normal in I-cell fibroblasts and its N-linked glycans never acquire M6P groups [56]. The lysosomal integral membrane protein type 2 (LIMP-2) was identified as the responsible protein for transport of GCase to lysosomes [57]. As described in more detail in section 1.4.2.1, LIMP-2 binds GCase in the ER and releases the enzyme at acid pH in lysosomes [58].

Alternative M6P independent transport mechanisms have also been described for other lysosomal enzymes like acid sphingomyelinase and cathepsins D and H. The type I transmembrane protein sortilin has also been proposed to be involved in targeting of some lysosomal proteins trought this alternative routing [59, 60]. There is more compelling evidence for an active role of sortilin in the transport to lysosomes of GM2 activator protein and prosaposin, the precursor of the small molecular weight sphingolipid activator proteins saposin A-D [61]. GM2 activator protein assists in the degradation of the ganglioside GM2 by β-hexosaminidases [62, 63]. Saposins enhance the activity of lysosomal hydrolases towards sphingolipid substrates by favouring the access to their hydrophobic lipid substrates. This facilitating action is essential for β-galactocerebrosidase (by saposin A), GCase (by saposin A and C), arylsulfatase A (by saposin B), α-galactosidase A (by saposin B) and sphingomyelinase (by saposin D) [64, 65]. The physiological importance of activator proteins is illustrated by the outcome of genetic deficiencies. For example, patients with a mutated saposin C develop a similar phenotype to those with a GCase deficiency [66].

1.3. Lysosomal storage disorders

LSDs are individually rare diseases, but as group they affect about 1 in 5,000 live births [67]. The prevalence in Portugal is similar, being about 1 in 4,000 live births [68]. However, the true incidence can exceed this due to misdiagnosed/undiagnosed cases. Besides defects in soluble hydrolases, LSDs can also be caused by defects in non enzymatic accessory proteins like activator proteins, transporters or proteins involved in post-translational modifications and trafficking of lysosomal proteins [5, 33, 69]. Lysosomes may also be defective due to mutations in structural membrane components, like the lysosome associated membrane protein 2 (LAMP-2) or LIMP-2, impairing mobility of lysosomes and their fusion with other cellular structures including autophagosomes [70, 71]. LSDs are generally still classified according to the nature of the substrate stored (Table 1.1). The traditional classification discerns: i) sphingolipidoses (sphingolipid accumulation); ii) mucopolysaccharidoses

(glycosaminoglycan accumulation); iii) oligosaccharidoses (oligosaccharide accumulation); iv) defects in membrane proteins and v) others [72].

Most LSDs are inherited in an autosomal recessive manner, with the exception of Fabry, Hunter and Danon diseases, being X-linked disorders [73]. LSDs usually display a very diverse clinical phenotype, manifesting as infantile, juvenile or adult forms. The clinical presentation of LSDs is heterogeneous, depending of the primary defect, the nature of the substrate and the affected organs, in particular the possible involvement of the central nervous system. Many patients with LSDs are asymptomatic at birth and young age, leading to a delay of several years until the correct diagnosis is made. Although many LSDs may present some characteristic neurological involvement, others entirely lack it, like Fabry disease and type 1 GD [72]. Prediction of severity of an LSD based on genotyping is increasingly employed. For some diseases, particular mutations in the corresponding gene result in a complete absence of enzymatic activity and therefore a severe disease while others result only in a slight decreased deficiency and milder clinical presentation. However, for several LSDs it is recognized that predictions of disease severity based on genotype are not accurate. Patients with the same mutant genotype can sometimes exhibit very different clinical symptoms and disease severity [74–76]. Although the genetic and biochemical background of the majority of the LSDs are well described, the way lysosomal storage interferes with other metabolic pathways and impairs cell function is still unknown. For most LSDs, it is still enigmatic how epigenetic and/or external factors can influence their progression [77, 78].

Sphingolipidoses comprise the most prevalent group of LSDs. These disorders result from a block in lysosomal degradation of sphingolipids due to an enzymatic deficiency. In sphingolipids, sphingoid bases are acylated with a fatty acid. These ceramide structures can carry hydrophilic headgroups (e.g. phosphorylcholine in the case of sphingomyelin, carbohydrate residues in the case of glycosphingolipids, and a phosphate moiety in the case of ceramide-1-phosphate). Glycosphingolipids are important components of cellular membranes and are expressed in a cell-type specific pattern [79, 80]. The presence of sialic acids in glycosphingolipids underlies their classification into neutral or acidic types [81, 82]. Major classes are gangliosides

and globosides. The shared precursor of most glycosphingolipid series is glucosylceramide (GlcCer). This lipid is synthesized at the cytoplasmic face of the Golgi membrane by the transfer of a glucose moiety from UDP-glucose to ceramide by the enzyme glucosylceramide synthase (GCS) (E.C. 2.4.1.80). [83]. All subsequent complex glycosphingolipids are the result of a stepwise addition of sugars to GlcCer in the lumen of the Golgi [5, 84, 85].

Degradation of glycosphingolipids largely occurs in lysosomes by sequential action of specialized glycosidases, ultimately rendering ceramide which on its turn is cleaved into sphingosine and free fatty acid by acid ceramidase [5, 84, 85].

Deficiencies in one of multiple glycosidases are the cause of various sphingolipidoses. The most frequent sphingolipidosis is Gaucher disease (GD). This recessively inherited disease is caused by deficiency in GCase, which degrades GlcCer intralysosomally [86]. In most GD patients with a non-neuronopathic disease, GlcCer storage is most prominent, even exclusive, in tissue macrophages [87]. The features and therapy of GD are described below in more detail in sections 1.3.1 and 1.3.2. Another prevalent sphingolipidosis is Fabry disease, in which globotriaosylceramide (Gb3) accumulates as the result of a deficient activity of α-galactosidase A [88]. Both in GD and Fabry disease, the primary storage lipids are partly converted to the corresponding sphingoid bases which are markedly elevated in plasma: glucosylsphingosine (GlcSph) from GlcCer in Gaucher patients and lysoGb3 from Gb3 in Fabry patients [89]. Lysosomal sphingolipid accumulation may also be caused indirectly. For example, accumulation of another substrate in lysosomes may interfere with local degradation of sphingolipids as occurs in Niemann–Pick disease type C (NPC). Defects in the lysosomal membrane protein NPC1, which mediates the efflux of cholesterol from lysosomes, not only leads to accumulation of cholesterol, but also to storage of sphingomyelin, several glycosphingolipids, sphingosine and others lipids [84, 90].

Table 1.1 – Lysosomal storage disorders. Adapted from [72].

	DISORDERS		ENZYME OR CO-FACTOR DEFICIENCY	MAIN STORAGE COMPOUNDS
Sphingolipidosis	Fabry		α-galactosidase A	Gb3 and blood-group-B compounds
	Farber lipogranulomatosis		Ceramidase	Ceramide
	Gaucher		β-glucocerebrosidase Saposin-C activator	Glucosylceramide/ Glucosylsphingosine
	GM1 gangliosidosis		β-galactosidase	GM1 ganglioside
	GM2 gangliosidosis	GM2-activator protein deficiency	GM2-activator protein	GM2 ganglioside and related glycolipids
		Sandhoff	β-hexosaminidase A and B	
		Tay Sachs	β-hexosaminidase A	
	Niemann-Pick A and B		Sphingomyelinase	Sphingomyelin
	Sphingolipid activator protein		Sphingolipid activator	Glycolipids
Mucopolysaccharidoses (MPS)	Morquio A disease		N-acetylglucosamine-6-sulphatesulphatase	Keratan sulphate, chondroitin-6-sulphate
	Morquio B disease		β-galactosidase	Keratan sulphate
	MPS I (Hurler, Scheie, Hurler/Scheie)		α-iduronidase	DS and HS
	MPS II (Hunter)		Iduronate-2-sulphatase	
	MPS III (Sanfilippo)	A	Heparan N-sulphatase (sulphamidase)	HS
		B	N-acetyl-α-glucosaminidase	
		C	Acetyl-CoA:α-glucosamide N-acetyl transferase	
		D	N-acetylglucosamine-6-sulphatase	
	MPS VI (Maroteaux-Lamy)		N-acetylgalactosamine-4-sulphatase (arylsulphatase B)	DS
	MPS VII (Sly)		β-glucuronidase	HS, DS, chondroitin-4-sulphate, chondroitin-6-sulphate
Oligosaccharidosis	Pompe (glycogen storage disease type II)		α-glucosidase	Glycogen
Defects in membrane proteins	Cystinosis		Cystinosin	Cystine
	Danon disease		LAMP-2	Cytoplasmic debris and glycogen
	Infantile sialic-acid-storage disease		Sialin	Sialic acid
	AMRF		LIMP-2	Glucosylsphingosine
	Mucolipidosis IV		Mucolipin-1	Lipids and acid mucopolysaccharides
	Niemann-Pick C		NPC1 and NPC2	Cholesterol and sphingolipids
	Salla disease		Sialin	Sialic acid
Others	Galactosialidosis		Cathepsin A	Sialyloligosaccharides
	ML II (I-cell and pseudo-Hurler polydystrophy)		N-acetylglucosaminyl-1-phosphotransferase	Oligosaccharides, mucopolysaccharides and lipids
	Multiple sulphatase deficiency		Cα-formylglycine-generating enzyme	Sulphatides
	Batten disease	NCL1	CLN1 (protein palmitoylthioesterase-1)	Lipidated thioesters
		NCL2	CLN2 (tripeptidyl amino peptidase-1)	Subunit c of the mitochondrial ATP synthase
		NCL3	Arginine transporter	

1.3.1 Gaucher disease

GD is the most frequent sphingolipidosis in Portugal with a prevalence of 1.4 per 100,000 live births [68]. A patient suffering from this recessively inherited disease was firstly described in 1982, by the French dermatologist Philippe Gaucher. GD results from a deficiency in the lysosomal hydrolase GCase, which is responsible for the intralysosomal hydrolysis of GlcCer into ceramide and glucose [87]. GCase is encoded by the *GBA* gene that has been mapped to chromosome 1q21 [91, 92]. The *GBA* gene is 7.5 kb long and contains 11 exons [93]. The enzyme consists of 497 aa, with 4-5 occupied N-glycosylation sites, with the mature glycosylated form with a molecular weight of 65 kDa [87]. A highly homologous pseudogene sequence located 16 kb downstream from *GBA* gene has also been described, presenting 96% of homology [93]. GCase does not acquire M6P residues in order to be sorted into lysosome [94], instead, its targeting to lysosomes is mediated by the LIMP-2 [57]. More than 200 different mutations have been described in *GBA* gene [95]. The most common mutation is the N370S aa substitution, constituting 70% of the mutant alleles within Ashkenazi Jews and 25% worldwide [96]. Presence of *GBA* N370S in patients, even in heteroallelic state, is sufficient to prevent neurological manifestations as seen in types 2 and 3 GD patients. Another common *GBA* mutation is the L444P aa substitution. In this case, the enzyme folds poorly in the ER and is largely degraded via ERAD [95, 97, 98]. Homozygosity for *GBA* L444P is associated with neuronopathic (type 2 or 3) GD [87]. Despite these trends, a strict *GBA* genotype - GD phenotype correlation does not exist [99, 100].

GD presents a large phenotypic variability, ranging from death at birth to asymptomatic adults [76]. The traditional classification of GD is based on presence and the age of onset of neurological involvement [87]. Most common is the non-neuronopathic type 1 GD (OMIM 230800), characterized by the absence of neurologic involvement and with a very variable age of onset. Type 1 GD has a frequency of 1:50,000 - 200,000 births, but is more prevalent in the Ashkenazi population (1:1,000 births) [68, 101]. Type 2 GD (OMIM 230900), is characterized by the development of severe neurological symptoms at infancy, with a survival

prognosis of less than two years. In type 3 GD (OMIM 231000), neuronopathic degeneration usually starts at the end of the first decade of life [87]. The neuropathic forms (types 2 and 3) comprises only 5 - 10% of GD births in Caucasians [102]. Complete absence of GCase activity leads to serious skin problems incompatible with life. Such cases are called "*collodion babies* " [103, 104].

GD is a multi-systemic disorder affecting most organs, resulting in cytopenia, hepatosplenomegaly and skeletal abnormalities [87, 105]. Bone involvement is the most disabling feature of adult GD patients and causes pain, immobility, bone fracture, frequently followed by infection and osteomyelitis [106]. Several attempts have been made to generate a genuine mouse model of GD presenting symptoms similar to Gaucher patients, however the *GBA* knock-out mice proved to be inviable [107–110]. Introduction of common aa substitutions in *GBA* mouse did not lead to a phenotypic copy of human disease, but resulted in far more severe disease in the animals. The best phenocopy of type 1 GD in mice is obtained by inducible knock-out of GCase expressed in the white blood cell lineage [111, 112].

Although the enzymatic activity of GCase is reduced in all cell types, only macrophages store large amounts of GlcCer in their lysosomes. The morphology of the lipid-laden macrophages is very characteristic and they are referred to as “Gaucher cells”. In type 1 GD, “Gaucher cells” are the hallmark of the disease [113, 114]. The prominent GlcCer storage in macrophages has been explained by the relatively large load of glycosphingolipids on the endo/lysosomal system of these cells. Macrophages phagocytoze old and damaged erythrocytes and leukocytes rich in glycosphingolipids [87]. Since “Gaucher cells” are the hallmark of GD disease, it is not surprising that the biomarkers discovered for GD manifestation are proteins that are selectively produced by alternatively activated macrophages. Such proteins are chitotriosidase, a chitinase, and CCL18, a chemokine, being on average 1000- and 40-fold elevated, respectively, in the plasma of symptomatic type 1 GD patients [115, 116]. The primary storage lipid in GD, GlcCer, is only modestly increased in plasma of symptomatic patients. Moreover, in most cell types of GD patients, abnormalities in GlcCer are not detected. A possible explanation for the modest GlcCer abnormalities is the deacylation of GlcCer to GlcSph. In plasma of type 1 GD patients, GlcSph is

200-fold increased [116, 117]. GlcSph was earlier noted to be increased in brain of type 2 and 3 GD [118, 119]. It is assumed that GlcSph is formed by intralysosomal deacylation of GlcCer by acid ceramidase (Ferraz et al, to be published). A type 3 GD like phenotype is observed in patients suffering from specific mutations in the prosaposin gene [64, 66, 120].

1.3.1.1 Pathologies associated with Gaucher disease

In recent years it has been recognized that some pathologies are linked to GD or GCase deficiency. It has been proposed by some clinical researchers that GD patients suffer from a significantly increased risk for cancer, particularly leukemias [121]. This is not unexpected since gammopathies occur frequently in GD patients, pointing to chronic stimulation of B cells [122]. Unexpected is the relatively recent finding that deficiency of GCase imposes a risk factor of α-synucleinopathies like Parkinson disease (PD) and Lewy-Body dementia [123–125].

Of interest, not only GD patients but even carriers of mutated *GBA* alleles are at increased risk for these neurodegenerative disorders. The exact mechanism by which GCase abnormalitiy promotes α-synuclein aggregation and the corresponding pathology is not known. However, evidence is present that GCase and α-synuclein may interact with each other and that abnormalities in GCase may drive a pathological cascade [126]. In brain of a neuronopathic GD mouse model, α-synuclein deposits are noticed and introduction of GCase by gene therapy ameliorates the aggregate [127, 128]. The same therapeutic effect has been noticed in a mouse model of PD [129].

Studies on GCase have enormously profited from the development of specific antisera and monoclonal antibodies since the eighties. These tools allowed new insights in the life cycle of the enzyme and have assisted in problematic diagnostic questions. Very recently, a completely novel research tool became available, the so-called activity-based probes (ABP), named inhibodies [130]. These probes are cyclophellitol epoxides with a fluorescent tag. They resemble the known suicide inhibitors of GCase, conduritol-β-epoxide (CBE) and cyclophellitol, that covalently,

and irreversibly, bind to the catalytic nucleophile (E340) in the pocket of GCase [131]. These inhibody probes covalently label only active GCase molecules. Due to their amphiphilic nature, inhibodies spontaneously cross membranes by diffusion, allowing GCase labelling *in vivo* in cells and mice. The availability of such probes allows therefore investigations on GCase in a disease condition [131–134]. The inhibodies can be also employed in diagnosis through the quantification of active GCase enzyme molecules [131]. Future applications may include *in vivo* monitoring of trace amounts of infused inhibody labelled therapeutic enzyme in GD patients. In this way the tissue distribution of the costly therapeutic enzyme may be non-invasively followed in individual patients. Finally, the generation of highly specific cyclophellitol epoxide type GCase inhibitors offers new possibilities to generate GD research animal models (mice, zebrafish).

1.3.1.2 *GBA2* and Gaucher disease

Lysosomal GCase is not the only cellular enzyme that can degrade GlcCer. Researchers in Amsterdam firstly noticed the existence of a non-lysosomal glucosylceramidase, now known as GBA2 [135]. This enzyme is not related to GCase and is encoded by a separate gene, the *GBA2* located on chromosome 9p13.3 [135, 136]. GBA2 degrades GlcCer in the cytosolic leaflet of membranes, but the precise cellular location of the enzyme is not entirely clear since it has been claimed to be associated with endosomes [137] as well as with the ER [138]. The levels of *GBA2* tend to be increased during GCase deficiency in GD patients [139] as well as in the modest GCase reduction in NPC [140, 141]. It has been speculated that compensatory over activity of GBA2 occurrence during reduced GCase activity, results in the formation of toxic levels of ceramide in the cytosol [142]. Inhibition of GBA2 might, in view of this, exert positive effects. Indeed, *Mistry* and colleagues demonstrated that genetic loss of GBA2 has beneficial effects in GD mice [143]. Consistent with this, a beneficial protective effect on Purkinje cell loss and associated deterioration of motor coordination has been noted in NPC mice upon genetic loss of

GBA2, as well as with pharmacological inhibition of GBA2 activity (Marques et al, unpublished results).

1.3.2 Therapy of Lysosomal storage disorders as illustrated by Gaucher disease

GD has been a frontrunner among the LSDs in development of therapy. Until twenty-five years ago, the only treatments available for GD were interventions to treat specific symptoms like splenectomy and hip replacement. Few patients were subjected to bone marrow transplantation in the eighties. Successes were reported, but this invasive procedure was rarely used given the high mortality risk associated [144].

Nowadays, there are two registered therapies for type 1 GD: enzyme replacement therapy (ERT) and substrate reduction therapy (SRT). Since tissue macrophages are the sole pathological cells in GD patients without neurological involvement, the so-called type 1, Brady and colleagues considered specific supplementation of these cells with lacking GCase. For this purpose, they developed a macrophage targeted human enzyme containing N-linked glycans with terminal mannose moieties, thus allowing selective endocytotic uptake by mannose receptors expressed at the surface of tissue macrophages [145, 146].

Initially, enzyme was isolated from human placenta and enzymatically modified in glycan structure. In 1994, recombinant enzyme became available for ERT of type 1 GD [147]. The ERT treatment implies bi-weekly intravenous administration of enzyme. As treated patients register reduction of organomegaly, pancytopenia and amelioration of skeletal disease, the clinical response is very satisfactory [145, 148]. Several recombinant enzyme preparations, including one produced in carrot cells, are now registered for ERT of type 1 GD. However the costs of the treatment remain very high (exceeding 200.000 €/adult patient/year) [149–151].

The success of ERT for GD, led to the development of several other recombinant enzymes for treatment of LSDs as it is the case of Fabry [152], Pompe [153], MPSI [154], MPSII [155], MSPVI [156] and Morquio IV A [157]. The remarkable

clinical success of ERT for type 1 GD, unfortunately it is not observed for most of the other disorders. Despite the success of ERT in type 1 GD, some limitations of the approach have become apparent. Most importantly, ERT is not able to prevent neurological symptoms in Gaucher patients with a neuronopathic course of disease (types 2 and 3). This failure is ascribed to the inability of the 60 kDa enzyme to pass the blood brain barrier (BBB).

As alternative to ERT, SRT was developed [158, 159]. SRT aims to reduce glycosphingolipid overload by inhibiting GCS. The first generation of suitable GCS inhibitors was azasugar, which mimics GlcCer. N-butyl-deoxynojirimycin (Zavesca®, *miglustat*, Actelion) was registered as therapeutic SRT drug for type 1 GD [160]. Clinical studies have revealed that oral SRT with Zavesca® is able to treat visceral symptoms in mild to moderately affected type 1 GD patients [160, 161]. However, Zavesca® is a relatively poor GCS inhibitor and high doses are poorly tolerated due to off target side effects. Prevention of neuropathology in type 2 or 3 GD patients with Zavesca® treatment is not feasible [162]. A new generation of more potent inhibitor iminosugars, resembling ceramide, has been designed. Very recently, Eliglustat, a low nanomolar GCS inhibitor was registered for SRT of type1 GD [163, 164]. Recent clinical investigations reported very beneficial clinical responses in patients, such as reduced organomegaly and hematological improvements [165, 166]. Again, Eliglustat offers no solution for neuronopathic GD patients since the compound is actively removed from the brain. To generate brain permeable GCS inhibitors, series of biphenyl-substituted iminosugars of both configurations (D-gluco and L-ido) have been designed [167]. One of these, it is the 1307RB20, which is very promising, showing an IC_{50} of 2.5 nM for GCS and not affecting GCase (IC_{50} >5 μM) (Fig. 1.1) [167]. The same compound also inhibits GBA2 (IC_{50}= 0.6 nM). Such inhibition is thought to be beneficial in individuals with reduced GCase activity (see section 1.3.1.2).

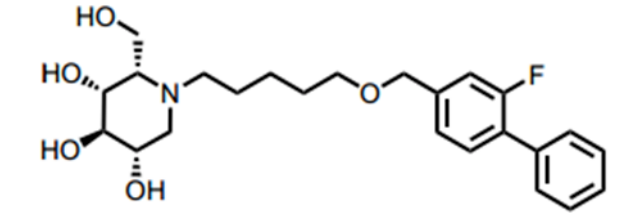

Figure 1.1 – Structure of the GCS inhibithor compound, the 1307RB20.

Under investigation are two other approaches to treat GD: chaperone therapy and gene therapy. Pharmacological chaperones are low molecular weight chemical compounds that through interaction with the catalytic pocket of GCase assist in the correct protein folding and stabilization of this proper fold. This approach is used in patients carrying specific mutated forms of GCase. A successful chaperone should increase the amount of mutant GCase that reaches lysosomes and improve degradative capacity [168]. Trials regarding gene therapy of type 1 GD were already conducted in the early nineties. The approach is based on *ex vivo* correction of hematopoietic stem cells with genetic information to produce the correct GCase and their subsequent re-introduction in patients. Technical limitations have hampered earlier attempts, but presently, approaches employing new generation lentiviral constructs have rendered very promising results in genuine type 1 GD mouse models [169]. Since gene therapy offers a cure, rather than chronic therapy, the outcome of translation of experimental gene therapy in mice to application in GD patients is eagerly awaited.

1.4. Lysosomal membrane proteins

The lysosomal membrane has a peculiar composition, being extremely rich in carbohydrates linked to membrane proteins, in cholesterol and with a characteristic phospholipid composition [170, 171]. Several LMPs have been identified by proteomic approaches [172–174]. The four most abundant LMP are LAMP-1 and 2, and LIMP-1 and 2 [70], representing approximately 50% of total LMPs. The LMPs generate a thick glycocalyx, which is thought to protect the limiting lysosomal membrane from

destruction by the luminal acid hydrolases. In addition, the integrity of the lysosomal membrane is essential to protect the cell against leakage of harmful components from the interior of the lysosome [70].

LAMPs are type I transmembrane proteins with a large luminal ectodomain and a short homologous cytoplasmic tail. LIMPs, on the other hand are type III transmembrane proteins [33, 70, 174]. The LMPs not only fulfil a structural role in the limiting lysosomal membrane but are also implicated in the sorting of lysosomal enzymes, fusion of lysosomes with other organelles, integrity of the endosomal/lysosomal compartment, transport of metabolites across the lysosomal membrane into the cytoplasm and chaperone mediated autophagy [70] .

1.4.1 Sorting of lysosomal membrane proteins to lysosomes

LMPs reach the lysosomes in different ways. One route is direct and runs from the TGN directly to endosomes and subsequently to lysosomes. The alternative route is indirect and involves routing trought plasma membrane via the secretory pathway, hereafter via endocytosis, reaching the lysosomes [175, 176]. In both cases, the transport of LMPs is dependent on tyrosine (YXX) or dileucine motifs (DXXLL) sorting signals, located in their cytoplasmic tail [7]. While LAMPs and LIMP-1 use the tyrosine motif, LIMP-2 requires the dileucine DXXLL motif in its cytoplasmic domain for efficient routing to lysosomes [177, 178]. These sorting signals in the cytoplasmic tails of LMPs are recognized by cytosolic APs, which are involved in the targeting to the lysosome [177, 179].

1.4.2 LIMP-2

Lysosomal integral membrane protein type 2 (LIMP-2) is encoded by the *SCARB2* gene. The gene is also known as *CD36L2*, *HLGP85* and *LIMPII.* It was firstly identified and biochemically characterized in 1985, without a specific function attributed to it [176]. As a type III transmembrane protein, LIMP-2 spans twice the lysosomal membrane, with its N-terminal and C-terminal both located in the cytosol

[180]. The luminal portion of LIMP-2 protein is highly conserved and contains a *coiled-coil* domain [57, 181, 182]. LIMP-2 is palmitoylated at cysteine residues, further anchoring it in the membrane [183].

LIMP-2 belongs to the cluster of differentiation 36 (CD36) superfamily, which includes several cell adhesion proteins, lipid receptors and other LMPs [184]. LIMP-2 is ubiquitously expressed in cells [185] and presents a 34% aa homology with the multifunctional CD36 [186]. CD36 is involved in binding of collagen, thrombospondin, erythrocytes parasitized with *plasmodium falciparum*, platelet aggregation, oxidized low density lipoproteins, native lipoproteins, oxidized phospholipids and long chain fatty acids [186, 187]. Another member of the CD36 scavenger receptor family is CLA1/SCARB1 isoform 1 (SR-BI) and its splice variant CLA2/SCARB1 Isoform 2 (SR-BII). Both proteins are involved in the import of cholesterol and cholesterol esters from HDL particles [188]. SR-BI and CD36 are both linked to lipid transport and are equipped for this with a presumed tunnel. Homology modelling suggests the presence of a similar tunnel in LIMP-2, which is conserved from zebrafish to man [189].

The *SCARB2* gene coding for LIMP-2 protein is located on the human chromosome 4 in the region 4q21.1 [190]. The gene comprises 52.7 kb and contains 12 exons. The human *SCARB2* and the mouse *LIMP-2* gene have a sequence identity of 84% at the nucleotide level and 85% at the aa level [191]. The cDNA encodes a protein of 478 aa, with a predicted molecular weight of 53 kDa. The real molecular weight of LIMP-2 is 73-85 kDa as the result of extensive N-glycosylation at potential 11 sites [180, 191–193]. The glycosylation of LIMP-2 is essential for its correct folding, sorting, lysosomal localization and stability [58, 194]. The C-terminal cytoplasmic tail of LIMP-2 has 20 aa, which contains the di-leucine motif (L475, I476) essential for sorting [195]. In the case of the LIMP-2, AP-3 mediates its intracellular sorting [196–198]. Mutations within the conserved consensus motif lead to the incorrect localization of the protein at the plasma membrane [195, 199]. Other mutations can also lead to its incorrect localization. For example, these LIMP-2 mutant forms may accumulate at early and late endosomes, or even, be retained in the ER [58, 185, 200, 201]. Surprisingly, a recent study suggests that LIMP-2

acquires M6P moieties [202]. The significance of this finding is questioned particularly since in I-Cell disease GCase is correctly targeted to the lysosome [56, 202].

1.4.2.1 Glucocerebrosidase and LIMP-2

Studies by Reijnbout *et al.* indicated that newly synthesized GCase soon gets membrane bound in the ER [203, 204]. The responsible membrane bound receptor remained enigmatic for several decades. Only in 2007, LIMP-2 was identified as the protein responsible for the targeting of GCase to the lysosome [57]. Binding of GCase to LIMP-2 occurs in the ER and disruption of the complex takes place at acidic pH, characteristic of late endosomes and lysosomes lumen [58] (Fig. 1.2). The highly conserved coiled-coil domain (aa 150-167) in the luminal domain was shown to bind to GCase [194]. The histidine residues in the coiled coil domain, particularly H171, are responsible for the pH dependence binding of GCase to LIMP-2. At acid pH the histidines are protonated and GCase is released from LIMP-2 [58]. Recently, Zhao *et al.* have claimed that H150 is also important in the pH dependent binding of GCase to LIMP-2 [202]. Moreover, it has been reported that two phosphatidylinositol 4 kinases (PI4K) are important in the trafficking of the LIMP-2/GCase complex to the lysosome: PI4KIIα and PI4KIIIβ. PI4KIIIβ was proposed to be involved in the transport through the complex in the Golgi apparatus, while PI4KIIα would be important to transport of the complex between TGN and late endosomes or lysosomes [205, 206].

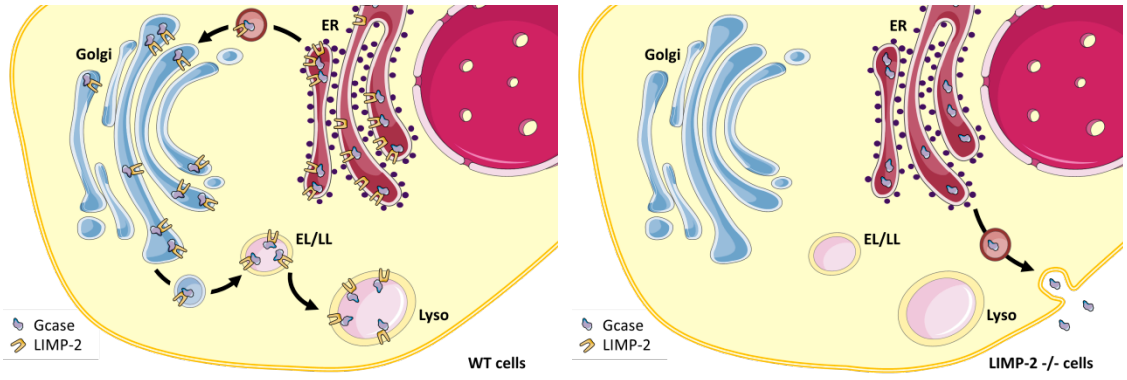

Figure 1.2 – Schematic representation of GCase sorting in wils type (WT) and LIMP-2 (-/-) deficient cells. "EL/LL" - Early and late endosome; "Lyso" – Lysosome; "ER" - Endoplasmatic reticulum.

1.4.2.2 *LIMP-2 KO* mice

In mice, the *LIMP-2* gene is located on chromosome 5 [190]. Saftig and co-workers, following their discovery of some of the functions of LIMP-2 protein, generated a *LIMP-2 KO* mouse [190]. The animals show increased postnatal mortality due to the hydronephrosis [190]. The main pathological change in the kidney, uni- or bilateral hydronephrosis, develops variably at the age of 3-16 months. It is caused by mislocalization of the protein uroplakin in the coating cells of the urothelium. In the *LIMP-2 KO* mice, uroplakin cannot protect the epithelium of the bladder and ureter from the acid urine and, consequently, there is hyperproliferation of the urothelium. This process leads to pathological thickening, causing reflux of urine into the kidney [190]. *LIMP-2 KO* mice also develop deafness and peripheral neuropathy [190]. The deafness and numbness of *LIMP-2 KO* mice might be due to mislocalization of the potassium channel KCNQ1, β-subunit KCNE1, and megalin in the stria vascularis of the inner ear, which contributes to the atrophy of the stria vascularis and collapse of the endochochlear potential [207]. The neuronal changes result from demyelination of the peripheral nervous system. The myelin proteins, the myelin basic protein (MBP) and the peripheral myelin protein 22 (PMP22), that are involved in the stability and in the strength of the concentric rings of myelin, are decreased in the *LIMP-2 KO* mice [190]. Characteristic of the *LIMP-2 KO* mice is the increased diameter of the peripheral nerves, next to the reduced number of fibers [190]. The same phenomenon occurs in the hereditary neuropathy Charcot-Marie-Tooth Disease. The so-called onion bulbs are formed due to hypomyelination of the peripheral nervous system and Schwann cell hypertrophy, resulting in constant de- and re-myelination. This results in reduced nerve conduction velocity and impaired muscle reflexes [208, 209]. LIMP-2 deficient Schwann cells also present abnormal inclusions and vacuoles in their cytoplasm [190]. Some changes observed in the brain of *LIMP-2 KO* mice are comparable to those seen in LIMP-2 deficient patients, such as intracellular deposits and inclusion bodies similar to those observed in certain cases of ataxia [210, 211].

1.4.2.3 LIMP-2 and Action Myoclonus Renal Failure Syndrome

LIMP-2 deficiency causes the Action Myoclonus Renal Failure Syndrome (AMRF, OMIM 254900). This autosomal recessive disorder has been unequivocally shown to be due to mutations in the *SCARB2* gene [194, 201, 210, 212, 213]. AMRF was initially described in Canada [214] and years later several patients were identified in other countries like Australia, Canada, Italy, Germany and Portugal [194, 201, 210, 212, 213, 215–218]. Nowadays, a wide spectrum of mutations in LIMP-2 has been identified, ranging from missense to nonsense mutations [194, 201, 210, 213, 215–217, 219] (Table 1.2). As in other LSDs, no strict genotype-phenotype correlation seems to exist [220].

Table 1.2 – Mutations in the *SCARB2* gene causing AMRF.

MUTATION	NUCLEOTIDE CHANGE	TYPE	REFERENCE
IVS10DS, G-T, +1	1239+1G-T	Splice-site mutation; premature truncation	[210]
2-BP INS, 435AG	c.435_436insAG	Frameshift, premature truncation	[210]
G288X	c.862C-T	Nonsense	[210]
W178X	c.533G-A	Nonsense	[201]
IVS8AS, A-C, -2	1116-2A-C	Intron mutation	[213]
1-BP DEL, 1258	c.1258delG	Nonsense	[213]
1-BP INS, T, IVS9	1187+3insT	Intron mutation	[221]

AMRF shows major phenotypic heterogeneity, including patients presenting classical features of the disease without any renal involvement [213, 216, 217, 222, 223]. However, most AMRF patients present renal dysfunction and failure due to focal glomerulosclerosis [210, 224]. In addition, they show myoclonic epilepsy and ataxia with progressive neurological impairment [201, 210, 212, 217]. The neurological symptoms usually appear between 15-25 years of age [220]. Patients first manifest tremors, which develop to progressive myoclonus, generalized seizures and later to ataxia. In *postmortem* brain biopsies, an extra brown pigment accumulation was detected. No cognitive deficit is noted [212, 216, 217]. AMRF patients, like *LIMP-2 KO* mice, develop neurological and renal symptoms [190, 210, 218].

1.4.2.4 LIMP-2 and other pathologies

Besides causing AMRF, *SCARB2* mutations also can influence the severity of GD manifestations. The heteroallelic *SCARB2* mutation was found to cause neuronopathic GD in patients with a *GBA* genotype normally associated with non-neuronopathic type I disease [225]. LIMP-2 is also partly present at the plasma membrane. There, it acts as a receptor for the Coxsackievirus [226, 227] and enterovirus 71 (EV71) [228, 229], that are responsible for causing Hand-Foot-Mouth Disease [230]. The region 142-204 aa of LIMP-2 protein was identified as essential for EV71 binding [231].

LIMP-2 is also important in the activation of the innate immune system during infection with *Listeria monocytogenes* by influencing the transport of bacteria to the phagosome [232]. It also acts as a functional receptor of β-catenin and N-cadherin within the intercalated discs of the cardiac muscle cells, and consequently linked to cardiac hypertrophy and heart failure [233]. For unknown reasons, LIMP-2 expression is found to be correlated with regeneration of injured sensory spinal axons [234].

Finally, mutations in the *SCARB2* gene, like those in the *GBA* gene, have been reported to impose an increased risk for developing PD [235]. In addition to this, LIMP-2, like GCase, has been shown to play an important role in the progression and development of α-synucleinopathies [236, 237].

2. AIMS

AIMS

AMRF is caused by mutations in the *SCARB2* gene encoding the lysosomal membrane protein LIMP-2. It has been recognized that LIMP-2 takes care of the transport of newly synthesized GCase to lysosomes where it degrades the glycosphingolipid GlcCer. In AMRF patients, a cell type dependent reduction of GCase activity occurs: GCase being markedly reduced in fibroblasts, but not in leukocytes.

In this thesis work, investigations are described on the function of LIMP-2, with focus on its crucial interaction with GCase. The consequences of LIMP-2 deficiency for GCase are broadly examined. In the reported investigations, besides AMRF patient's materials, use is made of *LIMP-2 KO* mice. GCase is investigated with classical research tools and new ones like ABPs. The lipid metabolites of GCase are studied with novel LC-MS/MS based measurements.

In chapter 2, the cell-type specific deficiency are analyzed in different type of cells either by using classic methods as well as the new developed ABP tools. Special attention is given to the fate of GCase in cultured fibroblast of AMRF patients, demonstrating partial secretion of active enzyme into the medium. Since phenotypically GD and AMRF are very distinct diseases, but share a common deficiency in GCase, glycosphingolipid GlcCer and its deacylated form GlcSph are measured in different samples. With the obtained results, a differential laboratory diagnosis is suggested for the correct and accurate identification of AMRF and GD patients.

In chapter 3, *LIMP-2 KO* mice are used to study the impact of the lysosomal membrane protein on GCase at cellular and tissue level. Highly purified lysosomes of hepatocytes from *LIMP-2 KO* mice are analyzed to identify new binding partners of LIMP-2. Since it is described a cell-type specific deficiency in AMRF patients as extensive biochemical analysis are performed regarding GCase activities. Subsequently, a correlation of the activities measured and its effect on direct and indirect catabolic pathways is evaluated. Attention is also paid to the cause of the high residual GCase activity in white blood cells of LIMP-2 mice, recapitulating findings in AMRF patients.

In chapter 4, investigations are described that aim to establish directions for treatment of AMRF. The impact of LIMP-2 on the efficacy of restoring lysosomal GCase capacity by exposure of cells to recombinant enzyme is described. Pilot studies on the use of substrate reduction by means of oral administration of a brain permeable inhibitor of glycosphingolipid synthesis are described.

The outcome of the various investigations and the envisioned future directions of research are discussed in the conclusions chapter.

3. LIMP-2 DEFICIENCY IN HUMANS: ACTION MYOCLONUS RENAL FAILURE SYNDROME

3.1 Abstract

The LIMP-2 has been identified as the receptor involved in the intracellular sorting and trafficking of the enzyme GCase to lysosomes. Deficiency of LIMP-2 causes AMRF. Fibroblasts of AMRF patients virtually lack GCase similarly to cells of patients with GD. GD is caused by mutations in the *GBA* gene encoding GCase, and is characterized by the accumulation of GlcCer-laden macrophages. Recently developed fluorescent ABPs allow a sensitive and specific visualization of active GCase. Using these probes, we show that GCase is incorrectly secreted in AMRF fibroblasts, leading to markedly reduced levels of active enzyme in those cells. In contrast, AMRF leukocytes present almost normal intracellular GCase levels. Our findings are consistent with the lack of lipid-laden white blood cells and the absence of increased plasma levels of macrophage markers such as chitotriosidase in AMRF patients, in contrast to Gaucher patients. We further evaluated the consequences of LIMP-2 deficiency with respect to plasma glycosphingolipid levels. Plasma GlcCer concentration was normal in the AMRF patients investigated as well as in *LIMP-2 KO* mice. However, a marked increase in the sphingoid base GlcSph was observed in AMRF patients and *LIMP-2 KO* mice. Our results suggest that combined measurements of chitotriosidase and GlcSph can be used for convenient differential laboratory diagnosis of AMRF and GD.

3.2 Introduction

Lysosomes contain a variety of integral membrane proteins among which the most abundant are LAMP-1, LAMP-2 and LIMP-2 [33]. Defects in LMPs may result in several pathologies [70]. An example are mutations in the LIMP-2 gene (*SCARB2*) causing AMRF, a fatal recessively inherited disorder characterized by glomerulosclerosis, progressive myoclonus epilepsy, ataxia and accumulation of undefined storage material in the brain [57, 194, 201, 210, 211, 238]. More recently it has become clear that not all AMRF patients develop renal complications [213, 217, 222, 223].

It has been demonstrated that LIMP-2 deficient fibroblasts of AMRF patients lack the lysosomal enzyme GCase, whereas this appears not to be the case for their white blood cells [201]. The transport of newly formed GCase to lysosomes has been an enigma for a long time. Earlier, it had been observed that GCase does not acquire M6P moieties [56]. GCase is not deficient in fibroblasts of ML II and III patients which suffer from defects in the formation of M6P recognition signals [56]. In contrast, most soluble lysosomal enzymes are incorrectly secreted in these fibroblasts since their sorting is dependent on M6PR [33]. GCase was shown to become membrane bound in the ER by interaction with an unknown protein [203, 204]. Only a few years ago the receptor protein was identified as LIMP-2 [57].

GCase, an acid β-glucosidase, catalyzes the lysosomal degradation of GlcCer into ceramide and glucose. GD is caused by mutations in the *GBA* gene encoding GCase. GD is clinically very heterogeneous, ranging from severe neonatal variants to very mild variants with onset at old age. The most common phenotype is the non-neuronopathic type 1, showing almost exclusive storage of GlcCer in tissue macrophages, the so-called “Gaucher cells” [114]. These lipid-laden macrophages accumulate in various tissues, such as spleen, liver, bone marrow and lung, resulting in clinical symptoms of which cytopenia, hepatosplenomegaly and skeletal abnormalities are the most prominent [87]. These “Gaucher cells” secrete a variety of cytokines and hydrolases [239]. Of interest, AMRF patients do not show the massive occurrence of lipid-laden macrophages and some of the characteristic clinical

symptoms of the GD patients [218]. Consistently, plasma chitotriosidase, a biomarker of Gaucher cells, is normal in AMRF patients but several hundred-fold elevated in GD patients [115, 201]. This suggests that their macrophages are not deficient in GCase. These findings point to cell-type specific consequences of LIMP-2 deficiency. Another biochemical characteristic of GD is the several hundred-fold increased plasma concentration of the sphingoid base GlcSph [117]. The sphingoid base is likely formed from accumulating GlcCer in GCase deficient cells.

GCase is a low abundant protein, particularly in leukocytes and difficult to detect with antibodies [240]. To study more closely GCase in leukocytes of AMRF patients, we employed novel ABPs that allow visualization of active GCase molecules [130, 131, 133]. It was recently shown that epoxides like CBE and cyclophellitol form a covalent bond with the nucleophile E340 in GCase. Attaching a BODIPY moiety through a linker to C6 of cyclophellitol resulted in an even more potent irreversible inhibitor of GCase. Different ABPs have been designed by variation of the BODIPY (MDW941, Inhibody Red; and MDW933, Inhibody Green) that allow ultrasensitive detection of GCase in cell types containing enzyme levels below the level of detection by antibodies. The probes have also the ability to spontaneously cross membranes allowing *in vivo* labelling studies [131]. The availability of ABPs allowing sensitive detection GCase in leukocytes prompted us to study the fate of GCase in different cell types obtained from AMRF patients as well as from *LIMP-2 KO* mice.

GCase is very unstable at neutral (plasma) pH and rapidly loses its enzymatic activity. This reduces the ABP labelling, since active enzyme molecules are required for labelling. More recently, an other ABP has been designed for labelling GCase, MDW1033 (Anybody Green), which besides labelling active enzymes also labels enzyme molecules that have lost enzymatic activity, but conserved their structure [133].

Here, we report the outcome of these investigations, confirming cell-type specific decreases in GCase caused by LIMP-2 deficiency. Furthermore, we studied the consequence of LIMP-2 deficiency for GlcCer and GlcSph levels, the products of degradation by GCase. In this chapter, we also highlight the outcome and possible use in differential diagnosis of AMRF and GD.

3.3 Methods

3.3.1 Activity-based probes, anybody and antibodies

MDW941 (Inhibody Red), MDW933 (Inhibody Green) and MDW1033 (Anybody Green) were synthesized as described earlier [131, 133]. The rabbit polyclonal anti-LIMP-2 antibody was acquired from Novus Biologicals, Littleton, USA (NB400-129).

3.3.2 Patients' samples

Materials from donors were obtained after informed consent. Leukocytes and fibroblasts were obtained from AMRF patients homozygous for the *SCARB2* mutation W178X [201], LIMP-2 obligate carriers of the same mutation, Gaucher patients with the *GBA* genotype L444P/L444P and control subjects. Fibroblasts obtained from skin biopsies were cultured in Dulbecco's modified Eagle's medium supplemented with 10% fetal bovine serum, 2 mM L-glutamine, 1% penicillin–streptomycin, 100 mg/ml kanamycin sulfate and 2.5 mg/ml fungizone (Gibco, Invitrogen). Cells were harvested when reaching confluence. Leukocytes were isolated from whole blood as described earlier [201].

Monocytes were isolated with CD14 MicroBeads (Miltenyi Biotec) according to the manufacturer's protocol. Isolated monocytes were differentiated into macrophages for 7 days in Roswell Park Memorial Institute medium (RPMI) supplemented with 10% human AB serum [115].

3.3.3 Mice

Mice were housed and plasma was collected according to the local protocol approval from the review board of the Christian-Albrechts-University in Kiel (Germany). *LIMP-2 KO* mice were generated as described earlier [190].

3.3.4 Preparation of cell lysates

Isolated fibroblasts, macrophages and leukocytes were homogeneized in potassium phosphate buffer (PBS) (25 mM, pH 6.5, 0.1% (v/v) Triton X-100). Protein was quantified with a BCA Kit (Thermo Scientific). Cell extracts were prepared by sonication (40% power, 40% amplitude for 6 s). All homogenates were stored at -80 ºC.

3.3.5 Labelling with activity-based probes

Cell homogenates were incubated with MDW941 (100 nM) in McIlvaine buffer (150 mM citrate-Na_2HPO_4, pH 5.2, 0.2% (w/v) sodium taurocholate, 0.1% (w/v) Triton X-100) for 30 min at 37 ºC. Subsequently proteins were denatured with 5x Laemmli buffer (50% (v/v) 1 M Tris-HCl, pH 6.8, 50% (v/v) glycerol, 10% (w/v) DTT, 10% (w/v) SDS, 0.01% (w/v) bromophenol blue) by boiling for 10 min at 100 ºC, and separated by electrophoresis on 10% acrylamide (w/v) SDS-PAGE gels running at 90 V [131, 133]. Wet slab gels were scanned for red fluorescence using a Typhoon variable mode imager (Amersham Bioscience), λ_{ex} 532 nm and λ_{em} 610 nm (band pass filter 30 nm).

Fibroblasts were incubated with MDW941 (5 nM) for 72 h. Subsequently, the culture medium was collected and the cells were harvested. Detection of fluorescent GCase in the culture medium was performed as described above upon capture of enzyme from 1 ml of medium using monoclonal antibody 8E4 immobilized in Sepharose beads [94].

For Fluorescence-Activated Cell Sorting (FACS), fibroblasts and macrophages were incubated with MDW933 (50 nM) for 5 h in the medium. Cells were harvested with 0.25% Trypsin prior analysis.

In the case of white blood cells, the leukocyte layer was collected from freshly drawn blood by centrifugation for 10 min at 2500 rpm. The remaining erythrocytes were lysed with lysis solution 0.8% (w/v) ammonium chloride at 4 ºC. Leukocytes were next incubated with MDW933 (100 nM) during 30 min in phosphate buffered

saline containing 1% (w/v) bovine serum albumin. FACS analysis was performed with a FACS Calibur Becton Dickinson (B.D. Bioscience), λ_{ex} 488 nm, λ_{em} 530 nm (band pass filter 30 nm) [131].

3.3.6 Western-Blotting

SDS–PAGE gels were electroblotted onto a nitrocellulose membrane (Schleicher&Schuell®). Membranes were blocked with 5% skimmed milk and 0.05% Tween-20 in Tris-buffered saline (TBS) for 1 h at room temperature and incubated overnight with the primary antibody at 4 °C. Membranes were then washed three times with 0.01% Tween-20 in TBS and incubated with the appropriate IRDye conjugated secondary antibody for 1 h at room temperature. After washing, detection was performed using the Odyssey® Clx, Infrared Imaging System (LI-COR).

3.3.7 Measurement of *in vivo* glucocerebrosidase activity

GCase activity in intact cells was measured using fluorescein di-β-D-glucopyranoside (FDG) as a substrate (20 μM for fibroblasts and 40 μM for leukocytes and macrophages). Cells were suspended by trypsinization and analyzed by FACS exactly as described by Witte et al [131].

3.3.8 Fluorescence microscopy

Fibroblasts were cultured on glass slides. Cells were incubated with MDW933 (50 nM) for 2 h in medium. Next, cells were washed, fixed with 3% (v/v) paraformaldehyde in PBS for 15 min, washed, incubated with 0.1 mM NH_4Cl in PBS for 10 min and then with 3% (w/v) bovine serum albumin (BSA) and 10% (w/v) goat serum albumin in PBS for 1 h. Nuclei were stained with DAPI. Filter blocks used were A4 (360/40 nm band pass excitation, 400 nm dichromatic mirror, 470/40 nm band pass suppression) for DAPI and K3 (470-490 nm band pass excitation, 510 nm

dichromatic mirror, 515 nm long pass suppression) for MDW933. Analysis was performed with multispectral imaging, essentially as detailed in [131].

3.3.9 Glucosylceramide and Glucosylsphingosine measurements

GlcCer and GlcSph in fibroblasts, leukocytes and plasma specimens were measured as described earlier [117, 241].

3.3.10 Enzymatic assays

Enzymatic assays were performed according to Aerts et al [242]. β-Glucosidase activity was measured with 3.73 mM 4-methylumbelliferyl-β-D-glucopyranoside (4-MU-β-D-Glc), dissolved in 150 mM McIlvaine buffer (pH 5.2 supplemented with 0.2 % (w/v) sodium taurocholate, 0.1% (v/v) Triton X-100 and 0.1% BSA. Chitinase enzyme was measured with 1 mM 4-methylumbelliferyl β-DNN'N"-triacetylchitotrioside (4-MU-TCT) in a citrate/phosphate buffer, pH 5.2. After stopping the reaction with NaOH-glycine (pH 10.3), fluorescence was measured with a fluorimeter LS55 (Perkin-Elmer, Beaconsfield, UK), λ_{ex} 366 nm and λ_{em} 445 nm.

3.3.11 Anybody labelling

GCase from fresh plasma was immunoprecipitated with the monoclonal antibody 8E4 immobilized in Sepharose beads according to Aerts et al [94]. After washing, the beads were incubated with MDW1033 (100 nM) for 30 min and then subjected to SDS-PAGE. Fluorescent GCase was visualized using a fluorescence scanner (Typhoon Variable Mode Imager, Amersham Biosciences) [131].

3.4 Results

3.4.1 Activity-based labelling of glucocerebrosidase in fibroblasts

To evaluate the amount of active GCase, fibroblasts homogenates from three AMRF patients (*SCARB2* W178X/W178X), two LIMP-2 carriers (*SCARB2* W178X/WT), two control subjects and one type 2 Gaucher patient (*GBA* L444P/L444P) were labelled with MDW941 (100 nM) for 30 min and then subjected to SDS-PAGE to detect active GCase molecules. Labelled GCase was detected by fluorescence imaging of the slab gel (Fig. 3.1). Fibroblasts of AMRF patients showed a markedly reduced amount of fluorescently labelled GCase. Similarly, the amount of labelled enzyme is markedly reduced in cells from the type 2 GD patient. In the case of the carriers of LIMP-2 deficiency a normal amount of labelled GCase was detected when compared to control individuals. These results highlight the absence of active GCase in fibroblasts of AMRF patients.

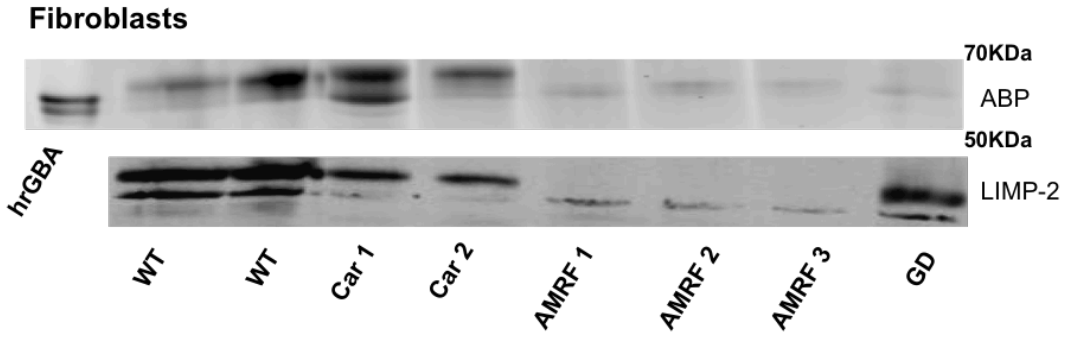

Figure 3.1 - Detection of GCase with fluorescent ABP MDW941 in homogenates from cultured fibroblasts (30 µg): labelling followed by SDS-PAGE and detection by fluorescence imaging. "WT" - Wild type; "AMRF" - AMRF patient (*SCARB2* W178X/W178X); "Car" - Carrier of AMRF (*SCARB2* W178X/WT); "GD" - Type 2 GD patient (*GBA* L444P/L444P); "hr*GBA*" - Recombinant GCase (Cerezyme®); "ABP" - Activity based probe; "LIMP-2" - Western-blot against LIMP-2 protein.

3.4.2 Fluorescence microscopy of glucocerebrosidase

Using multi-spectral imaging analysis, which allows identifying and distinguishing the respective fluorescence emission spectra from autofluorescence, intact fibroblasts were incubated with MDW933 to visualize by fluorescence

microscopy the active GCase molecules (Fig. 3.2). We observed almost no labelling of GCase in AMRF fibroblasts when compared to the control fibroblasts (Fig 3.2). AMRF fibroblasts were found to be clearly deficient in lysosomal GCase when compared to WT, in line with the results described in Fig. 3.1.

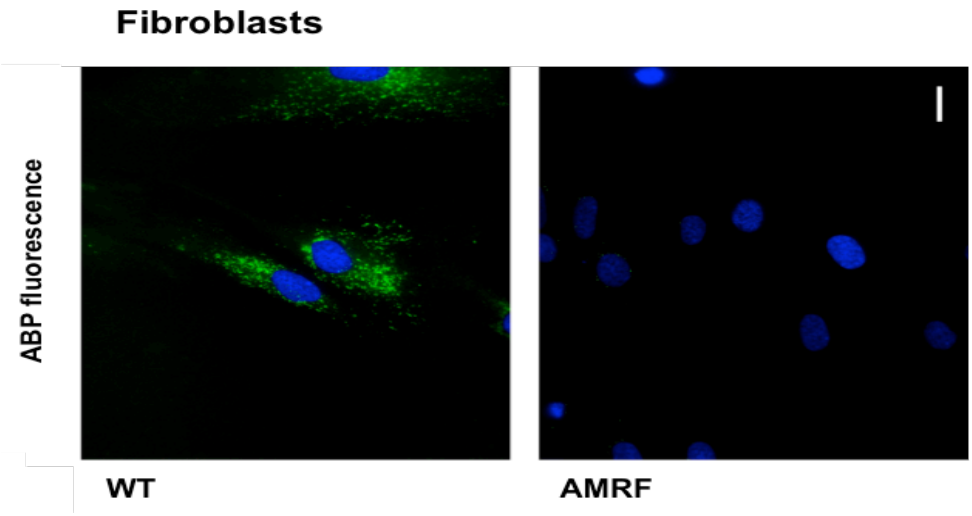

Figure 3.2 - Visualization of GCase with fluorescent ABP MDW933 by fluorescence microscopy. Fibroblasts were labelled *in vivo* with MDW933 and DAPI. Left micrograph: Wild type fibroblasts; Right micrograph: AMRF patient. The scale bar represents 20 µm.

3.4.3 Activity based labelling of glucocerebrosidase in leukocytes and macrophages

Leukocyte lysates were labelled *in vitro* with MDW941 (100 nM) for 30 min and subjected to SDS-PAGE. The findings from leukocytes of an AMRF patient are very different from those obtained in the fibroblasts. The amount of active GCase in leukocytes was similar for all subjects (control, LIMP-2 deficient carrier and AMRF patients) (Fig. 3.3A). Western-blot analysis using anti-LIMP-2 antibody showed that LIMP-2 protein was expressed at higher levels in fibroblasts compared to leukocytes. LIMP-2 protein was decreased in fibroblasts of LIMP-2 deficient carriers when compared to controls (Fig. 3.1 and 3.3A).

Next, GCase was analyzed in monocyte–derived macrophages. Monocytes were isolated from blood of an AMRF patient and a healthy subject, and differentiated

into macrophages. Detection of active GCase in homogenates of the generated macrophages revealed again only a slight reduction of GCase in the patient's cells (Fig. 3.3B).

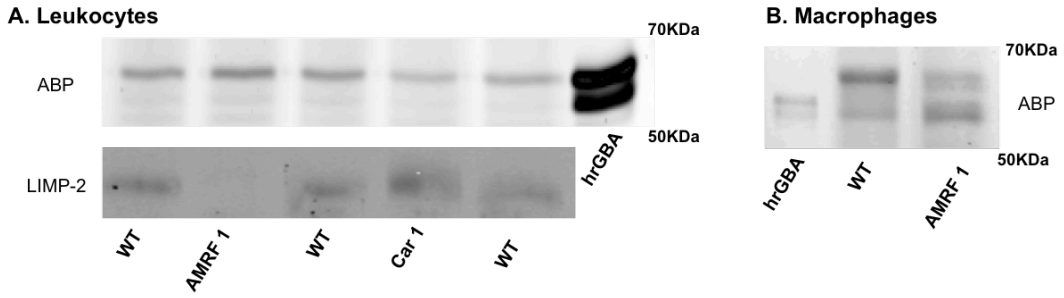

Figure 3.3 - Detection of GCase in homogenates of leukocytes (50 µg) (A) and cultured macrophages (20 µg) (B): labelling followed by SDS-PAGE and detection by fluorescence imaging. "WT" - Wild type; "AMRF" - AMRF patient (*SCARB2* W178X/W178X); "Car" - Carrier of AMRF (*SCARB2* W178X/WT); "hrGBA" - Recombinant GCase (Cerezyme®); "ABP" - Activity based probe; LIMP-2 - Western-blot against LIMP-2 protein.

3.4.4 FACS analysis

The amount of active GCase in intact cells was assessed by FACS analysis, either by labelling it with ABP MDW933 or by measuring the GCase activity with the substrate FDG (Fig. 3.4). The labelling of GCase in fibroblasts with MDW933 showed that control fibroblasts presented higher labelling when compared to the AMRF fibroblasts (Fig. 3.4A and 3.4C). GCase enzyme activity of fibroblasts towards FDG was measured using FACS (Fig. 3.4B and 3.4C). The results obtained were identical to those with MDW933. Control fibroblasts showed higher GCase activity when compared to AMRF fibroblasts. Similar experiments showed that the amount of active GCase is relatively high in different blood cells types of an AMRF patient, especially when compared to levels found in fibroblasts (Fig. 3.4C). Significant residual GCase levels (values >30%) were noted in lymphocytes, monocytes and cultured macrophages of the AMRF patient, both with ABP labelling and PFB-FDG incubation. The same finding was made for total leukocytes from *LIMP-2 KO* mice (Fig. 3.4C).

These results are in line with GCase enzymatic activity measured in cell lysates using the artificial substrate 4-MU-β-D-Glc, as it was previously published [201].

A. FACS: ABP labeled fibroblasts

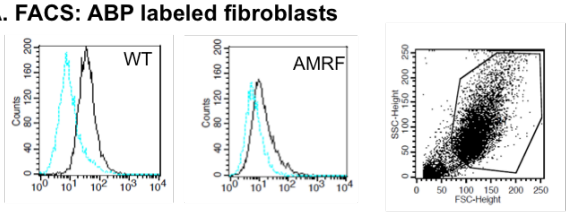

B. FACS: FDG treated fibroblasts

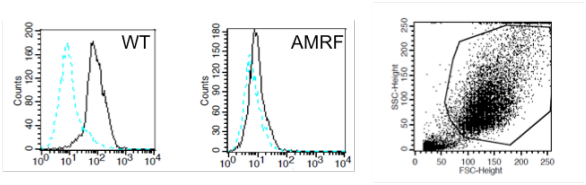

C. Residual GBA (percentage of normal)

	Cell type	ABP	FDG
AMRF 1	Fibroblasts	15	3
AMRF 2	Fibroblasts	23	4
AMRF 3	Fibroblasts	7	2
AMRF 1	Lymphocytes	39	35
AMRF 1	Monocytes	41	47
AMRF 1	Macrophages	40	32
LIMP2 -/- mouse	Total leukocytes	47	ND

Figure 3.4 – FACS analysis of active GCase detected with ABP MDW933 and FDG as substrate. A: Example of FACS analysis of fibroblasts with ABP. Left panel: Primary FACS data (dotted line not labelled with MDW933, solid line labelled with MDW933). Right panel: Representative FACS dot plot. B: Example of FACS analysis of fibroblast enzymatic activity toward FDG. Similar to A. C: Overview of detected residual active GCase by analysis of cells with ABP and FDG.

3.4.5 Secretion of glucocerebrosidase by LIMP-2 deficient fibroblasts

Misrouting of GCase to lysosomes may result in its accumulation in the extracellular space. To study this, cultured fibroblasts were labelled with MDW941 for 72 h and the culture medium was collected. Labelled GCase present in 1 mL of medium was immunoprecipitated with the anti-GCase monoclonal antibody 8E4 and visualized after SDS-PAGE in a fluorescent scanner (Fig. 3.5). Labelled GCase was

clearly detected in the medium of cells from AMRF patients and it was almost absent in the case of controls and LIMP-2 deficient carriers.

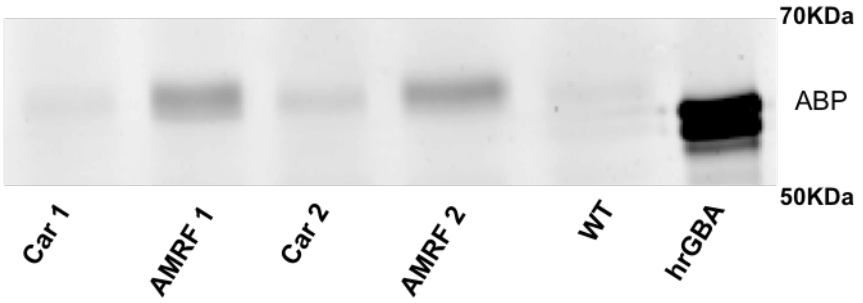

Figure 3.5 – Partial secretion of GCase by fibroblasts. Fibroblasts were labelled for 72 h with MDW941. From 1 ml medium GCase was immunoprecipitated with anti-GCase monoclonal antibody 8E4 immobilized in Sepharose beads. The immunoprecipitate subjected to SDS-PAGE and fluorescent GCase labelled with MDW941 was visualized by imaging. "WT" - Wild type; "AMRF" - AMRF patient (*SCARB2* W178X/W178X); "Car" - Carrier of AMRF (*SCARB2* W178X/WT); "hrGBA" - Recombinant GCase (Cerezyme®); "ABP" - Activity based probe.

We next looked for the presence of GCase in the plasma of AMRF patients by measuring its enzymatic activity with the artificial substrate 4-MU-β-D-Glc. We noted an increased activity in the case of fresh specimens from AMRF patients when compared to healthy subjects Fig. 3.6A. Such increase was only detected in freshly obtained plasma. Storage of plasma, even frozen, led to inactivation of the enzymatic activity of GCase (in samples frozen for a long period at - 20 ºC, less than 2% of original GCase activity was detected). In line with the data obtained for the freshly AMRF patient plasma, *LIMP-2 KO* mice also showed increased GCase in fresh plasma specimens (Fig. 3.6B). Using another sensitive probe developed, MDW1033 (Anybody Green), a large amount of GCase was found in the plasma of AMRF patient upon imunoprecipitation, when compared to control plasma (Fig. 3.6C). Given the loss of enzyme activity in plasma, measurement of plasma GCase activity is in practice not a very reliable test to identify AMRF patients.

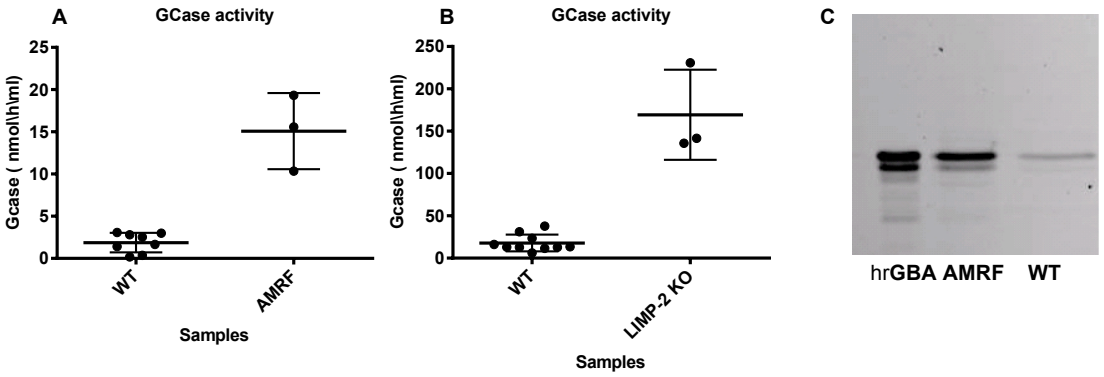

Figure 3.6 – Detection of GCase in the plasma specimen. Measurement of GCase activity in human plasma (A) and in mice plasma (B). GCase detection in human plasma using the probe MDW1033 (C). "WT" - Wild type; "AMRF" - AMRF patient (*SCARB2* W178X/W178X); "*LIMP-2 KO" - LIMP-2 KO* mice; "hrGBA" - Recombinant GCase (Cerezyme®)

To evaluate the macrophage involvement in the disease, chitotriosidase levels were measured in the plasma specimens from AMRF patients and *LIMP-2 KO* mice (Fig. 3.7).

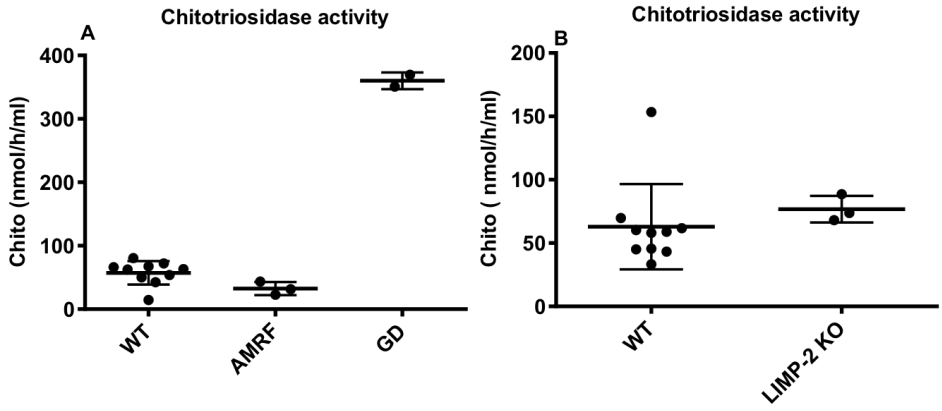

Figure 3.7 - Detection of chitotriosidase in the plasma specimen. Measurement of chitotriosidase activity in human (A) and in mice (B) plasma. "WT" - Wild type; "AMRF" - AMRF patient (*SCARB2* W178X/W178X); "GD" - Gaucher patients; "*LIMP-2 KO" - LIMP-2 KO* mice.

As it was expected, both AMRF patients and *LIMP-2 KO* mice didn´t present increased levels of chitotriosidase when compared to control samples (Fig. 3.7).

3.4.6. Lipid abnormalities in LIMP-2 deficiency

The lack of lysosomal GCase as a result of LIMP-2 deficiency might theoretically result in abnormalities in GlcCer breakdown as seen in Gaucher patients. We therefore determined GlcCer and GlcSph concentrations in fibroblasts and plasma from AMRF patients as well as in plasma of *LIMP-2 KO* mice.

In AMRF fibroblasts GlcCer was not elevated when compared to the control subjects (Fig. 3.8A). Importantly, a marked increase in GlcSph was noted (Fig. 3.9A). The same was found in leukocytes (Fig. 3.9B). Also in plasma of three AMRF patients we could detect elevated GlcSph levels (Fig. 3.9C). However, no clear concomitant increase in GlcCer was observed when compared to the matched control plasmas (Fig. 3.8B). To further validate the finding of the sphingoid base abnormality we also examined plasma of *LIMP-2 KO* mice. Again, a clear elevation in GlcSph concentration was observed (Fig. 3.9D).

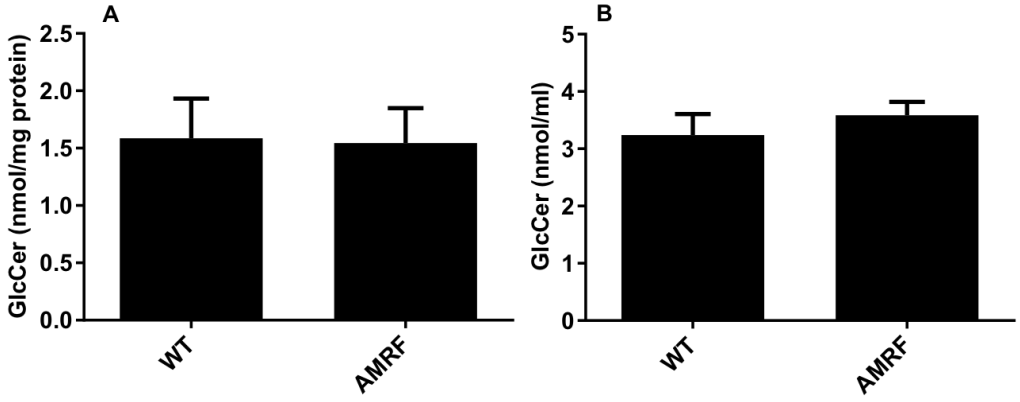

Figure 3.8 - GlcCer levels in fibroblasts (A) and plasma (B). "WT" - Wild type; "AMRF" - AMRF patient (*SCARB2* W178X/W178X).

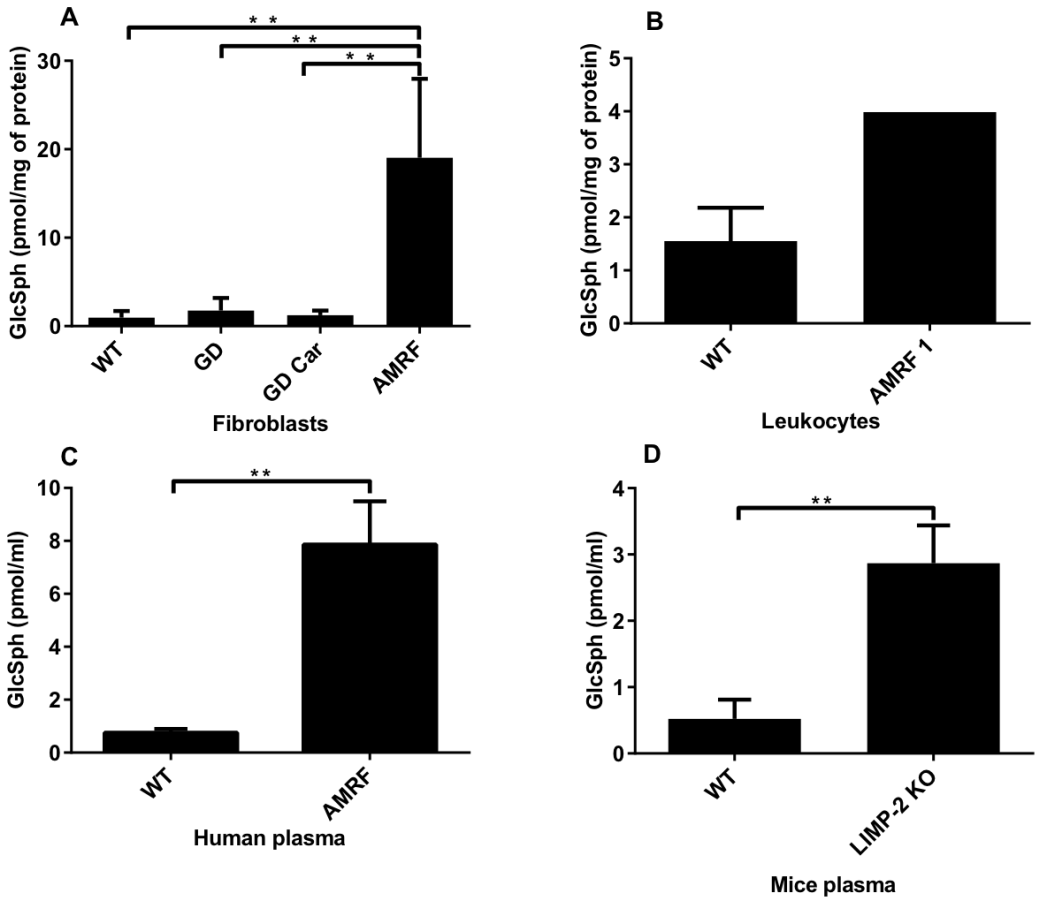

Figure 3.9 - GlcSph content of cells and plasma. Upper panels: GlcSph (pmol/mg total protein); Lower panel: GlcSph (pmol/ml); (A) Fibroblasts, (B) Leukocytes, (C) Human plasma and (D) Mice plasma. "WT" - Wild type; "AMRF" - AMRF patient (*SCARB2* W178X/W178X); "GD" - Gaucher patients; "GD car" - Carriers of mutations in the *GBA* gene; "*LIMP-2 KO" - LIMP-2 KO* mice.

3.5 Discussion

The intracellular sorting of GCase has been an enigma for a long time. It was clear that it is transported to the lysosomes independently of the M6PR system. The study by Reczeck and coworkers firstly revealed that the LIMP-2 mediates the trafficking of GCase [57]. Soon afterwards, Berkovic *et al.* and Balreira and colleagues [201, 210], demonstrated that LIMP-2 deficiency is the the basis of AMRF. Surprisingly, AMRF patients do not show lipid-laden macrophages, but present a cell-type specific GCase deficiency [201, 218]. In Gaucher patients, with a primary defect in GCase, macrophages are particularly sensitive to store GlcCer and form the so-called “Gaucher cells”. These cells produce and secrete unique marker proteins such as chitotriosidase and CCL18 [113]. In contrast, AMRF patients do not show elevated levels of chitotriosidase like Gaucher patients do. This suggests that macrophages in AMRF individuals degrade GlcCer and that GCase is correctly present in their lysosomes. This paradox may be explained by our present findings. Using ABPs we were able to examine very sensitively GCase in leukocytes. We noted that in white blood cells of AMRF individuals the levels of enzymatically active GCase are almost normal, in sharp contrast to fibroblasts.

Firstly, we showed that in homogenates of AMRF fibroblasts much less active GCase can be detected with ABP. In white blood cells and cultured macrophages this abnormality is far less striking. Next, we labelled intact cells with ABP and noted by FACS analysis that AMRF fibroblasts are markedly deficient in active GCase. Significant amount of active GCase was again detected in lymphocytes, monocytes and cultured macrophages. The same phenomenon was observed in an independent manner by exploiting PFB-FDG as substrate for *in vivo* detection of GCase enzymatic activity. Again, FACS analysis revealed a marked deficiency in AMRF fibroblasts, but considerable residual enzyme in white blood cell types. We then looked into the fate of GCase in fibroblasts of AMRF patients, observing that these cells abnormally secrete some active GCase to the medium where the enzyme rapidly loses its enzymatic activity. In freshly obtained plasma from AMRF patients, a labile GCase activity is demonstrable, either by measuring its activity or by using a different probe that allows labelling of GCase at higher pH, despite its inactivity. Apparently, another

mechanism can compensate in white blood cells, but not in fibroblasts, for the absence of LIMP-2 and mediate the trafficking of GCase to lysosomes. The most likely explanation is the presence of a receptor involved in this alternative sorting of GCase whose identity is not yet known and warrants further investigation. It also cannot be discarded the possible phenomenon in which secreted GCase might be taken up by an endocytic process and delivered via this secretion-recapture manner to lysosomes of white blood cells.

In lysosomes, assisted by the activator protein saposin C, GCase takes care of degradation of GlcCer. Deficiency of GCase causes formation of GlcCer storage tubules, most prominent in macrophages. Of interest, part of the accumulating GlcCer during GCase deficiency is deacylated into the sphingoid base GlcSph which can leave lysosomes and cells [117]. This explains the marked increase in GlcSph in plasma of Gaucher patients. Our investigation of GlcCer and GlcSph concentrations in cultured fibroblasts of AMRF patients revealed that only the sphingoid base GlcSph is markedly increased. In agreement, GlcSph is abnormally high in plasma of AMRF patients. This finding was also made with plasma specimens of *LIMP-2 KO* mice. Apparently, other cells in AMRF patients than macrophages can also form GlcSph during GCase deficiency, which is partly released into circulation. Our investigation renders a workflow suitable for laboratory diagnosis of AMRF, prior to sequencing of the *SCARB2* gene. If markedly increased plasma GlcSph is detected in an individual, in the absence of elevated chitotriosidase, this is an indication for AMRF. Measurement of GCase activity in white blood cells will not be very informative, but in fibroblasts enzymatic activity must be reduced to further consider the diagnosis of AMRF. Such diagnosis can be validated with the sequencing of the *SCARB2* gene. Demonstration of a cell-type specific functional GCase deficiency by detection of abnormally high GlcSph in plasma should be considered as an important step in the identification of individuals suffering from a truly functional deficiency in LIMP-2.

4. TISSUE AND CELL-TYPE DEPENDENT IMPACT OF SECONDARY GLUCOCEREBROSIDASE ABNORMALITIES DUE TO LIMP-2 DEFICIENCY

4.1 Abstract

Degradation of GlcCer in lysosomes is mediated by the enzyme GCase. Primary defects in this enzyme resulting from mutations in the *GBA* gene cause GD. Mutations in the *SCARB2* gene cause defects in the protein LIMP-2, which mediates transport of newly formed GCase to lysosomes. The corresponding disease, AMRF, differs clinically from GD. The marked phenotypic difference between GD and AMRF prompted us to study more closely the abnormalities in GCase and the functionally related lipid abnormalities in tissues of *LIMP-2 KO* mice. We first determined the proteome of isolated lysosomes from hepatocytes of wild type and *LIMP-2 KO* mice. No significant differences were noted in lysosomal matrix proteins, except for a major deficiency in GCase. Next, we analyzed the level of active GCase molecules in various tissues of *LIMP-2 KO* mice using recently developed ABP. Here, we report a gradient in deficiency of functional GCase along LIMP-2 deficient tissues. The GCase reductions are very prominent in organs like the liver, but more benign in others like brain and in leukocytes. The concentrations of GlcCer did not correlate with the extent of GCase deficiency. For example, GlcCer was normal in liver despite the severe GCase reduction. Another outspoken lipid abnormality in *LIMP-2 KO* mice is the elevation of GlcSph, which correlates with GCase deficiencies in tissues. Here, we also firstly document another metabolite abnormality in *LIMP-2 KO* mice, i.e. elevated levels of GlcChol. Experimentally we studied the potential cause for the considerable high residual GCase activity in LIMP-2 deficient leukocytes, sharply contrasting with the low residual GCase in fibroblasts. An explanation can be provided by our finding of considerable endocytotic re-uptake of enzyme by cultured lymphoblasts but not fibroblasts. In conclusion, among cell types and tissues of *LIMP-2 KO* mice, marked differences exist in the degree of deficiency of GCase and related lipid abnormalities. These findings may help to understand the remarkable difference in clinical and biochemical manifestation associated with primary GCase deficiency in Gaucher patients and that associated with secondary GCase deficiency in AMRF patients.

4.2 Introduction

Marked differences exist in the clinical picture of patients with GD suffering from primary defects in GCase, when compared to patients with bi-allelic mutations in the gene encoding LIMP-2. Gaucher patients largely develop a storage macrophage driven disease, characterized by hepatosplenomegaly, skeletal deterioration and pancytopenia [87]. On the other hand, mutations in *SCARB2* gene cause AMRF, a rare form of progressive myoclonic epilepsy (PME). It is associated with nephritic range of proteinuria, kidney failure, histological appearances of collapsing focal and segmental glomerular sclerosis (FSGS) and neurological symptoms including PME and ataxia with uncharacterized storage material in brain, but without cognitive decline [201, 210, 211, 218, 243]. While the majority of the initially reported AMRF patients had severe renal disease, a small group has subsequently been reported with disease restricted to the neurological system [211, 213, 217, 223].

To date, several *SCARB2* mutations have been identified in AMRF, as well as in some PME cases [201, 210, 211, 213, 215, 216, 222, 223, 244, 245]. The difference in clinical expression between GD and AMRF patients is surprising since LIMP-2 has been unequivocally shown to play an essential role in transport of newly formed GCase to lysosomes [57, 201, 210]. LIMP-2 belongs to the CD36 superfamily and it is among the most abundant proteins of the lysosomal membrane [33, 184, 246]. It is a type III membrane glycoprotein that transverses the membrane twice with a large luminal domain and a second membrane spanning domain preceding a 20 aa cytoplasmic tail at the C-terminal. A leucine-isoleucine motif within the C-terminal cytoplasmic tail of LIMP-2 determines its lysosomal localization [178, 195, 247]. In the endoplasmic reticulum the integral membrane protein LIMP-2 binds through its conserved coiled-coil domain (aa 152-167) to the correctly folded GCase [194]. The LIMP-2/GCase complex is next transported to acidic (pre)lysosomal compartments where dissociation occurs [58, 202].

Cell studies showed that absence of functional LIMP-2 has a devastating impact on the routing of GCase to lysosomes. Enzyme that manages to pass the

endoplasmic reticulum appears to be exclusively secreted to the extracellular space [248, 249]. In view of this, prominent lipid storage in macrophages of AMRF patients might have been expected, however clinical evidence for this is not observed [201, 218]. For example, circulating markers of lipid-laden macrophages, like chitotriosidase and CCL18, are markedly increased in Gaucher patients [89, 130], however this was not observed in the AMRF patients [201, 218].

The deficiency in active GCase molecules and its consequences at the lipid metabolite level remains to be studied in detail in the AMRF patients, largely due to the scarcity of patients for investigation. Fortunately, *LIMP-2 KO* mice have been generated by Saftig and co-workers [190], and shown to be a valid disease model with similar symptoms to those seen in AMRF and PME patients [190, 201, 210, 212, 213, 215, 216, 218, 224, 243, 250, 251]. These animals allow investigation on the biochemical impact of the absence of the lysosomal membrane protein LIMP-2. In this regard, attention for the lipid metabolites resulting from GCase activity is required. The deficiency of GCase in Gaucher patients is known to be not only restricted to the accumulation of GlcCer, but also by storage of GlcSph, which is markedly increased in tissue as well as plasma [89, 116, 117, 130].

Recently, GlcCer was also described as a glucose donor for the reaction catalyzed by GCase, which leads to the formation of cholesterol-glucoside (1-O-cholesteryl-β-D-glucopyranoside) (GlcChol) [252]. The occurrence of GlcChol and its potential abnormalities have not been studied so far in the context of LIMP-2 deficiency. Next, to the determination of lipid metabolites like GlcCer, GlcSph and GlcChol, the impact of LIMP-2 deficiency on GCase can be studied using recently developed ABP that specifically labels active GCase molecules through covalent binding to the catalytic nucleophile residue [131, 132, 134, 253].

Here, we report our investigation of functional deficiency of GCase in mice lacking LIMP-2 protein by the measurements of active GCase levels and abnormalities in lipids in various tissues in mice with increasing age. Marked cell-type and tissue specific differences in deficiency of functional GCase in the absence of LIMP-2 were observed. Strikingly, white blood cells present high residual levels of

GCase. We offer a possible explanation for this phenomenon based on the demonstration of compensatory endocytotic uptake of GCase by lymphocytes, but not fibroblasts, obtained from AMRF patients.

4.3 Methods

4.3.1 Animal studies

Breeding pairs of *LIMP-2 KO* mice were kindly provided by Prof. Paul Saftig (Kiel. Germany) [190]. Homozygous WT animals (LIMP-2 $^{+/+}$) and homozygous affected animals (LIMP-2 $^{-/-}$) were generated by crossing heterozygous (LIMP-2 $^{+/-}$) mice. Genotyping was determined by PCR using genomic DNA isolated from a small piece of the ear. Principles of laboratory animal care were followed, and approval for the study was obtained from the ethics committee of Academic Medical Center, Amsterdam, The Netherlands. A total of 45 animals were used, equally distributed in genotype (wild type; *LIMP-2 KO*), gender (male; female) and in age (2, 4, 6 and 12 months).

4.3.2 Tissue collection

Animals were first anesthetized with a dose of Hypnorm (0.315 mg/ml phenyl citrate and 10 mg/ml fluanisone) and Dormicum (5 mg/ml midazolam) according to their weight. The given dose was 80 µl/10 g body weight. Blood was collected by heart puncture into EDTA tubes and used for lipid measurements. Tissues and organs were collected by surgery and rinsed with PBS. Each one was sliced in half: one half was directly snap-frozen in liquid nitrogen and stored at -80 °C and the other half was conserved in 10% (v/v) formaldehyde for posterior pathology analysis. Bile was collected for 15 min via cannulation of the gall bladder. Urine was collected through aspiration of the bladder.

4.3.3 Bone marrow isolation

Bone marrow was extracted from the hind legs. The skin and flesh were removed in order to expose the tibia and femur. Both ends of the collected femur

were excised and bone marrow was removed by rinsing with ice cold PBS and the fluid was collected in a 50 ml tube. The cells in the aspirate were centrifuged for 10 min at 2.500 rpm (4 °C). The supernatant was discarded and the pellet was washed again. The pellet was taken up in 1 ml ice cold PBS, transferred to a 1.5 ml Eppendorf tube and centrifuged for 5 min at 13.200 rpm (4 °C). The supernatant was discarded and the pellet stored at -80 °C.

4.3.4 Plasma and leukocytes isolation

Blood collected in EDTA tubes was centrifuged for 10 min at 4.000 rpm. Plasma was collected in an Eppendorf tube and stored at -80 °C. The leukocyte layer was transferred to a 50 ml tube with 45 ml of erythrocyte lysis buffer (NH_4Cl/EDTA buffer, pH 7.4). After 20 min shaking in the cold room, on a roller mixer, the tube was centrifuged at 4 °C at 2.500 rpm for 10 min. The supernatant was discarded and 45 ml of lysis buffer was added. This procedure was repeated to remove all erythrocytes. The pellet was then resuspended in 1 ml ice cold PBS and transferred to a 1.5 ml Eppendorf tube and centrifuged for 5 min at 13.200 rpm (4 °C). The supernatant was discarded and the leukocyte pellet was stored at -80 °C.

4.3.5 Tissue homogenization

Homogenization procedures were performed with RNAse-free glass beads in 2 ml screwcap Eppendorf tubes. Twenty-five mM potassium phosphate buffer (pH 6.5), containing 0.1% (v/v) Triton X-100 and protease inhibitor cocktail (Roche) was added to tissue in a 1:5 ratio. Samples were homogenized with a Tissue Lyzer FastPrep (R)-24 M. P. Biomedicals (Irvine, CA, USA) set 6 ms^{-1} for 30 s. Homogenates were cooled for 1 min on ice between runs. Smaller tissues (eye, salivary gland, sciatic nerve, lymph node, epididymis and adrenal gland) were homogenized by sonication (40% power, 40% amplitude for 6 s) using the sonicator Vibra Cell$^{(TM)}$ Model no. CV18. Sonics (Danburry, CT, USA). These were similarly cooled. In the case of

leukocyte and bone marrow preparations, 100 µl of the same extraction buffer was added to the pellets and these were homogenized by sonication as described above. All homogenates were stored at -80 ºC.

4.3.6 Protein measurement with the Bicinchoninic acid (BCA™) assay

Protein content measurement was performed according to the manufacturer's protocol with Pierce™ BCA Protein Assay Kit (Pierce Biotechnology Inc., No. 23225), when necessary diluted with MilliQ water.

4.3.7 Lysosomes isolation (Tritosomes)

The lysosome enriched samples (tritosomes) were obtained from Dr. Markus Damme and Prof. Paul Saftig (University of Gottingen and University of Kiel, respectively). Briefly, mice were treated with a single injection of 0.75 mg of tyloxapol (Triton WR1339, Sigma) per g of body weight, 4 days prior to liver withdrawal. This treatment leads to the accumulation of the non-digestible Triton WR 1339 in lysosomes in the liver cells. Four days after the tyloxapol administration, animals were sacrificed and the livers collected. Cells were gently disrupted leaving lysosomes intact. The density of tyloxapol-laden lysosomes (named tritosomes) is below 1 g/mL, facilitating their separation from other cell organelles. The isolation of tritosomes from tyloxapol-treated mice included differential centrifugation and isopycnic centrifugation and resulted in a lysosome enriched fraction as described earlier [1, 254, 255].

4.3.8 LC-MS/MS proteomics

Tritosomes for LC-MS/MS were prepared using Rapigest detergent (Waters Corporation) and tryptic fragments were analyzed by label free data independent LC-MS/MS as previously described [256].

4.3.9 *In vitro* activity-based probe labelling of glucocerebrosidase

Homogenate (50 µg total protein) was incubated with 100 nM cyclophellitol-epoxide type activity based probe with a red BODIPY-containing fluorophore MDW941, the so-called Inhibody Red [131]. The incubation of tissue homogenate with MDW941 was performed in 150 mM McIlvaine buffer (150 mM citrate-Na_2HPO_4, pH 5.2, with 0.2% (w/v) sodium taurocholate and 0.1% Triton X-100) supplemented with protease inhibitor cocktail (Roche) for 45 min at 37 °C. Subsequently, protein was denatured with 5x Laemmli buffer (50 % (v/v) 1 M Tris-HCl, pH 6.8, 50% (v/v) glycerol, 10% (w/v) DTT, 10% (w/v) SDS, 0.01% (w/v) bromophenol blue) by boiling for 10 min at 100 ºC. and separated by electrophoresis on 10% (w/v) acrylamide SDS-PAGE gels running at 90 V [131, 133]. Wet slab gels were scanned for red fluorescence using a Typhoon variable mode imager (Amersham Bioscience) using λ_{ex} 532 nm and λ_{em} 610 nm (band pass filter 30nm). ABP-emitted fluorescence was quantified using ImageJ software (NiH). Gels were electroblotted onto a nitrocellulose membrane (Schleicher&Schuell®) and the protein bands detected with Ponceau S staining.

4.3.10 Enzymatic assays

Enzymatic assays were performed according to Aerts et al [242]. GCase activity was measured with 3.73 mM 4-MU-β-D-Glc, dissolved in 150 mM McIlvaine buffer (pH 5.2) supplemented with 0.2% (w/v) sodium taurocholate, 0.1% (v/v) Triton X-100) and 0.1% BSA. After stopping the reaction with NaOH-glycine (pH 10.3), fluorescence was measured with a fluorimeter LS55 (Perkin-Elmer, Beaconsfield, UK) at λ_{ex} 366 nm and λ_{ex} 445 nm.

4.3.11 HPLC and MS/ MS lipid measurements

Neutral glycosphingolipids, lysoGb3, GlcSph and GlcChol were determined in the homogenates as described earlier [117, 241, 257, 258]. An internal standard mix

($^{13}C_5$-Lyso-Gb3. $^{13}C_5$-GlcSph and $^{13}C_6$-GlcChol) was added to the samples for calculation. After protein precipitation with $CHCl_3$:MeOH 1:1 (v:v), one step of extraction and two washing steps were carried out, always with the ratio $CHCl_3$:MeOH:H_20 1:1:0.9 (v:v:v). With this procedure, lysoGb3 and GlcSph are in the hydrophilic phase (upper phase), and GlcChol and neutral lipids will be in the hydrophobic phase (lower phase). The upper phase was dried under N_2 gas stream and the pellet redissolved in MeOH (LysoGb3 and GlcSph). The lower phase was halved. One half, for GlcChol measurement, was dried under a N_2 gas stream and the pellet redissolved in solution A (100% MeOH, 10 mM ammonium formate). Lipids were measured using an Acquity TQD (Waters Inc.). For determination of neutral glycosphingolipids, a known amount of internal standard (C_{17}-Sphinganine) was added to the sample and then deacylated with 0.1 M NaOH in MeOH in a microwave for 1 h at 60 ºC. Neutral lipids were next analyzed using a Dionex HPLC system with a C18 reversed-phase chromatography and automated derivatisation with fluorescent o-phthaldialdehyde (OPA). The fluorescent derivatized structures derived from glycosphingolipids were quantitatively detected by measurement of fluorescence at λ_{ex} 340 nm and λ_{ex} 435 nm. Quantification of GlcCer in brain and sciatic nerves required an optimized protocol given the abundant presence of interfering galactosylceramide in these materials. After total lipid extraction by modified Folch extraction [259], neutral lipids glycosphingolipids (ceramides and phospholipids) were separated by solid phase extraction (SPE) using a silica gel (SiOH) SPE column. After deacylation with sphingolipid ceramide N-deacylase (SCDase, Takara Bio Inc., Japan), GlcCer was digested with recombinant GCase (Imiglucerase, Genzyme). The subsequent increase in ceramide levels after digestion, measured as described above, was assumed as derived from GlcCer degradation.

4.3.12 Lymphocyte immortalization

Materials from donors and patients were obtained after informed consent. B95–8 culture supernatants containing the transforming strain of Epstein-Barr virus

(EBV) were used to establish a lymphoblastoid cell lines *in vitro* as described earlier [260]. Briefly, leukocytes from healthy donors and from two LIMP-2 deficient patients homozygous for the *SCARB2* mutation W178X [201] were isolated by sedimentation on Ficoll-Hypaque density gradients. Mononuclear cells were resuspended in RPMI 1640 medium containing 10% fetal calf serum and viral supernatants (10^7 mononuclear cells/ml) and incubated for 2 h at 37 °C. Cultures were maintained in 25 cm^2 tissue culture flask for 3 weeks containing 1 µg/ml cyclosporin A. The cells were washed twice with PBS and then cultured in RPMI 1640 medium containing 10% fetal calf serum and 5% (v/v) Pen/Strep (Life Technologies).

4.3.13 Generation of lentivirus particles and infection

Recombinant lentivirus particles encoding shRNAs targeting *SCARB2* were produced, concentrated and titrated as described previously [261]. Cultured THP-1 were infected with recombinant lentivirus particles for 24 h in 400 ml of RPMI 1640 medium containing 10% fetal calf serum and 5% Pen/Strep. In the next day, 400 ml RPMI 1640 medium containing 10% fetal calf serum and 5% Pen/Strep were added. After 48 h, the cells were carefully washed and cultured for another 48 h, to be finally harvested. Transduction efficiency was determined by western-blot and qRT-PCR.

4.3.14 RNA extraction and quantitative RT-PCR

Total RNA was harvested from cells using the Total RNA mini kit (Bio-Rad) or Trizol reagent (Invitrogen) according to the manufacturer's instructions. cDNA was made using the iScript cDNA synthesis kit (Bio-Rad). Real-time reverse transcription PCR was performed using the MyIQ system (Bio-Rad) and the primer LIMP-2 forward 5′-TTGGCCCTCTGGACATTATC-3′ and the LIMP-2 reverse 5′-AGAACCGCATGAAGTGAACC-3′. Acidic ribosomal phosphoprotein P0 was determined as an internal control for cDNA content of the samples with the primer P0

forward 5′-TCGACAATGGCAGCATCTAC-3′ and P0 reverse 5′-ATCCGTCTCCACAGACAAGG-3′.

4.3.15 Western-Blotting

Homogenates containing 20 µg of total protein were denatured with 5x Laemmli buffer (50% (v/v) 1 M Tris-HCl, pH 6.8, 50% (v/v) glycerol, 10% (w/v) DTT 10% (w/v) SDS and 0.01% (w/v) bromophenol blue) by boiling for 10 min at 100 ºC, and separated by electrophoresis on 10% acrylamide (w/v) SDS-PAGE gels running at 90 V [131, 133]. SDS–PAGE gels were electroblotted onto a nitrocellulose membrane (Schleicher&Schuell®). Membranes were blocked with 5% skimmed milk and 0.05% Tween-20 in TBS for 1 h at room temperature and incubated overnight with the rabbit polyclonal anti-LIMP-2 antibody (NB400-129, Novus Biologicals) at 4 °C. Membranes were then washed three times with 0.01% Tween-20 in TBS and incubated with the appropriate IRDye conjugated secondary antibody for 1 h at room temperature. After washing, detection was performed using the Odyssey® Clx. Infrared Imaging System (LI-COR).

4.3.16 Inhibition of endocytosis

Immortalized lymphocytes and THP-1 cells were seeded at $1x10^6$ cells/well in 6-well plates containing 1 mL of medium RPMI 1640 with 5% Pen/Strep. Fibroblasts were obtained from skin biopsies of control subjects and AMRF patients after informed consent. The patients' cells were homozygous for the *SCARB2* mutation W178X [201]. Fibroblasts were cultured in Dulbecco's modified Eagle's medium supplemented with 10% fetal bovine serum, 2 mM L-glutamine, 1% Pen/Strep, 100 mg/ml kanamycin sulfate and 2.5 mg/ml fungizone (Gibco, Invitrogen). Fibroblasts were cultured in 6-well plates almost to confluency. Next, the medium was changed to 1 ml of Dulbecco's modified Eagle's medium supplemented with 1% penicillin–streptomycin (Gibco, Invitrogen). A pre-dilution of Dynasore to 160 µM was made in

RPMI 1640 or Dulbecco's modified Eagle's medium containing 5% Pen/Strep. One ml of this solution was added to cells to achieve a final concentration of 80 μM. After 8 h of incubation, the cells were washed with PBS and collected. Treatment of cells with mannan at a concentration of 1 mg/ml was performed overnight. Cells were disrupted by sonication (40% power, 40% amplitude for 6 s) in the sonicator Vibra Cell (TM) Model no. CV18. Sonics (Danburry, CT, USA).

4.3.17 *In vitro* activity-based probe labelling of glucocerebrosidase in THP-1

THP-1 homogenates (20 μg total protein) were incubated with 100 nM Inhibody-Red MDW941 [131] in 150 mM McIlvaine buffer (pH 5.2, with 0.2% (w/v) sodium taurocholate, 0.1% Triton X-100) and protease inhibitor cocktail (Roche) for 30 min at 37 °C. Subsequently, protein was denatured with 5x Laemmli buffer (50% (v/v) 1 M Tris-HCl, pH 6.8. 50% (v/v) glycerol, 10% (w/v) DTT, 10% (w/v) SDS, 0.01% (w/v) bromophenol blue) by boiling for 10 min at 100 ºC and separated by electrophoresis on 10 % acrylamide (w/v) SDS-PAGE gels running at 90 V [131, 133]. Wet slab gels were scanned for red fluorescence using a Typhoon variable mode imager (Amersham Bioscience) using λ_{ex} 532 nm and λ_{em} 610 nm (band pass filter 30nm). ABP emitted fluorescence was quantified using ImageJ software (NiH). Gels were electroblotted onto a nitrocellulose membrane (Schleicher&Schuell®) and the proteins bands were detected with Ponceau S staining.

4.4 Results

4.4.1 Impact of LIMP-2 deficiency on the protein composition of lysosomes.

Presently, it is unknown whether lack of LIMP-2 also impairs other lysosomal proteins besides GCase. To address this, we analyzed the protein composition of isolated lysosomes from mice treated with non digestible Triton WR1339, so-called tritosomes**.**

We employed non labelled quantitative proteomics using LC-MS^{e} as described earlier [256]. No significant differences in any of the lysosomal proteins other than GCase were noted, when comparing the protein composition of tritosomes isolated from wild type and *LIMP-2 KO* mice (Table S4.1. supplemental data). Around 70 lysosomal matrix proteins were identified and quantified. Table 4.1 shows that sphingomyelinase and lysosomal acid lipase tended to be about two fold decrease in tritosomes from *LIMP-2 KO* mice. About two-fold increase was noted for Cathepsin H and N-acetylglucosamine 6 sulfatase. In cases like α–galactosidase, the amount of protein was at the level of detection, not being detectable in some samples and making the data not interpretable. Importantly, both GCase and LIMP-2 protein were found to be absent in tritosomes from *LIMP-2 KO* mice.

This finding indicates that LIMP-2 deficiency results in a very specific deficiency in GCase and does not affect other lysosomal proteins, at least in the studied hepatocytes.

Table 4.1 – Examples of proteins in tritosomes from *LIMP-2 KO* mice that were changed in comparison to wild type.

Nº	Protein Name	Accesion No.	Description	Ratio
30	LICH_MOUSE	Q9Z0M5	Lysosomal acid lipase cholesteryl ester hydrolase OS Mus musculus GN Lipa PE 2 SV 2	0.44
32	ASM_MOUSE	Q04519	Sphingomyelin phosphodiesterase OS Mus musculus GN Smpd1 PE 2 SV 2	0.59
65	E9Q2Q0_MOUSE	E9Q2Q0	Uncharacterized protein OS Mus musculus GN Ctsc PE 3 SV 1	0.59
66	F7AF87_MOUSE	F7AF87	Uncharacterized protein Fragment OS Mus musculus GN Glb1 PE 4 SV 1	0.60
61	D3Z437_MOUSE	D3Z437	Uncharacterized protein OS Mus musculus GN Ctsh PE 4 SV 1	2.14
33	GALNS_MOUSE	Q571E4	N-acetylgalactosamine 6 sulfatase OS Mus musculus GN Galns PE 2 SV 2	2.16

4.4.2 Analysis of pathology

Disease manifestation is relatively benign in *LIMP-2 KO* mice. As shown in Fig. S4.1 (supplemental data), despite the clear absence of lysosomal GCase in hepatocytes, no abnormalities in the liver are observed. Actually, no overt pathology was detected by an experienced pathologist in any organs of mice of 6 and 12 months of age with the exception of signs of nephrohydrosis in the absence of clear abnormalities in the glomerulus. Of interest, a markedly thickness of sciatic nerve without apparent phenotypic consequences was observed in Fig. S4.2 (supplemental data).

4.4.3 Levels of active glucocerebrosidase in tissues by enzymatic activity measurement

Various tissues were collected from *LIMP-2 KO* and wild type mice of 4 months of age. In tissue homogenates, GCase activity was measured with the fluorogenic substrate 4-MU-β-D-Glc, (Table 4.2). Very little activity was detected for many of the tissues analyzed (eye, pancreas, heart, spleen, liver and lungs) when compared to wild type. In the case of the intestine (divided in duodenum, ileum and jejunum), no

clear differences were observed in the enzymatic activity between the genotypes, probably due to the abundance of bacterial glycosidases as well as endogenous lactase phloridzin hydrolase (LPH) which also hydrolyzes the artificial substrate [262, 263]. Of interest, in the case of the sciatic nerve, leukocytes, brain and skin, no major reduction of GCase activity was found in *LIMP-2 KO* mice. Of note, plasma from wild type animals contains virtually no GCase activity, but it is detectable in plasma of *LIMP-2 KO* mice, likely due to faulty secretion of the mistargeted enzyme.

Table 4.2 - GCase activity (nmol/h/mg protein or ml) in several tissues obtained from *LIMP-2 KO* mice and matched wild type animals of 4 months of age.

Tissue	**GCase activity**	
Genotype	**Wild type**	***LIMP-2 KO***
Duodenum	728.58 ± 262.33	463.51 ± 54.80
Jejunum	660.35 ± 167.74	812.48 ± 23.79
Liver	142.05 ± 31.02	22.65 ± 11.43
Ileum	114.95 ± 20.20	78.20 ± 51.22
Testis (TE)	103.23 ± 10.02	39.85 ± 3.32
Thymus	98.06 ± 35.16	27.23 ± 9.45
Abdominal fat (AF)	96.79 ± 33.68	16.44 ± 3.79
Bone Marrow (BM)	96.34± 7.65	21.09± 1.06
Pancreas	94.77 ± 20.09	9.81 ± 2.20
Omental fat (OF)	93.13 ± 22.63	16.16 ± 2.47
Epidydimal fat (EF	90.02 ± 35.69	16.96 ± 3.96
Epidydimis (EP)	88.01 ± 26.59	45.33 ± 32.51
Inguinal fat (IF)	79.57 ± 24.69	10.81 ± 6.32
Lymph node (LN)	62.88 ± 2.21	20.59 ± 1.93
Spleen	60.30 ± 13.20	10.79 ± 2.52
Adrenal gland (AG)	58.00 ± 3.82	18.64 ± 0.35
Lungs	57.36 ± 12.87	9.59 ± 0.83
Salivary gland (SG)	55.97 ± 10.60	16.27 ± 1.52
Brain	54.20 ± 0.69	32.14 ± 2.74
Brown adipose tissue (BAT)	48.92 ± 1.35	11.41 ± 4.02
Leukocytes (PBMC)	46.78± 2.98	31.73± 1.47
Kidney	34.94 ± 4.11	9.76 ± 0.51
Skin	33.39 ± 4.24	18.75 ± 2.03
Heart	29.32 ± 6.03	3.95 ± 1.29
Sciatic nerve (SN)	23.97 ± 0.46	22.36 ± 12.78
Eye	4.65 ± 2.05	0.85 ± 0.28
Plasma	0.78 ± 0.0	8.48 ± 1.59

4.4.4 Detection of active glucocerebrosidase molecules in tissues by activity-based probes labelling.

Tissues were collected from *LIMP-2 KO* and wild type mice of 4 months of age. The following abbreviations are used hereafter: IF (Inguinal fat), AF (Abdominal fat), OF (Omental fat), EF (Epididymal fat), BM (Bone marrow), BAT (Brown adipose tissue), SG (Salivary gland), AG (Adrenal gland), LN (Lymph node), TE (Testis) and SN (Sciatic nerve).

Tissue homogenates were incubated with ABP MDW941 to detect active GCase following SDS-PAGE and fluorescence scanning (Fig. 4.1). Most tissues of *LIMP-2 KO* mice showed absence or a strongly reduced amount of active GCase, when compared to the controls. Only a few tissues of *LIMP-2 KO* mice, such as the brain and the leukocytes, showed considerable amounts of labelled GCase, although less than the corresponding wild type material.

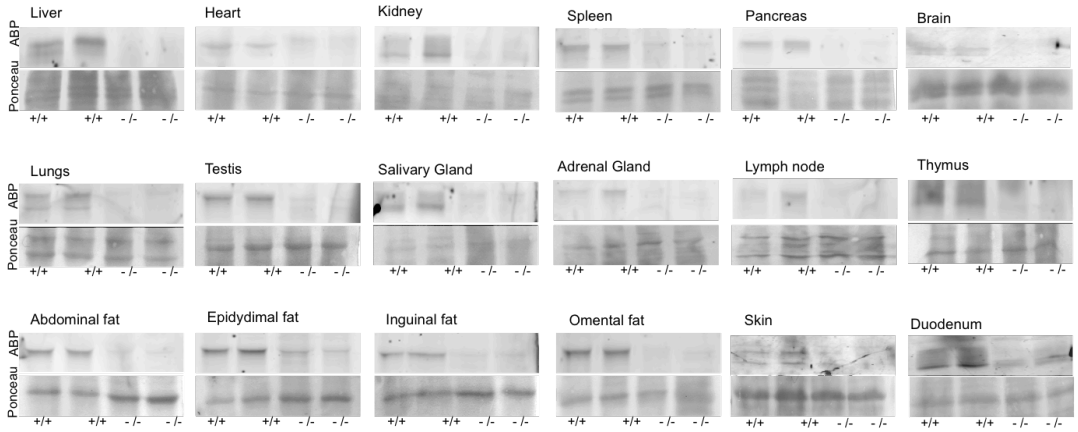

Figure 4.1 - Visualization of GCase with fluorescent ABP MDW941. Detection of active GCase in tissues and organs homogenates (50 µg) labelled with ABP followed by SDS-PAGE and visualization by fluorescence imaging. (+/+) - Wild type; (-/-) - *LIMP-2 KO* mice.

Quantification of labelled GCase molecules and comparison with measured residual enzyme activity in tissue homogenates showed a good correlation. In Fig. 4.2, tissues are ranked based on the residual enzyme activity measured *in vitro* (Fig. 4.2A) and a comparison is provided for the residual GCase activity determined by enzymatic assay and ABP labelling (Fig. 4.2B). A very strong correlation between the

results obtained with both methods is apparent. Figure 4.2 illustrates the marked tissue dependence of deficiency of GCase in LIMP-2 deficiency. Of note, high residual GCase was detected for brain, leukocytes and SN when determined either by enzymatic assay and ABP labelling.

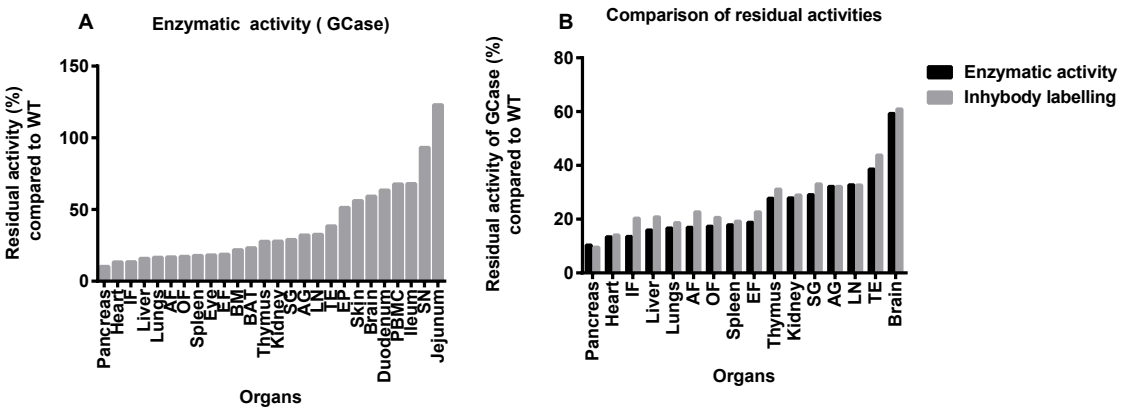

Figure 4.2 – Residual GCase activity in *LIMP-2 KO* mice. A - Ranking of the homogenates according to the residual enzymatic activity. B - Comparison of residual GCase activity determined as by enzymatic assay and ABP labelling.

4.4.5 Detection of lipid metabolite abnormalities in *LIMP-2 KO* mice.

To assess the functional deficiency of GCase, we analyzed lipid metabolites in various tissues of *LIMP-2 KO* mice. Given the fact that GlcCer is the primary storage lipid during GCase deficiency, we first determined its concentration in various tissues of *LIMP-2 KO* and wild type animals. Table 4.3 shows that GlcCer concentrations vary among tissues and that it is most prominently elevated in PBMC, OF, AF and LN of *LIMP-2 KO* mice. Of note, the presented values for GlcCer in brain and SN are suboptimal given the interference of the abundant isomer galactosylceramide in the GlcCer determination [80, 81].

Table 4.3 – GlcCer levels (nmol/wet weight tissue or mg protein or ml) in several tissues and organs of *LIMP-2 KO* and wild type mice. Lipid level for plasma bile and urine is presented as nmol/ml. Right column - Fold increase in *LIMP-2 KO* mice compared to wild type. "*" - (Gly)cosylceramide = galactosylceramide plus GlcCer.

Tissue/ Organ	**GlcCer levels**		**Fold of increase in the LIMP-2 deficiency**
Genotype	**Wild type**	***LIMP-2 KO***	
Pancreas	9.55±4.3	15.38±1.9	1.61
Heart	4.18±2.6	2.99±0.4	0.72
IF	8.15±6.3	27.48±11.9	3.37
Liver	22.18±13.3	23.43±13.0	1.06
Lungs	30.52±9.5	42.55±14.8	1.39
AF	8.75±5.1	57.70±29.3	6.59
OF	3.39±1.5	14.76±4.4	4.35
Spleen	75.04±8.0	73.77±6.6	0.98
Eye	571.77±179.1	171.03±107.2	0.30
EF	3.50±2.0	3.95±0.4	1.13
BM	0.49±0.3	0.73±0.4	1.49
BAT	32.57±15.2	41.16±10.2	1.26
Thymus	70.54±13.6	70.95±15.4	1.01
Kidney	17.86±4.5	7.80±10.2	0.44
SG	22.62±8.6	41.44±9.6	1.83
AG	33.18±12.4	53.36±26.2	1.61
LN	40.02±20.2	97.47±28.5	2.44
TE	13.42±2.5	13.32±6.0	0.99
EP	13.31±6.7	14.00±5.9	1.05
Skin	23.34±5.1	23.71±14.2	1.02
Brain*	3067.43±837.8	3248.91±473.7	1.06
Duodenum	64.33±7.1	68.37±9.0	1.06
PBMC	0.10±0.1	0.73±0.8	7.30
Ileum	25.10±3.8	28.08±5.5	1.12
SN*	10493.84	4898.21±1016.1	0.47
Jejunum	41.35±9.2	47.93±11.2	1.16
Plasma	3.17±0.9	1.80±1.1	0.57
Bile	4.78±5.7	2.07±0.8	0.43
Urine	0.26±0.1	0.19±0.1	0.73

Next, we determined the concentrations of GlcSph, the deacylated form of GlcCer, known to be prominently increased in GD. Much clearer abnormalities were detected for GlcSph, being increased in almost every tissue, most strikingly in pancreas, heart and OF (Table 4.4). A trend can be noted between GlcSph accumulation and residual GCase activity in tissues. Exceptions in this regard are OF, kidney, SG, LN and the different parts of the intestine.

To establish if other catabolic pathways are also affected in the LIMP-2 deficiency, the globoside Gb3 and its deacylated form, lysoGb3, were also measured. No significant increase in these lipids was detected (Fig. S4.3 and S4.4, in supplemental data). Interestingly, the levels of these lipids in spleen, thymus and testis were about half of those in wild type materials (Fig. S4.3 and S4.4, in supplemental data). The concentrations of GlcChol in tissues of *LIMP-2 KO* and wild type mice are presented separately. Very recently, an accurate LC-MS/MS for quantification of GlcChol was developed, employing an isotope $^{13}C_6$-labelled internal standard (Marques *et al.*, unpublished results). The presence of GlcChol in various tissues was demonstrable (Fig. 4.3). The lipid was found to be increased in most tissues, most clearly in adipose tissues (IF, AF, OF and BAT) (Fig. 4.3).

Table 4.4 – GlcSph levels (pmol/wet weight tissue or mg protein or ml) in several tissues and organs of *LIMP-2 KO* and wild type mice. Lipid level for plasma bile and urine is presented as nmol/ml. Right column - Fold increase in *LIMP-2 KO* mice compared to wild type. "*" - (Gly)cosylsphingosine.

Tissue	**GlcSph levels**		**Fold of increase in the LIMP-2**
Genotype	**Wild type**	***LIMP-2 KO***	
Pancreas	2.33±0.7	178.35±24.1	76.55
Heart	3.33±1.0	86.70±20.5	26.04
IF	3.00±0.9	31.93±17.5	10.64
Liver	32.06±2.6	214.91±157.9	6.70
Lungs	34.86±8.0	738.37±285.0	21.18
AF	1.94±0.7	40.50±35.7	20.88
OF	0.97±0.7	128.44±41.0	132.41
Spleen	20.65±2.3	399.98±143.7	19.37
Eye	62.92±5.7	892.64±189.7	14.19
EF	4.23±1.9	11.04±0.2	2.61
BM	0.20±0.1	2.01±0.8	10.05
BAT	4.07±1.7	49.67±38.8	12.20
Thymus	13.44±2.4	85.63±23.1	6.37
Kidney	25.82±0.7	557.45±115.4	21.59
SG	4.97±1.6	95.17±37.4	19.15
AG	7.04±5.1	75.69±65.1	10.75
LN	4.97±4.3	95.56±69.0	19.23
TE	5.18±1.8	24.69±4,68	4.77
EP	29.42±4.3	233.17±112.1	7.93
Skin	9.26±4.9	29.62±13.6	3.20
Brain*	112.80±5.8	230.53±14.5	2.04
Duodenum	8.79±3.8	139.00±26.5	15.81
PBMC	0.30±0.3	1.67±0.3	5.57
Ileum	9.31±1.3	180.50±22.9	19.39
SN*	1111.88±651.5	860.89±543.6	0.77
Jejunum	8.16±1.6	140.69±15.3	17.24
Plasma	1.14±1.3	3.57±1.7	3.13
Bile	1.39±0.5	6.31±2.2	4.54
Urine	0.65±1.2	0.36±0.2	0.55

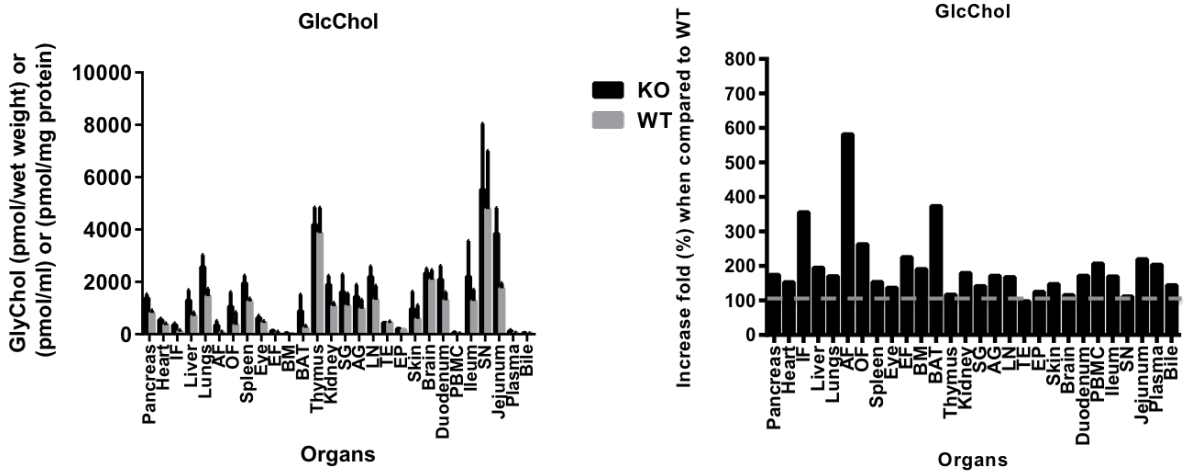

Figure 4.3 – GlcChol measured in the several homogenates from the *LIMP-2 KO* and wild type mice. Left panel - Absolute amounts; Right panel - Relative amount of increase when compared to wild type. Dashed line marks the normal values obtained in wild type mice.

4.4.6 Biochemical course of disease

Given the detected abnormalities in lipid metabolites in tissues of *LIMP-2 KO* mice of 4 months of age, we next studied how these abnormalities develop with age in several tissues. GlcCer changes were very small in all tissues from *LIMP-2 KO* mice when examined at various ages (Fig. 4.4). Only a very slight increase was noticed for the kidney and salivary gland at older age. In the case of the eye of *LIMP-2 KO* mice, a significant reduction of GlcCer was observed. In sharp contrast, GlcSph elevation was already detectable in animals of 2 months of age and generally did not further increase with age (Fig. 4.5). Only in the case of the thymus, IF, OF and the eye of *LIMP-2 KO* mice, the levels of GlcSph increased with age. The concentrations of globosides Gb3 and lysoGb3 were also determined in various tissues with increasing age. No differences in the wild type animals were detected, except for reduced levels in spleen (Fig. S4.5 and S4.6, in supplemental data).

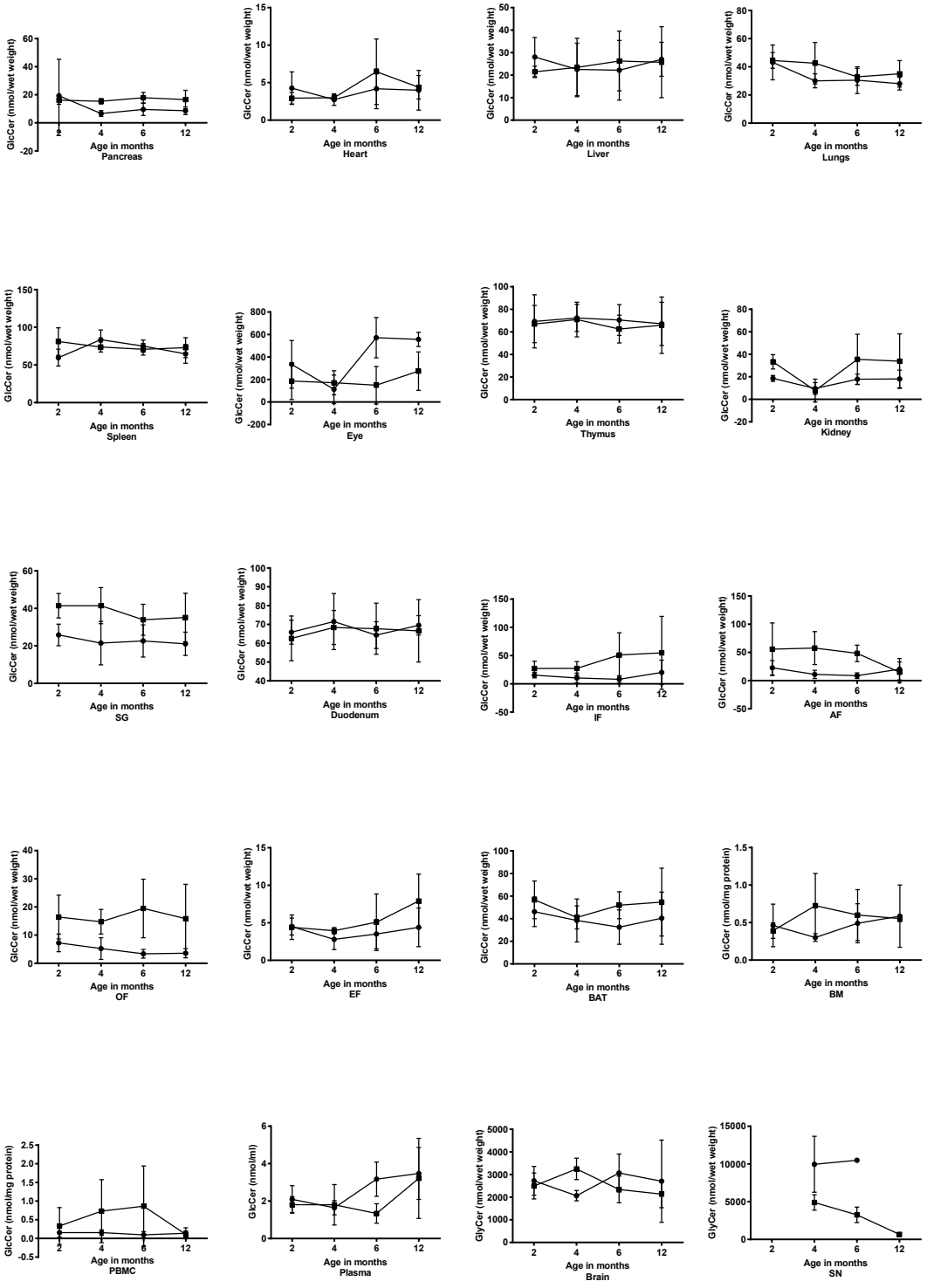

Figure 4.4– GlcCer levels in wild type and *LIMP-2 KO* mice at different ages. Black circle - wild type; Black square - *LIMP-2 KO* mice.

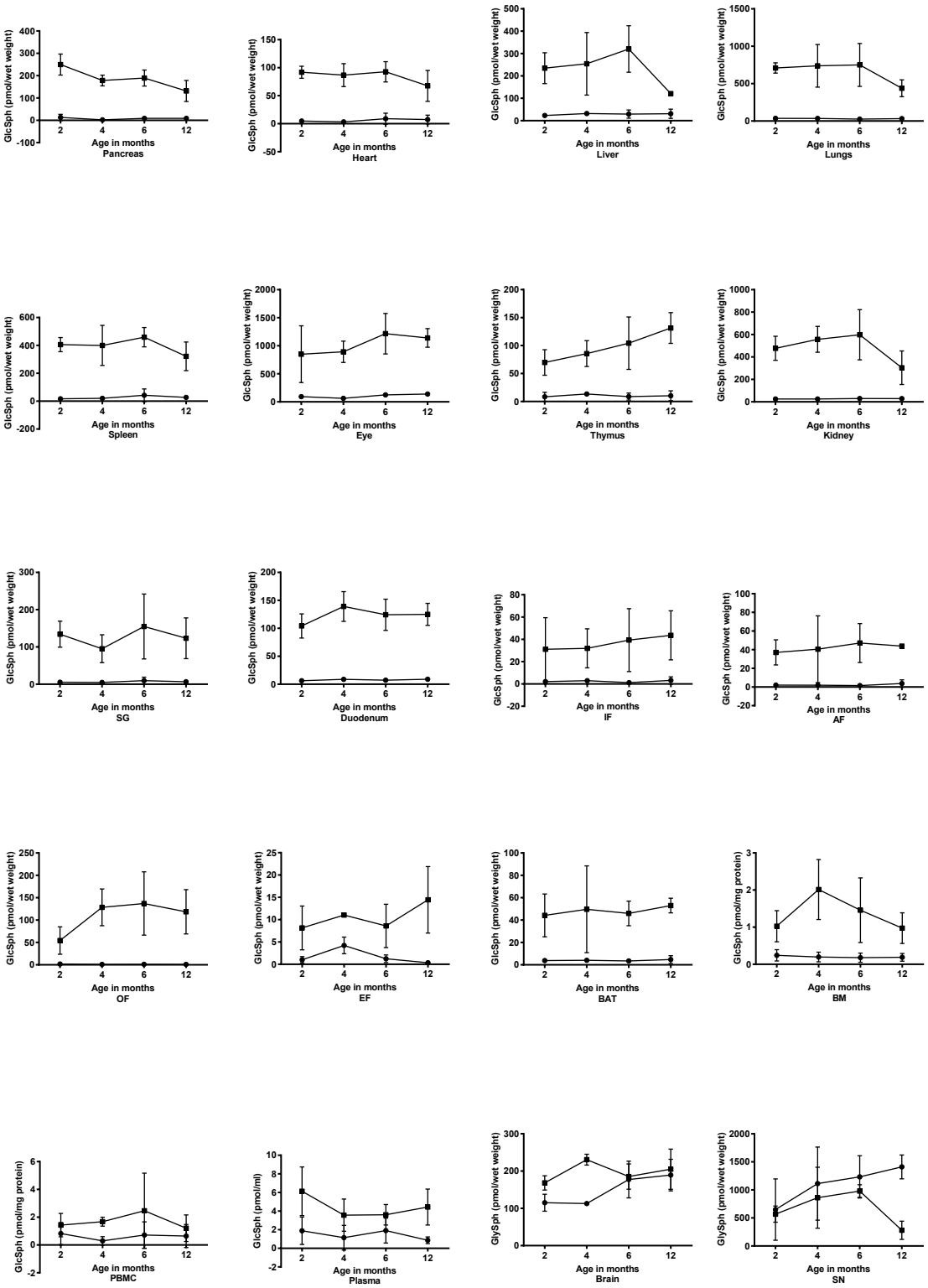

Figure 4.5 – GlcSph levels in wild type and *LIMP-2 KO* mice at different ages. Black circle - wild type; Black square - *LIMP-2 KO* mice.

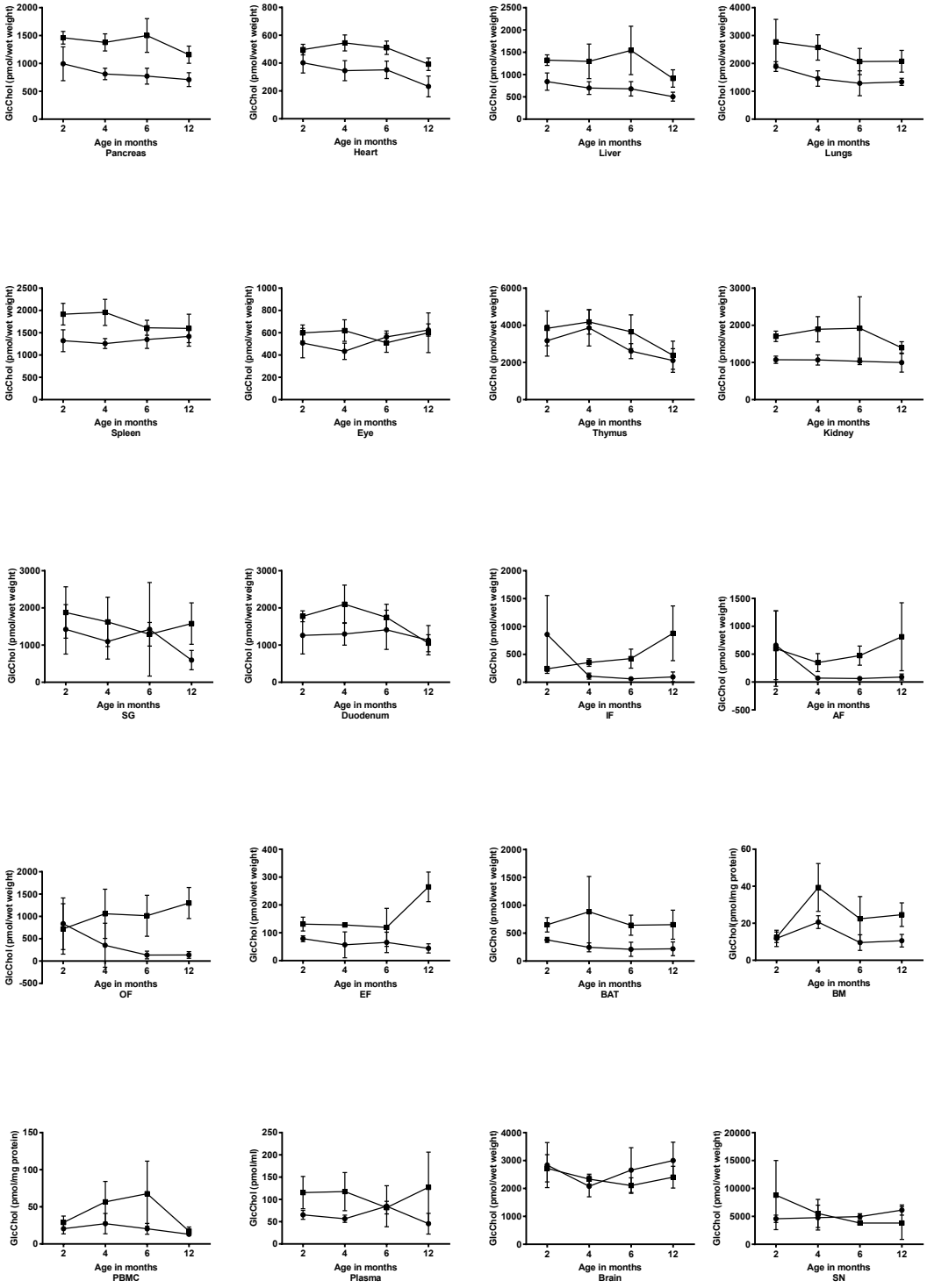

Figure 4.6 – GlcChol levels in wild type and *LIMP-2 KO* mice at different ages. Black circle - wild type; Black square - *LIMP-2 KO* mice.

Determination of GlcChol in tissues from *LIMP-2 KO* mice revealed that the glucosylated sterol was already increased at the youngest age examined (2 months). In none of the tissues a marked accumulation of GlcChol with increasing age was observed (Fig. 4.6).

4.4.7 Lipids in brain and sciatic nerve

In most tissues GlcCer concentrations are known to be far higher than those of galactosylceramide. However in brain and nerves, galactosylceramide is abundant. The same holds for the sphingosine forms of these monoglycosylceramides. Our LC-MS/MS procedure does not discriminate between GlcCer and galactosyceramide or between GlcSph and galactosylsphingosine. In the case of the brain of *LIMP-2 KO* mice, we observed no differences in the levels of (gly)ceramide and (gly)sphingosine. (see Fig. 4.4 and 4.5, respectively). In the case of the SN, (gly)ceramide was significantly reduced and less prominently (gly)sphingosine. Treatment of brain and SN homogenates with excess recombinant GCase allows the discrimination between GlcCer and galactosylceramide since the recombinant enzyme only degrades GlcCer. In the brain, almost no differences between wild type and *LIMP-2 KO* mice were observed, at any age analyzed, in the total (gly)ceramide (GlcCer+ galactosylceramide) (Fig. 4.4). Treatment with recombinant GCase reveals that the GlcCer content of brain from *LIMP-2 KO* mice is normal (Fig. 4.7). Only a small decrease in galactosylceramide is demonstrable. In the SN, clear abnormalities in (gly)ceramide are detected, in particular a prominent reduction in galactosylceramide is apparent with increasing age. Already at young age the concentration of ceramide is elevated in the SN, reaching a maximum at 4 months and being reduced after that.

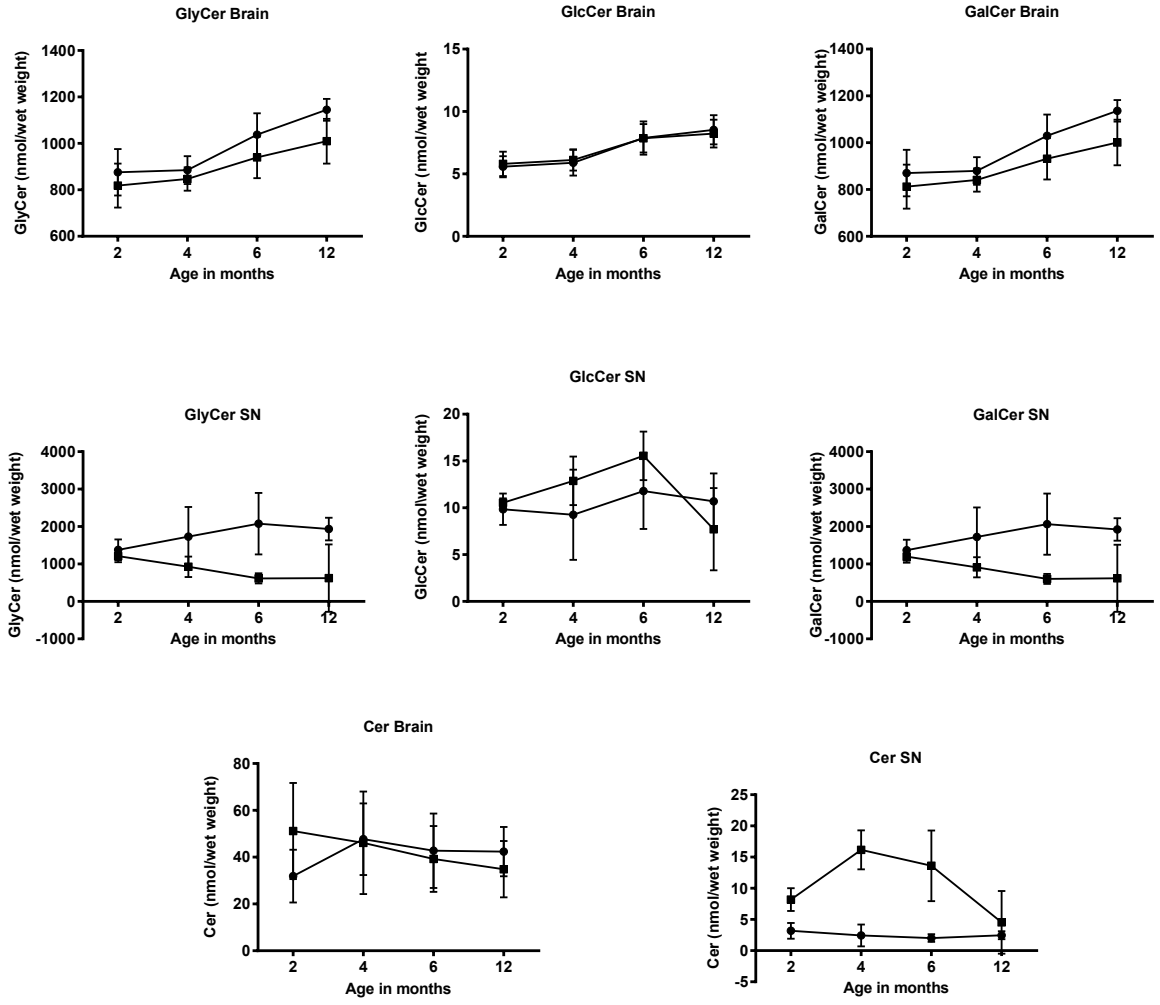

Figure 4.7 – Glycosphingolipids and ceramide levels in brain and SN, before and after the treatment with recombinant GCase.

4.4.8 Secretion and re-capture of glucocerebrosidase

The mechanism by which GCase reaches lysosomes in the absence of LIMP-2 is unknown. One of the cell types in AMRF patients and *LIMP-2 KO* mice with high residual GCase activity are the leukocytes. To generate AMRF-like leukocytes, THP-1 cells were infected with lentiviral *SCARB2* shRNA. The reduced expression of *SCARB2* (qPCR and Western Blot) and the accompanying GCase activity were determined (Fig. S4.7, in supplemental data). Immortalized AMRF lymphocytes,

fibroblasts, AMRF-like THP-1 cells and the corresponding control cells were cultured in the presence of a potent inhibitor of dynamin (Dynasore), which inhibits endocytosis [264]. Dynasore treatment led to a 50% reduction in the cellular GCase activity in the immortalized AMRF lymphocytes and *SCARB2* knocked-down THP-1 cells. In the case of the AMRF fibroblasts, no alterations were observed (Fig. 4.8).

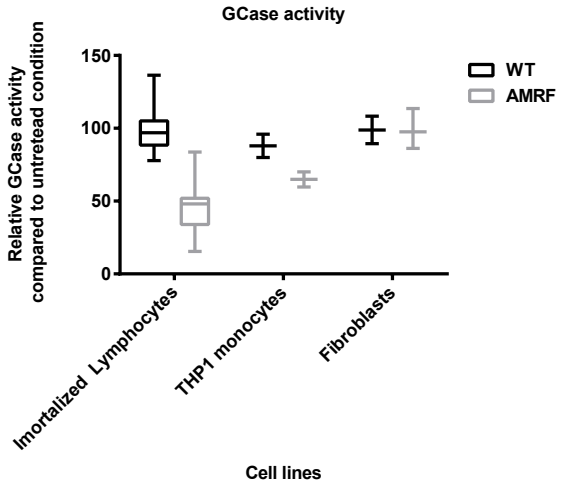

Figure 4.8 – Relative amount (%) of remaining GCase activity in different cell lines after treatment with Dynasore, compared to the non treated condition.

Using ABP labelling of GCase, similar results were obtained for THP-1 cell lines (Fig. 4.9). The Dynasore treatment reduced the amount of active GCase detected by ABP labelling. The concomitant presence of mannan in the culture medium did not influence the cellular content on active GCase (Fig. 4.9). This finding suggests that a mannose lectin receptor is not responsible for the endocytotic uptake of GCase.

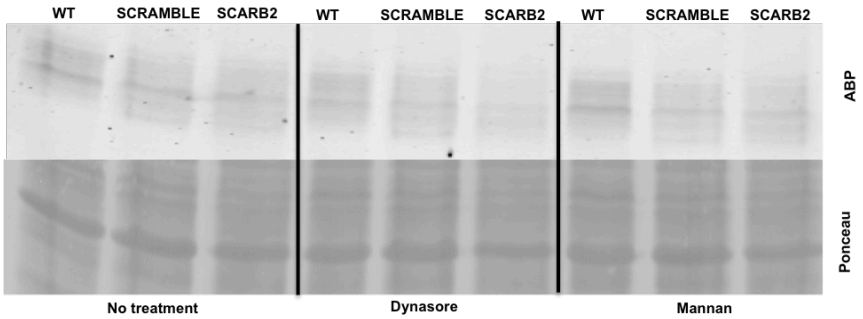

Figure 4.9 – Active GCase labelled with ABP in THP-1 cell lines.

4.5 Discussion

Primary GCase deficiency caused by mutations in the *GBA* gene occurs in all cells and tissues of GD patients [87]. Such GCase deficiency may lead to different phenotypes of GD, ranging from type 1 (non-neuronopathic manifestation) to type 2 and 3 (neuropathic) manifestations [87]. With every phenotypic variant, storage of the substrate GlcCer in lysosomes from tissue macrophages is a distinctive feature. Presence of the GlcCer-laden macrophages, named “Gaucher cells”, is reflected by a marked increase in plasma concentrations of proteins specifically secreted by these abnormal cells, like chitotriosidase and CCL18 [89, 130]. Interestingly, secondary GCase deficiency as the result of a defective LIMP-2 protein does not result in a phenocopy of GD. Instead, it results in AMRF, a disorder with distinct symptoms from GD and lacking the formation of significant amounts of “Gaucher cells” [218]. The availability of a genuine mouse model of AMRF, *LIMP-2 KO* mice, allowed us to carefully investigate abnormalities in GCase in various cells and tissues and find clues for the discordant manifestation of GD and AMRF. Firstly, we studied the composition of highly purified lysosomes from liver cells obtained from *LIMP-2 KO* and wild type mice. Except for the absence of GCase, no major differences in lysosomal matrix proteins were observed. Of note, the lack of GCase did not appear to affect hepatocytes as indicated by pathology examination. Next, we investigated how the absence of LIMP-2 influences the levels of active GCase molecules. For this purpose, we first used enzymatic activity measurements with an artificial fluorogenic substrate, 4-MU-β-D-Glc. A variable deficiency in GCase activity was observed for various organs. In addition, we used an independent method to assess the presence of active GCase molecules by employing our recently developed fluorescent ABP, a suicide substrate which specifically covalently labels GCase. Consistent marked differences in relative decrease in GCase activity among tissues were found. Importantly, the findings made with both methods were similar. Some tissues, like pancreas, heart and liver contain very little GCase in *LIMP-2 KO* mice. In sharp contrast, leukocytes show a relatively high residual GCase. Next, we addressed the

functional consequences of the reductions in GCase activity in various tissues of *LIMP-2 KO* mice. For this purpose, we measured concentrations of GlcCer, the primary storage lipid, and GlcSph, a water-soluble metabolite of GlcCer formed by deacylation [89, 117]. In most tissues we hardly observed any increase in GlcCer, suggesting that the small amount of residual GCase is sufficient for its lysosomal degradation and/or that accumulating GlcCer is efficiently converted to GlcSph. Indeed, GlcSph was found to be highly increased in many tissues from *LIMP-2 KO* mice, suggesting that metabolism of GlcCer by its deacylation seems a remarkably effective pathway to avoid GlcCer accumulation. It is noteworthy that those tissues with low GCase activity tend to show the highest levels of GlcSph as, for example, the pancreas and the heart. The marked deficiency of GCase in most tissues of *LIMP-2 KO* mice has therefore remarkably little consequences regarding GlcCer accumulation. Lysosomes seem to cope surprisingly well with the undegraded GlcCer. For example, we observed no abnormalities in lysosomal catabolism of globosides as reflected by normal Gb3 and lysoGb3 concentrations. In contrast, in Gaucher patients significant increase in lysoGb3 can be observed, suggesting secondary impaired lysosomal degradation and alternative metabolism of Gb3 (Ferraz et al, unpublished results).

Our findings on peripheral blood leukocytes from *LIMP-2 KO* mice deserve special discussion. Only in these cells a significant, although modest, increase in GlcCer was demonstrable. On the other hand, the concentrations of GlcSph in leukocytes were meanwhile not exceptionally high when compared to other tissues of *LIMP-2 KO* mice. It therefore seems that peripheral leukocytes manage less well than other tissues to avoid GlcCer accumulation trough its conversion to GlcSph. In this regard, it is of interest to point out that of all materials studied, leukocytes of *LIMP-2 KO* mice show high levels of residual GCase activity, reaching even about 60% of normal levels. Apparently, such residual capacity is sufficient to avoid prominent formation of GlcCer-laden macrophages, a characteristic feature in GD patients. Thus, it is not surprising that mutations in the *SCARB2* gene have been reported to aggravate the severity of clinical manifestation in Gaucher patients [225, 265]. In this

work, we analyzed relatively young *LIMP-2 KO* mice. At older age animals are known to present tubular proteinuria associated with a reduced ability of endosomes, containing reabsorbed proteins, to fuse with lysosomes in the proximal convoluted tubule (PCT) of the kidney [190, 210, 243]. In the studied animals, no overt proteinuria had been developed yet. Residual GCase, measured by enzymatic assay or ABP labelling, was not strikingly different from other tissues. Likewise, lipid abnormalities were comparable to those in other tissues examined.

Another tissue from *LIMP-2 KO* mice that deserves discussion is the brain. Only severe cases of GD develop characteristic neuropathology. However, carriers of GD also have been reported to have an increased risk of developing Parkinson and Lewy-Body dementia [123, 124]. The neurological manifestation of AMRF is distinct and is characterized by epileptic attacks, thus mimicking PME. Brain of *LIMP-2 KO* mice showed relatively high residual levels of GCase and no clear increase in GlcCer. At present, it is therefore unclear why this tissue is particularly vulnerable to pathology. Possibly, we missed in our analysis of total brain lipids abnormalities in specific neuronal cells associated with epileptic attacks. It cannot even be excluded that such cells metabolize GlcCer to other toxic metabolites causing epilepsy. Taking this into account, our observation of the occurrence of GlcChol is of interest. The glucosylated sterol has recently been identified in mammals and has been suggested to be formed by GCase through transglucosylation of cholesterol molecules. Abnormalities in this pathway related to GCase deficiency might cause neurological disease manifestations. Absence of LIMP-2 led to modestly increased levels of GlcChol in all examined tissues of mice. This finding suggests that GCase plays a physiologically role in degradation of GlcChol, rather than in its synthesis through transglucosylation as recently proposed [252].

A known feature of LIMP-2 deficiency is the occurrence of peripheral demyelinating neuropathy, being absent in neurons from the central nervous system as a consequence of repeated de- and re-myelination [190]. In view of this, our findings with the sciatic nerve (SN) are intriguing. A grossly swollen SN develops in *LIMP-2 KO* mice. Residual GCase is relatively high in the SN of *LIMP-2 KO* mice and

GlcCer appears relatively normal. In contrast, the concentrations of galactosylceramide and GlcSph are markedly abnormal. Galactosylceramide becomes markedly reduced in the SN of *LIMP-2 KO* mice, likely reflecting ongoing peripheral demyelination and explaining the tremors observed in animals.

During our investigation, we have dedicated particular attention to the influence of the age of *LIMP-2 KO* mice with respect to lipid abnormalities. Interestingly, in almost all tissues, abnormalities in GlcSph and GlcChol were already present at 2 months of age and did not dramatically worsen with age. Only in the case of thymus and adipose tissues, a continuous increase of GlcSph with age in *LIMP-2 KO* mice was observed. Our findings with *LIMP-2 KO* mice differ quite clearly from those observed in GD patients and mouse models, in which there is as increasing accumulation of GlcCer. A possible explanation for this may be that in *LIMP-2 KO* mice a new equilibrium is soon established by metabolism of excessive GlcCer to GlcSph. The latter may egress from lysosomes and then be degraded by the cytosolic enzyme *GBA2* or even leave the body via the bile. Apparently, such pathway is not efficient enough in Gaucher patients to prevent accumulation of lipid-laden Gaucher cells.

Our study fully confirms the earlier notion that LIMP-2 is essential in lysosomal targeting of GCase [57]. The observed relative high residual levels of GCase in leukocytes led us to look for alternative mechanisms of delivery of GCase in these particular cells. We obtained evidence for the uptake of GCase by lymphoblasts of AMRF patients and normal individuals, but not by the corresponding fibroblasts. The uptake seems to be mediated by endocytosis since it could be blocked by the dynamin inhibitor, Dynasore, although the receptor that is involved in this capture mechanism is presently not known. Mannan was not able to efficiently inhibit the endocytosis of GCase. Presently, it seems that the endocytic capture of secreted GCase offers an explanation for the relatively high residual GCase activity in leukocytes, being sufficient to prevent formation of GlcCer-laden Gaucher cells in AMRF patients. Indeed, in freshly obtained plasma of AMRF patients significant circulating GCase has been detected to allow such mechanism [248].

In conclusion, this work sheds some new light on the consequences of LIMP-2 deficiency on residual GCase activity in various cells and tissues. Most tissues suffer from a marked deficiency in GCase. However, this does not lead to striking GlcCer accumulation but rather to elevated GlcSph. The water-soluble metabolite is either further degraded or able to exit the body via bile. In this way, a new equilibrium is established during LIMP-2 deficiency. Leukocytes seem to profit from their ability to re-uptake secreted GCase, acquiring sufficient residual enzyme activity to prevent formation of GlcCer-laden macrophages, the hallmark of GD.

4.6 Supplemental data

Table S4.1 – List of the lysosomal matrix proteins identified in the tritosomes. "n.d." - not detectable.

Nº	Protein Name	Acces Nº	Description	Countinj	Ratio
1	A2BFA6_MOUSE	A2BFA6	Alpha N acetylglucosaminidase Sanfilippo disease IIIB OS Mus musculus GN Naglu PE 4 SV 1	9	1.06
2	ARL8B_MOUSE	Q9CQW2	ADP ribosylation factor like protein 8B OS Mus musculus GN Arl8b PE 2 SV 1	9	1.10
3	CATH_MOUSE	P49935	Pro cathepsin H OS Mus musculus GN Ctsh PE 2 SV 2	9	1.22
4	CATL1_MOUSE	P06797	Cathepsin L1 OS Mus musculus GN Ctsl1 PE 1 SV 2	9	0.98
5	CATZ_MOUSE	Q9WUU7	Cathepsin Z OS Mus musculus GN Ctsz PE 2 SV 1	9	1.12
6	CREG1_MOUSE	O88668	Protein CREG1 OS Mus musculus GN Creg1 PE 2 SV 1	9	1.45
7	DPP2_MOUSE	Q9ET22	Dipeptidyl peptidase 2 OS Mus musculus GN Dpp7 PE 2 SV 2	9	0.87
8	GNS_MOUSE	Q8BFR4	N acetylglucosamine 6 sulfatase OS Mus musculus GN Gns PE 2 SV 1	9	0.92
9	LAMP1_MOUSE	P11438	Lysosome associated membrane glycoprotein 1 OS Mus musculus GN Lamp1 PE 1 SV 2	9	1.12
10	LAMP2_MOUSE	P17047	Lysosome associated membrane glycoprotein 2 OS Mus musculus GN Lamp2 PE 2 SV 2	9	1.06
11	LGMN_MOUSE	O89017	Legumain OS Mus musculus GN Lgmn PE 1 SV 1	9	0.96
12	LYAG_MOUSE	P70699	Lysosomal alpha glucosidase OS Mus musculus GN Gaa PE 1 SV 2	9	1.07
13	MA2B1_MOUSE	O09159	Lysosomal alpha mannosidase OS Mus musculus GN Man2b1 PE 2 SV 4	9	0.84
14	MANBA_MOUSE	Q8K2I4	Beta mannosidase OS Mus musculus GN Manba PE 2 SV 1	9	0.76
15	NAGAB_MOUSE	Q9QWR8	Alpha N acetylgalactosaminidase OS Mus musculus GN Naga PE 2 SV 2	9	0.91
16	NPC2_MOUSE	Q9Z0J0	Epididymal secretory protein E1 OS Mus musculus GN Npc2 PE 2 SV 1	9	1.08
17	PLBL2_MOUSE	Q3TCN2	Putative phospholipase B like 2 OS Mus musculus GN Plbd2 PE 1 SV 2	9	0.93
18	PPA5_MOUSE	Q05117	Tartrate resistant acid phosphatase type 5 OS Mus musculus GN Acp5 PE 2 SV 2	9	0.72
19	PPT2_MOUSE	O35448	Lysosomal thioesterase PPT2 OS Mus musculus GN Ppt2 PE 2 SV 1	9	1.12
20	RISC_MOUSE	Q920A5	Retinoid inducible serine carboxypeptidase OS Mus musculus GN Scpep1 PE 2 SV 2	9	1.12
21	RNT2_MOUSE	Q9CQ01	Ribonuclease T2 OS Mus musculus GN Rnaset2 PE 2 SV 1	9	0.82

22	NCUG1_MOUSE	Q9JHJ3	Lysosomal protein NCU G1 OS Mus musculus PE 1 SV 1	8	1.72
23	PCP_MOUSE	Q7TMR0	Lysosomal Pro X carboxypeptidase OS Mus musculus GN Prcp PE 2 SV 2	8	0.64
24	CATF_MOUSE	Q9R013	Cathepsin F OS Mus musculus GN Ctsf PE 2 SV 1	7	0.62
25	CATS_MOUSE	O70370	Cathepsin S OS Mus musculus GN Ctss PE 2 SV 2	7	0.78
26	HEXB_MOUSE	P20060	Beta hexosaminidase subunit beta OS Mus musculus GN Hexb PE 2 SV 2	7	1.37
27	CATC_MOUSE	P97821	Dipeptidyl peptidase 1 OS Mus musculus GN Ctsc PE 2 SV 1	6	n.d.
28	E9PVY4_MOUSE	E9PVY4	Uncharacterized protein OS Mus musculus GN Ppt1 PE 4 SV 1	6	0.96
29	GLCM_MOUSE	P17439	Glucosylceramidase OS Mus musculus GN *GBA* PE 1 SV 1	6	n.d.
30	LICH_MOUSE	Q9Z0M5	Lysosomal acid lipase cholesteryl ester hydrolase OS Mus musculus GN Lipa PE 2 SV 2	6	0.44
31	ARSB_MOUSE	P50429	Arylsulfatase B OS Mus musculus GN Arsb PE 2 SV 3	5	0.92
32	ASM_MOUSE	Q04519	Sphingomyelin phosphodiesterase OS Mus musculus GN Smpd1 PE 2 SV 2	5	0.59
33	GALNS_MOUSE	Q571E4	N acetylgalactosamine 6 sulfatase OS Mus musculus GN Galns PE 2 SV 2	5	2.16
34	NICA_MOUSE	P57716	Nicastrin OS Mus musculus GN Ncstn PE 1 SV 3	5	1.15
35	SCRB2_MOUSE	O35114	Lysosome membrane protein 2 OS Mus musculus GN *SCARB2* PE 1 SV 3	5	n.d.
36	ASAH1_MOUSE	Q9WV54	Acid ceramidase OS Mus musculus GN Asah1 PE 1 SV 1	4	n.d.
37	E9PW67_MOUSE	E9PW67	Uncharacterized protein OS Mus musculus GN Hexa PE 4 SV 1	4	0.97
38	NPC1_MOUSE	O35604	Niemann Pick C1 protein OS Mus musculus GN Npc1 PE 1 SV 1	4	n.d.
39	PPT1_MOUSE	O88531	Palmitoyl protein thioesterase 1 OS Mus musculus GN Ppt1 PE 2 SV 2	4	0.69
40	SIAE_MOUSE	P70665	Sialate O acetylesterase OS Mus musculus GN Siae PE 2 SV 3	4	n.d.
41	ARL8A_MOUSE	Q8VEH3	ADP ribosylation factor like protein 8A OS Mus musculus GN Arl8a PE 2 SV 1	3	n.d.
42	E9Q9I3_MOUSE	E9Q9I3	Uncharacterized protein OS Mus musculus GN Acp2 PE 4 SV 1	3	n.d.
43	RAB7A_MOUSE	P51150	Ras related protein Rab 7a OS Mus musculus GN Rab7a PE 1 SV 2	3	n.d.
44	AGAL_MOUSE	P51569	Alpha galactosidase A OS Mus musculus GN Gla PE 1 SV 1	2	n.d.

45	CD1D1_MOUSE	P11609	Antigen presenting glycoprotein CD1d1 OS Mus musculus GN Cd1d1 PE 1 SV 3	2	n.d.
46	DIAC_MOUSE	Q8R242	Di N acetylchitobiase OS Mus musculus GN Ctbs PE 2 SV 2	2	n.d.
47	E9Q515_MOUSE	E9Q515	Uncharacterized protein OS Mus musculus GN 4930471M23Rik PE 4 SV 1	2	n.d.
48	HEXA_MOUSE	P29416	Beta hexosaminidase subunit alpha OS Mus musculus GN Hexa PE 2 SV 2	2	n.d.
49	HGNAT_MOUSE	Q3UDW8	Heparan alpha glucosaminide N acetyltransferase OS Mus musculus GN Hgsnat PE 1 SV 2	2	n.d.
50	Q3U2B2_MOUSE	Q3U2B2	Uncharacterized protein OS Mus musculus GN Npc1 PE 2 SV 1	2	n.d.
51	CATB_MOUSE	P10605	Cathepsin B OS Mus musculus GN Ctsb PE 1 SV 2	9	0.98
52	Q8C243_MOUSE	Q8C243	Uncharacterized protein OS Mus musculus GN Ctsd PE 2 SV 1	9	0.94
53	SAP_MOUSE	Q61207	Sulfated glycoprotein 1 OS Mus musculus GN Psap PE 1 SV 2	9	0.81
54	SAP3_MOUSE	Q60648	Ganglioside GM2 activator OS Mus musculus GN Gm2a PE 1 SV 2	9	0.68
55	TPP1_MOUSE	O89023	Tripeptidyl peptidase 1 OS Mus musculus GN Tpp1 PE 1 SV 2	9	1.22
56	PPGB_MOUSE	P16675	Lysosomal protective protein OS Mus musculus GN Ctsa PE 1 SV 1	8	1.40
57	F6Y6L6_MOUSE	F6Y6L6	Uncharacterized protein Fragment OS Mus musculus GN Ctsd PE 3 SV 1	7	0.95
58	PAG15_MOUSE	Q8VEB4	Group XV phospholipase A2 OS Mus musculus GN Pla2g15 PE 1 SV 1	4	n.d.
59	CATD_MOUSE	P18242	Cathepsin D OS Mus musculus GN Ctsd PE 1 SV 1	3	n.d.
60	VA0D1_MOUSE	P51863	V type proton ATPase subunit d 1 OS Mus musculus GN Atp6v0d1 PE 1 SV 2	9	1.07
61	D3Z437_MOUSE	D3Z437	Uncharacterized protein OS Mus musculus GN Ctsh PE 4 SV 1	6	2.14
62	E9Q5W3_MOUSE	E9Q5W3	Uncharacterized protein OS Mus musculus GN Ctsz PE 3 SV 1	4	n.d.
63	F6QKK2_MOUSE	F6QKK2	Uncharacterized protein Fragment OS Mus musculus GN Arl8a PE 3 SV 1	4	n.d.
64	VATB2_MOUSE	P62814	V type proton ATPase subunit B brain isoform OS Mus musculus GN Atp6v1b2 PE 1 SV 1	4	n.d.
65	E9Q2Q0_MOUSE	E9Q2Q0	Uncharacterized protein OS Mus musculus GN Ctsc PE 3 SV 1	3	0.59
66	F7AF87_MOUSE	F7AF87	Uncharacterized protein Fragment OS Mus musculus GN Glb1 PE 4 SV 1	3	0.60
67	CD68_MOUSE	P31996-2	Isoform Short of Macrosialin OS Mus musculus	2	n.d.

			GN Cd68		
68	HGNAT_MOUSE	Q3UDW8-2	Isoform 2 of Heparan alpha glucosaminide N acetyltransferase OS Mus musculus GN Hgsnat	2	n.d.
69	LTOR3_MOUSE	O88653	Ragulator complex protein LAMTOR3 OS Mus musculus GN Lamtor3 PE 1 SV 1	2	n.d.
70	STOM_MOUSE	P54116	Erythrocyte band 7 integral membrane protein OS Mus musculus GN Stom PE 1 SV 3	2	n.d.

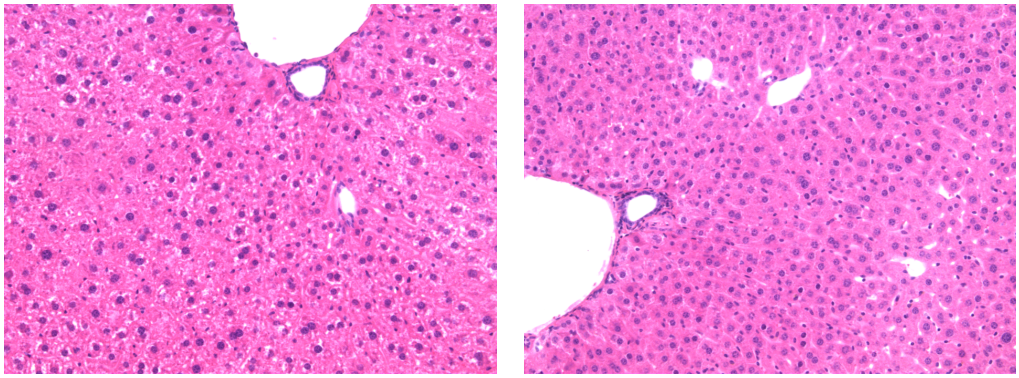

Wild type ***LIMP-2 KO***

Figure S4.1 – Hepatocyte from wild type and *LIMP-2 KO* mice, 6 months of age.

Figure S4.2 – Sciatic nerves from a wild type (left) and *LIMP-2 KO* mice (right).

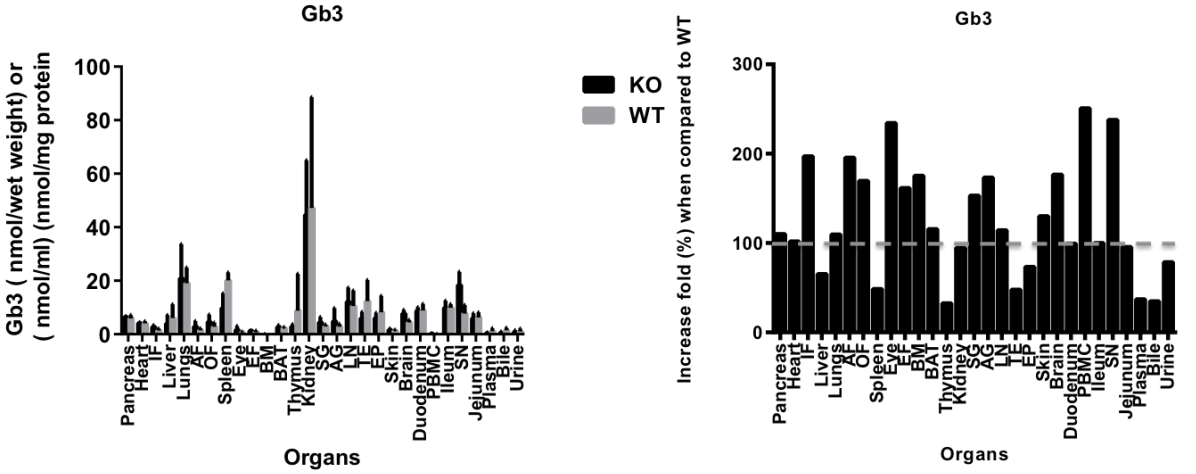

Figure S4.3 – Gb3 in the tissues of *LIMP-2 KO* and wild type mice. Left panel - Absolute amounts; Right panel - Relative increase when compared to wild type. Dashed line marks the normal values obtained in wild type mice.

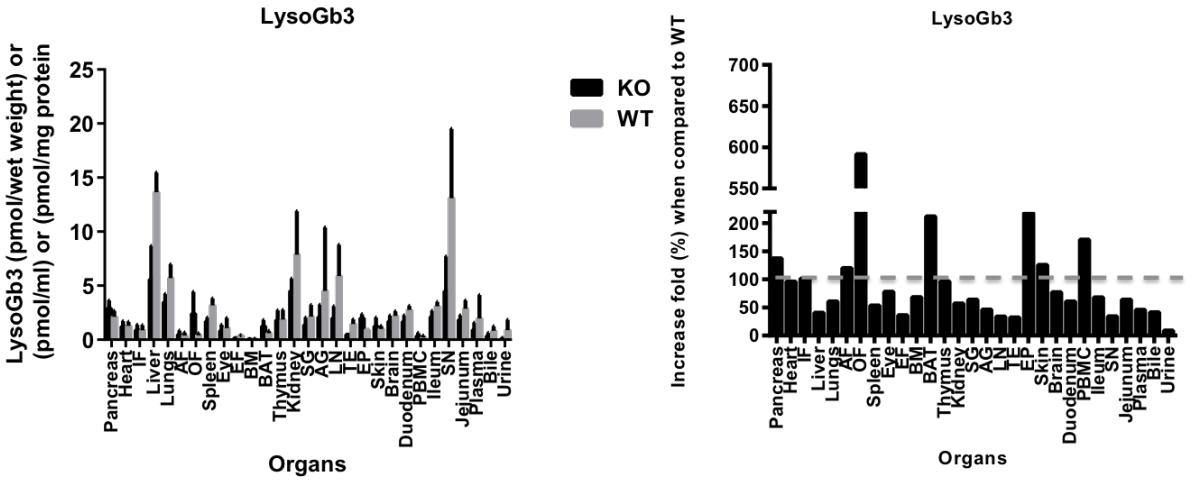

Figure S4.4 – LysoGb3 measured in tissues of *LIMP-2 KO* and wild type mice. Left panel - Absolute amounts; Right panel - Relative increase when compared to wild type. Dashed line marks the normal values obtained in wild type mice.

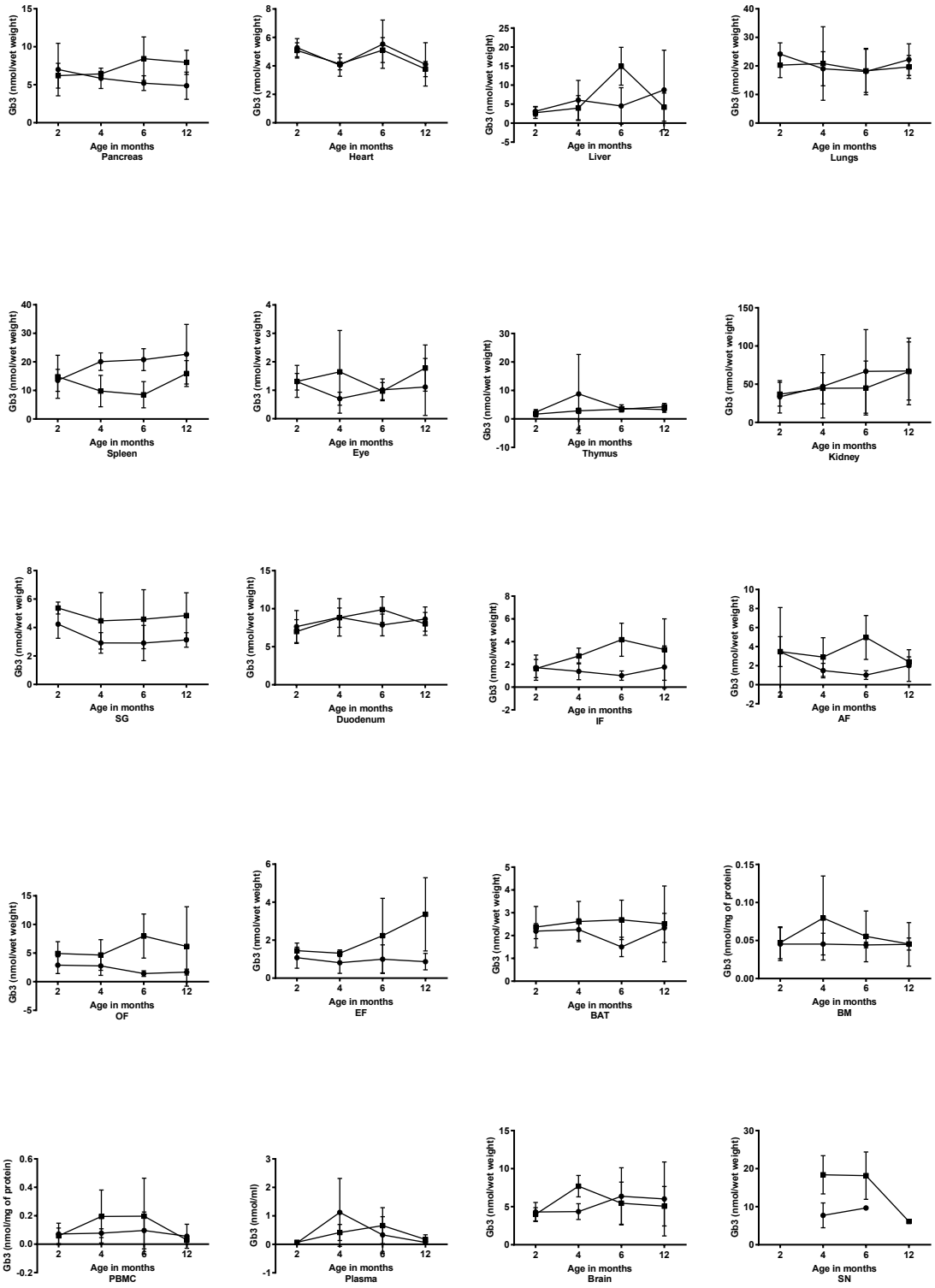

Figure S4.5 – Gb3 levels in wild type and *LIMP-2 KO* mice at different ages. Black circle - wild type; Black square - *LIMP-2 KO* mice.

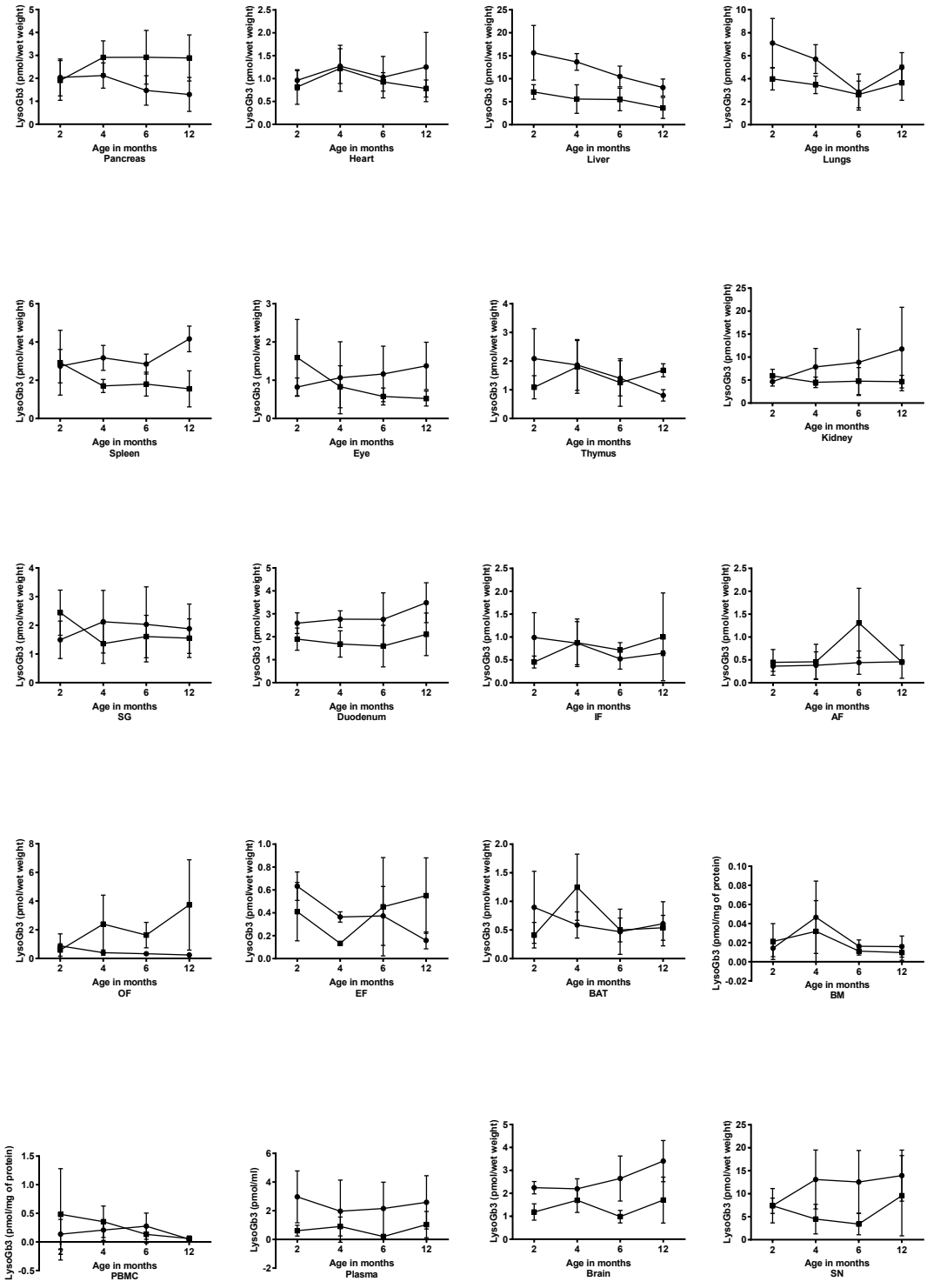

Figure S4.6 – LysoGb3 levels in wild type and *LIMP-2 KO* mice at differents ages. Black circle - wild type; Black square - *LIMP-2 KO* mice.

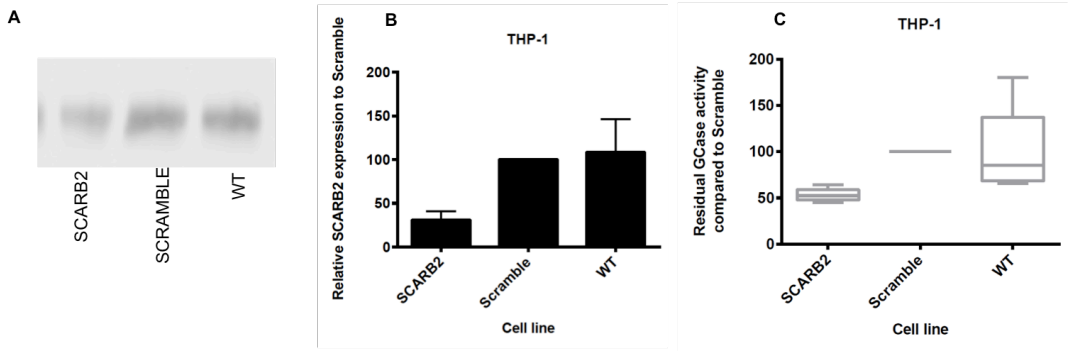

Figure S4.7 – Analysis of the THP-1 cell line with lentiviral *SCARB2* knock-out. A - Western-blot against LIMP-2 protein in THP-1 cells treated with *SCARB2* siRNA and scrambled siRNA; B - *SCARB2* gene expression; C - GCase activity measured with 4-MU-β-D-Glc.

5. LIMP-2 DEFICIENCY: THERAPEUTIC APPROACHES

5.1 Abstract

Deficiency of the lysosomal enzyme GCase is encountered in patients with GD as well as in individuals with AMRF. GD is caused by mutations in the *GBA* gene encoding GCase, whilst AMRF is due to mutations in the *SCARB2* gene encoding the lysosomal membrane protein LIMP-2, which governs the transport of newly formed GCase to lysosomes. In AMRF patients, GCase deficiency is secondary, being the result of impaired transport of enzyme to lysosomes. AMRF manifest primarily as a neurological disorder without major visceral complications except for late onset renal disease. In the common non-neuronopathic (type 1) manifestation of GD, storage of the GCase substrate GlcCer almost exclusively occurs in macrophages. Two different kinds of therapies are registered for type 1 GD: macrophage-targeted ERT and glycosphingolipid SRT. No treatment is presently available for AMRF.

Since GCase is the prominent biochemical abnormality in AMRF patients, we studied the feasibility to supplement LIMP-2 deficient cells with recombinant GCase (hrGBA). Studies were conducted with normal and AMRF fibroblasts as well as normal and LIMP-2 deficient HEK293T cells transduced with mannose receptor to promote uptake of mannose-terminated hrGBA. With both cell types we observed that following its endocytotic uptake and delivery to lysosomes, GCase is rapidly degraded in LIMP-2 deficient lysosomes. The half-life of the enzyme in LIMP-2 lysosomes is much shorter than in corresponding normal organelles. This finding suggests that, also intralysosomally, transient interactions of GCase with LIMP-2 stabilize the conformation of the enzyme and thus prevent proteolytic breakdown. This finding indicates that an intrinsic limit, installed by LIMP-2 presence, may exist in the efficacy of supplementing the GCase capacity of lysosomes by ERT. Next, we examined the feasibility of glycosphingolipid substrate reduction therapy. For this purpose *LIMP-2 KO* mice were orally treated with a newly developed brain permeable azasugar. The dose used proved to be too small to render sufficient inhibition of glycosphingolipid synthesis.

In conclusion, ERT does not seem an attractive approach for treatment of AMRF and further investigations are warranted regarding the potential efficacy of SRT using oral inhibitors of GlcCer synthesis.

5.2 Introduction

GD is an autosomal recessive disorder caused by impaired GlcCer catabolism as the result of GCase deficiency. The defect leads to prominent storage of GlcCer in lysosomes of macrophages that lead to the formation of “Gaucher cells” (lipid-laden macrophages), the hallmark of the disease [87, 114]. GCase is encoded by the *GBA* gene and more than 200 different mutations have been described in GD patients [95, 266, 267]. The symptomatology of GD is remarkably heterogeneous ranging from severe neonatal forms to an almost asymptomatic course until old age. Based on the occurrence and age of onset of the neurological involvement, GD has been classified into acute and juvenile neuronopathic forms and non-neuronopathic forms. The non-neuronopathic form, type 1 GD, is the most common and may manifest either in childhood or adulthood. Type 2 GD is characterized by infantile onset and severe neurological involvement. Type 3 GD type is a less severe and slowly progressive neuronopathic form [87, 105]. Although there are no strict genotype-phenotype correlations, some mutations are associated with type 1 GD, like the homo- or heteroallelic presence of *GBA* with the N370S mutation. On the other hand, homozygosity for the *GBA* allele with the L444P mutation is associated with a neuronopathic form of the disease [266]. The accumulation of GlcCer in “Gaucher cells” leads to characteristic visceral features of the disease such as cytopenia, hepatosplenomegaly and skeletal abnormalities [113].

For a long time, it remained unknown how GCase reaches the lysosome. In contrast to other lysosomal enzymes, GCase does not acquire any phosphomannosyl moieties in its 4 N-linked glycans. Clearly, the enzyme has to be targeted to the lysosomes by a mechanism independent of the M6PR [203, 204]. Only in 2007, LIMP-2 was identified as the protein responsible for the sorting of GCase to the lysosome, since its absence leads to GCase deficiency in almost all organs [57]. Mutations in the *SCARB2* gene, which encodes the LIMP-2 protein, are the cause of a disorder called AMRF. This disease is characterized by reduced levels of GCase in the majority of the cells, and clinical symptoms such as glomerulosclerosis, progressive myoclonus epilepsy, and ataxia [201, 210, 212, 218]. In addition,

accumulation of undefined storage material in the brain has been reported [211]. Although, LIMP-2 deficient individuals share a GCase deficiency with GD patients, the clinical presentation of AMRF is markedly different from GD. Most striking is the absence of “Gaucher cells” in AMRF patients and the corresponding lack of elevated plasma chitotriosidase and CCL18. AMRF patients do not show visceromegaly or neurological symptoms seen in severe GD patients [218].

In addition to GD, alterations in the *GBA* gene have been recently also linked to PD. More specifically, *GBA* mutations have been found to be associated to an increased risk for α-synucleinopathies such as PD and Lewy-Body dementia [123, 124]. This increased risk has also been reported for mutations in the *SCARB2* gene [235, 268, 269]. In mice treated with the GCase inhibitor CBE, the reduction in GCase activity induces the storage of α-synuclein [126, 270]. Consistently, adenoviral overexpression of GCase in the brain decreases α-synuclein in transgenic mouse models of GD and PD [128]. Recently, α-synuclein storage was also described in *LIMP-2 KO* mice [236].

Several treatments have been developed, or are under investigation, for GD. Already in 1991, ERT was firstly introduced for type 1 GD using alglucerase (Ceredase®) (GCase isolated from human placenta). In 1994 imiglucerase (Cerezyme®) (hr*GBA*), a recombinant enzyme produced in chinese hamster ovary cells [147] was firstly employed for ERT of type 1 GD. Only a few years ago, in 2010, an alternative recombinant enzyme preparation became available following the registration of velaglucerase alfa (VPRIV®) produced in a human fibroblast cell line [271]. In all cases, (recombinant) GCases were remodeled to expose terminal mannose residues in order to be efficiently captured by the mannose receptor expressed by macrophages, the most prominently affected cells in type 1 GD patients. Recently a new recombinant enzyme was registered, Taliglucerase alfa (Elelyso®), produced in carrots, avoiding possible contamination with mammalian viruses [272, 273]. All ERT treatments are found to be effective for the majority of type 1 GD patients, but their inability to cross the BBB, makes them ineffective to treat or prevent neuropathology in type 2 and type 3 GD patients. An entirely different approach to treat GD is SRT. This aims to reduce the levels of GlcCer by inhibiting

the biosynthetic enzyme GCS [274]. SRT offers an alternative to ERT in those patients that are not willing to undergo, or do not tolerate, chronic bi-weekly enzyme infusions. The first compound registered for SRT was N-butyldeoxynojirimycin (Miglustat®), also named Zavesca® [160]. N-butyldeoxynojirimycin resembles in its structure GlcCer and inhibits GCS, but also, even more potently, the β-glucosidase *GBA2* [158]. Since 2003, Miglustat (Zavesca®) has been used for SRT, although it is a relatively poor GCS inhibitor with a IC_{50} of 25 μM [158, 274–276]. Very recently, eliglustat tartrate (Cerdelga®) has been registered for use in SRT of type 1 GD [163–165]. This compound is a ceramide mimic, being a far more potent GCS inhibitor with IC_{50} of about 50 nM and without inhibitory effects on β-glucosidases. Unfortunately, Eliglustat does not penetrate into the BBB and therefore is only registered for treatment of type 1 GD patients. The compound is also subjected to CYP2B metabolism and cannot be used in individuals with abnormalities in this detoxification enzyme. In the meantime, N-(5'-adamantane-1'-yl-methoxy)-pentyl-1-deoxynojirimycin (AMP-DNM) [277] also named MZ21, was also developed and tested as GCS inhibitor. This compound shows an IC_{50} for GCS of 150 nM and is BBB permeable, although it was never developed as a drug, due to the lack of industrial interest given its concomitant potent inhibition of *GBA2* and to a lesser extent, also of the lysosomal GCase. It was observed that *ido*-variants of the deoxynojirimycins like AMP-DNM inhibit GCS with the same efficacy but with much less affinity for GCase. Based on these compounds, a new generation of deoxynojirimycin type GCS inhibitors with IC_{50} values in the very low nanomolar range has been recently developed [167]. One of the most promising compounds in this category is 1307RB20 [167]. Another approach for treating GD is the use of pharmacological chaperones. They are compounds that are able to promote folding of mutant GCase, promoting its delivery to lysosomes. Inside the lysosome, the chaperone and GCase ideally dissociate and the enzyme becomes thus available to degrade the substrate [278]. At present, no effective chaperone has yet been developed to treat neuronopathic GD, in part because the GD patients with neurological forms generally show almost no residual GCase activity [87]. Also, at the experimental stage as GD treatments are gene therapies approaches as well as

treatments aiming to beneficially manipulate downstream pathways that are affected in GD [127, 169].

Presently, there is no therapy available for AMRF. Although GD and AMRF differ in phenotype, they both share the deficiency in GCase activity. It is therefore of interest to investigate the potential beneficial impact of treating AMRF with approaches similar to the ones successfully employed for GD. Here, we report the outcome of supplementing AMRF cell lines with Cerezyme® (hr*GBA*) and the treatment of *LIMP-2 KO* mice with one of the most promising compounds in SRT, the 1307RB20. These investigations aim to obtain insight into whether treatments available for GD might be potentially beneficial for individuals suffering from LIMP-2 deficiency.

5.3. Impact of LIMP-2 on GCase: Consequences for Enzyme Replacement Therapy

5.3.1 Methods

5.3.1.1 Patients' samples

Materials used from donors and the respective culturing procedures are described in section 3.3.2.

5.3.1.2 *SCARB2* gene Knock-out in HEK293T cells

SCARB2 gene knock-out in Human Embryonic Kidney 293 (HEK293) cells (ATCC CRL 1573) was generated using the CRISPR/Cas9 system. Guide RNA sequences were selected using the optimized CRISPR design tool (http://crispr.mit.edu) using the individual *SCARB2* exon sequences as template. For the selected guides two complementary oligo´s containing the *SCARB2* guide sequences and BbsI ligation adapters were annealed and ligated into pX335 (pX335-U6-Chimeric_BB-CBh-hSpCas9n (D10A, Nickase, Addgene plasmid #42335) digested with BbsI according to the protocol described [279]. Primers used for *SCARB2* exon 1 were: guide 1 5'- CACCGGACGTTGTCCCTGCTCCTGC-3 and 5'-AAACGCAGGAGCAGGGACAACGTCC-3'. *SCARB2* exon 1 guide 2 5'-CACCGCCGCCGTGTAGAAGCAGCAT-3' and 5'-AAACATGCTGCTTCTACACGGCGGC-3'. For targeting the *SCARB2* exon 7, the primers were: guide 1 5'-CACCGTATACCTGAGGGAAACTGCC-3' and 5'-AAACGGCAGTTTCCCTCAGGTATAC-3'. guide 2 5'-CACCGGCCGGCATTGTCTGACGTAT-3' and 5'-AAACATACGTCAGACAATGCCGGCC-3'.

HEK293T cells were transfected with a 1:1 ratio of pX335 guide 1 and pX335 guide 2 for either exon 1 or exon 7 of the *SCARB2* gene using FuGene6 (Roche) with a FuGene: DNA ratio of 3:1. Two days after transfection single cell clones were isolated. Clones were checked by PCR and sequencing for the presence of indels. One clone (N1F8) with sequence confirmed indels was shown to secrete GCase. Western-blot analysis (data not shown) showed that clone N1F8 lacks any LIMP-2

protein. HEK293T cells were cultured in DMEM with high glucose supplemented with 10% FBS and 100 units/ml Pen/Strep.

5.3.1.3. Transfection of HEK293T cells with macrophage mannose receptors

HEK293T cells were cultured in DMEM with high glucose supplemented with 10% FBS and 100 units/ml Pen/Strep. One day before transfection 4 x 10^5 cells/well were seeded in a 6 well plate. HEK293T cells and HEK293T *SCARB2* knock-out cells (clone N1F8) were infected with a human Mannose Receptor (CD206) pLenti6.3/TO/V5-DEST construct, generated via PCR and the Gateway cloning system (Invitrogen) using primers 5'-GGGGACAAGTTTGTACAAAAAAGCAGGCTTCGGTACCACCATGAGGCTACCCCTGC-3' and 5'-GGGGACCACTTTGTACAAGAAAGCTGGGTCGATGACCGAGTGTTCATTCTG-3', and pDONR221 as the cloning intermediate. All constructs were verified by sequencing. To produce lentiviral particles HEK293T cells were transfected with pLenti6.3-CD206 in combination with the envelope and packaging plasmids pMD2G, pRRE and pRSV. Subsequently, culture supernatant containing viral particles was collected and used for infection of HEK293T cells and HEK293T *SCARB2* knock-out cells (clone N1F8). Infected cells were selected using blasticidin (Sigma) 2.5 µg/ml.

5.3.1.4 Cell culture and experiments

Fibroblasts were cultured in DMEM medium supplemented with 10% fetal bovine serum and 1% Pen/Strep. HEK293T cells were seeded one day before the experiment at 1 × 10^6 cells/well in a 6 well plate. The cells were subjected to the following 4 conditions during 4 days: no treatment; supplemented 20 µM of leupeptin (a broad spectrum cathepsin inhibitor); supplemented each day with 32 ng/µl of human recombinant GCase (hr*GBA*); and supplemented with 32 ng/µl of hr*GBA* each day, 1 h after the single addition of 20 µM of leupeptin. At the fourth day of exposure, the cells were harvested.

In a parallel experiment, to evaluate the effect of leupeptin in hrGBA, cells were exposed to leupeptin and hrGBA and only hrGBA. At the fourth day, the cells were washed with cold PBS, and the cells were cultured with or without leupeptin, as previous.

5.3.1.5 Uptake of human recombinant glucocerebrosidase

HEK293T cells were seeded one day prior to the experiment at 1×10^6 cells/well in a 6 well plate. The cells were subjected to the following condition: 32 ng/µl of hr*GBA*, one hour after the addition of 20 µM of leupeptin. The following time points were collected: 0, 10, 20, 30 min.

5.3.1.6 Preparation of cell lysates

Isolated fibroblasts and HEK293T cells were homogenized and protein content quantified as described in section 3.3.4.

5.3.1.7 Labelling of glucocerebrosidase with activity-based probes

Cell homogenates were incubated with MDW941 (100 nM) in McIlvaine buffer as described in detail in section 4.3.9.

5.3.1.8 Western-Blotting

Performed exactly as described in section 3.3.6.

5.3.1.9 Immunofluorescence

Fibroblasts were cultured on glass slides. The cells were subjected to the following 4 conditions during 4 days: no treatment; supplemented witg 20 µM of leupeptin; supplemented with 32 ng/µl of hr*GBA* each day and supplemented with 32

ng/µl of hr*GBA* each day one hour after of a single addition of 20 µM of leupeptin. Cells were incubated with 1 nM MDW941 overnight in HAM/DMEM with 10% FCS. Next, cells were washed, fixed with 3% (v/v) paraformaldehyde in PBS for 1 h, washed with PBS and incubated with 0.1% saponin in PBS. They were washed again with PBS, incubated with 0.1 mM NH_4Cl in PBS for 10 min and then with normal antibody diluent (BD09-999; Immunologic, Duiven, The Netherlands) for 2 h. Nuclei were stained with DAPI, LIMP-2 protein with an rabbit IgG anti-LIMP-2 antibody (NB400-129, Novus Biologicals, Abingdon, UK) and the LAMP-2 protein with a mouse IgG1 anti-LAMP-2 antibody (clone H4B4; 9840-01, Southern Biotechnology Associates, Birmingham, AL). Second step antibodies were Alexa Fluor 488-conjugated goat IgG anti-rabbit (A11034; Life Technologies, Bleiswijk, The Netherlands) and ATTO647N-conjugated goat IgG anti-mouse IgG (610-156-121; Rockland, Limerick, PA). Slides were mounted using ProLong Gold (Life Technologies). Imaging was performed by confocal laser scanning microscopy using a TCS SP8 X mounted on a DMI 6000 microscope with a Plan APO 63x/1.40 Oil CS2 objective. For excitation were applied a 405 nm UV diode for DAPI, and a 470-670 nm WLL Pulsed laser, sequentially set at 488 nm, 592 nm and 647 nm for the respective fluorochromes. PMT and HyD detection was applied. Recorded images were analyzed and overlayed using LAS X software (Leica Microsystems, Son, The Netherlands).

5.3.1.10 Enzymatic assays

Enzymatic assays were performed according to section 3.3.10.

5.3.2 Results

5.3.2.1 Human recombinant glucocerebrosidase and inhibitors of cathepsins

To evaluate the proteolytic degradation inside the lysosome, fibroblasts (wild type, GD and AMRF) were treated during 4 days with leupeptin, a cysteine protease cathepsin inhibitor, to inhibit intralysosomal proteolytic degradation of GCase (Fig. 5.1). The presence of leupeptin resulted in increased cellular GCase activity, detected by enzymatic assay (Fig. 5.1, left panel) and by ABP labelling of active GCase molecules (Fig. 5.1, right panel). Both the detection of GCase activity with a fluorescent substrate or labelling of GCase with ABP showed that the presence of leupeptin led to an increase in GCase in wild type and AMRF fibroblasts. No significant changes were observed in the case of the L444P homozygous GD cells. The latter finding is not surprising since the L444P mutation results in misfolding of the enzyme in the ER and its subsequent proteosomal degradation.

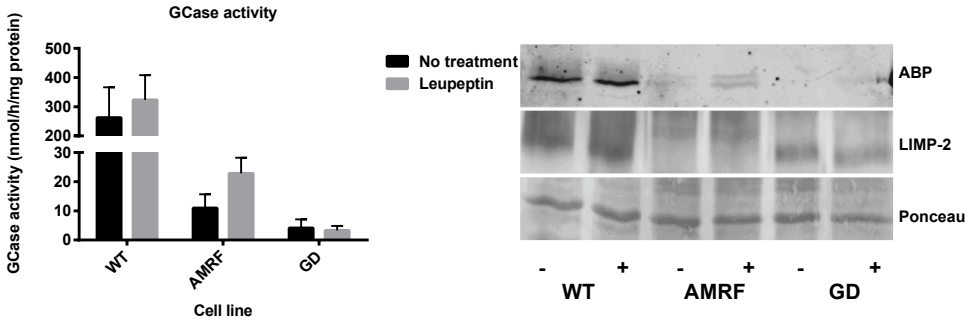

Figure 5.1 – Effect of leupeptin on cellular GCase. Left panel - GCase enzymatic activity determined with 4-MU-β-D-Glc; Right panel - ABP labelling followed by SDS-PAGE. Detection of LIMP-2 by Western blot. Symbols: "-" no treatment; "+" Leupeptin 20 μM; "WT" - wild type; "AMRF" - LIMP-2 deficient cell line; "GD" - Gaucher cell line; "ABP" - activity based probe.

The same fibroblast cell lines were then supplemented with recombinant GCase (hr*GBA*) in the medium for 4 days, in the presence or absence of leupeptin (Fig. 5.2). Addition of hr*GBA* to the medium led to an increase in cellular GCase in the case of control fibroblasts and GD cell lines. The increase observed was almost null in the case of AMRF cultured in the absence of leupeptin. The increase, in all the cell lines analyzed, was more prominent in the presence of leupeptin, pointing to a higher stabilization of GCase in the lysosomes (Fig. 5.2, left panel). Analysis of GCase by

ABP labelling gave similar results (Fig. 5.2, right panel). Of note, the stabilizing effect of leupeptin was more striking in the case of the AMRF fibroblasts, suggesting that endocytozed GCase is particularly sensitive to lysosomal degradation in AMRF fibroblasts.

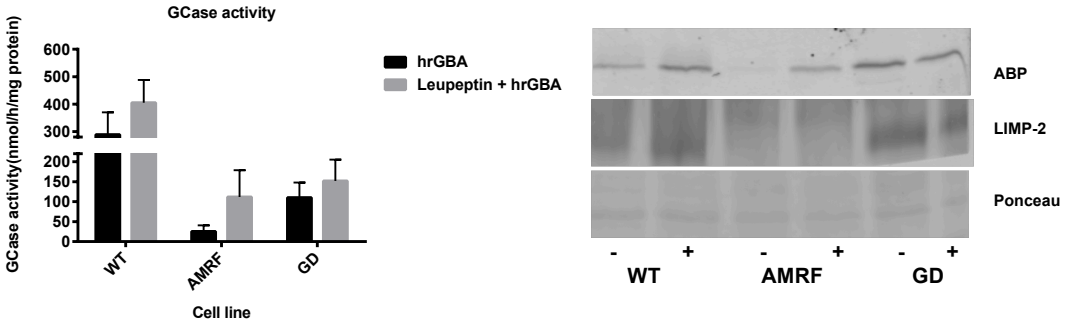

Figure 5.2 – Supplementation of fibroblasts with hr*GBA*, cultured with or without leupeptin. Left panel - GCase enzymatic activity with 4-MU-β-D-Glc; Right panel - ABP labelling followed by SDS-PAGE. Detection of LIMP-2 by Western blot. Symbols: "-" hr*GBA*; "+" Leupeptin 20 μM plus hr*GBA*; "WT" - wild type; "AMRF" - LIMP-2 deficient cell line; "GD" - Gaucher cell line; "ABP" - activity based probe.

5.3.2.2 Cellular localization of endocytozed human recombinant glucocerebrosidase

To assess whether hr*GBA* indeed reaches the lysosome in the case of LIMP-2 deficiency, immunofluorescence experiments were carried out with wild type and AMRF fibroblasts. For this purpose, we combined detection of GCase by ABP labelling with immune-detection of the lysosome with the markers LAMP-2 and LIMP-2 (Fig. 5.3). Cells were pre-treated, or not with leupeptin and they were cultured in the presence or absence of hr*GBA*. In all the conditions tested, we observed that GCase co-localized with the lysosome marker (LAMP-2) in control fibroblasts. With the three treatments (leupeptin, hr*GBA* or leupeptin plus hr*GBA*) the amount of active GCase inside the lysosomes of wild type fibroblasts increased when compared to non-treated cells (Fig. 5.3, left panel). Regarding AMRF fibroblasts treated with leupeptin, some lysosomal GCase colocalization with lysosomes was detected, particularly when it is followed by exposure of cells to hr*GBA* (Fig. 5.3, right panel). When only hr*GBA* is added, almost no increase of lysosomal GCase is observed (Fig. 5.3, right panel).

Again, these findings suggest that GCase, either endogenous or exogenously added, is particularly sensitive to lysosomal degradation in AMRF fibroblasts.

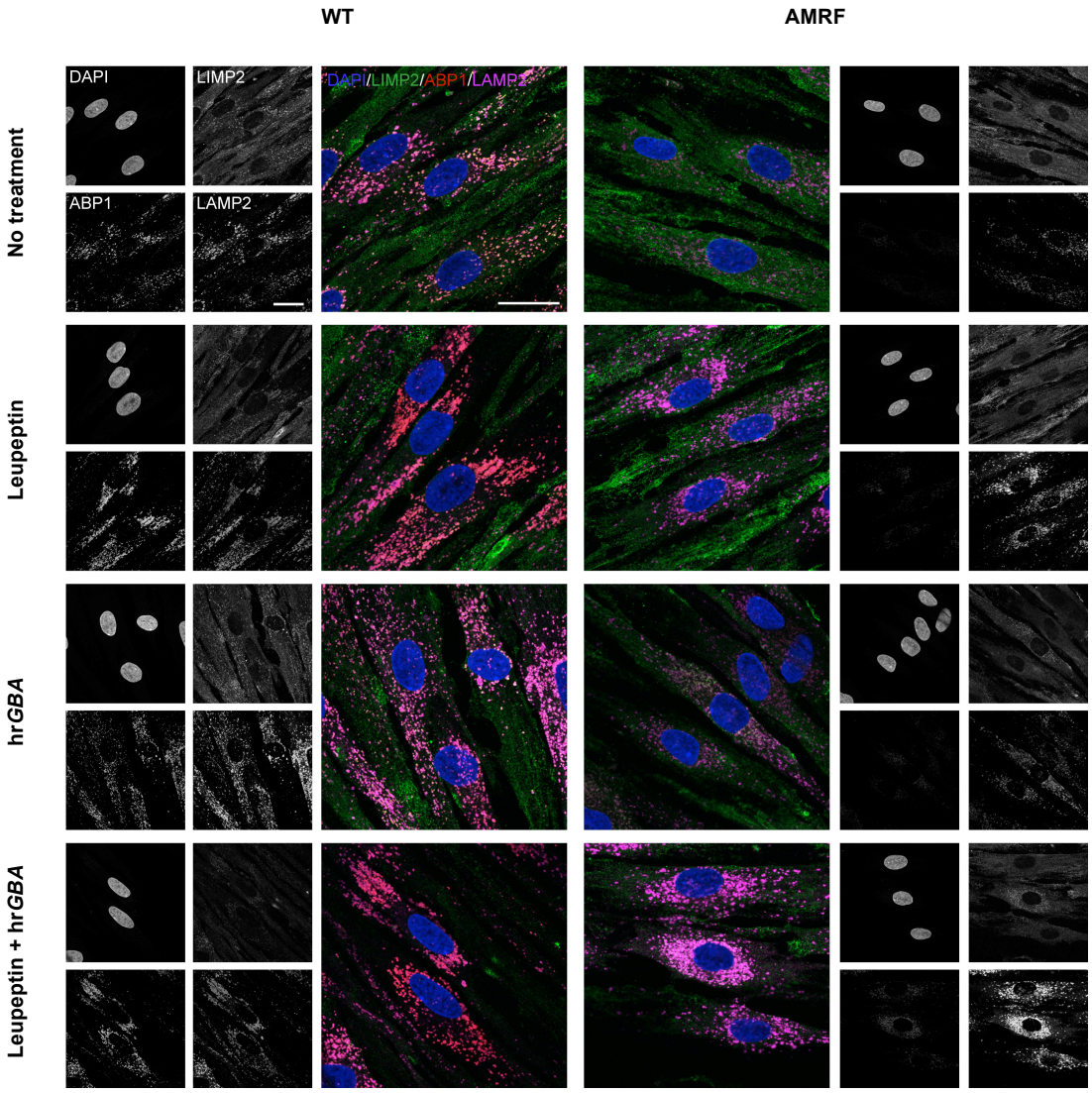

Figure 5.3 – Detection of GCase in wild type and AMRF fibroblasts. Cells were treated with or without leupeptin and with hr*GBA*, Left panel - wild type fibroblasts; Right panel - AMRF fibroblasts; "ABP1" - Activity based probe; "DAPI" - Nucleus staining.

5.3.2.3 Role of LIMP-2 in stability of human recombinant glucocerebrosidase as assessed in modified HEK293T cells

Given the observed lability of GCase in lysosomes of AMRF fibroblasts, we attempted to recapitulate this finding by constructing HEK293T cells deficient in LIMP-

2. For this purpose, in HEK293T cells, *SCARB2* gene was knocked-out by CRISPR technology [279]. In addition, HEK293T cells were stably transfected with cDNA encoding the mannose receptor. Mannose receptor positive cells allow a more efficient uptake of hr*GBA* with terminal mannose residues in its N-linked glycans. Having available the different HEK293T cell lines, the experiments conducted with fibroblasts described above were repeated (Fig. 5.4). As observed with the wild type fibroblast cell lines (Figs 5.1 and 5.2), control HEK293T cells showed an increase in GCase in the presence of leupeptin, either transfected or non-transfected with mannose receptor. In the cases of the LIMP-2 deficient HEK293T cells, the presence of leupeptin also resulted in increased GCase activity, despite still being very low (Fig. 5.4, left panel). Upon addition of hr*GBA* to the HEK293T cell lines, a marked increase in cellular GCase became apparent, particularly in cells transfected with the mannose receptor. GCase activity increased mostly when hr*GBA* was added after the treatment with leupeptin (Fig. 5.4, right panel). Just adding hr*GBA* alone to the LIMP-2 deficient HEK293T cells, hardly resulted in increased cellular GCase activity (Fig 5.4, right panel). The concomitant presence of leupeptin during incubation in LIMP-2 deficient cells expressing mannose receptor with hr*GBA* resulted in a very prominent increase of cellular GCase activity. Levels of GCase became almost identical to those seen in corresponding wild type cells (Fig 5.4, right panel). Thus, the findings with fibroblasts were recapitulated: endogenous as well as exogenous GCase in lysosomes of LIMP-2 deficient cells are prone to leupeptin sensitive proteolytic degradation. This finding suggests that the presence of LIMP-2 in lysosomes strongly stabilizes GCase.

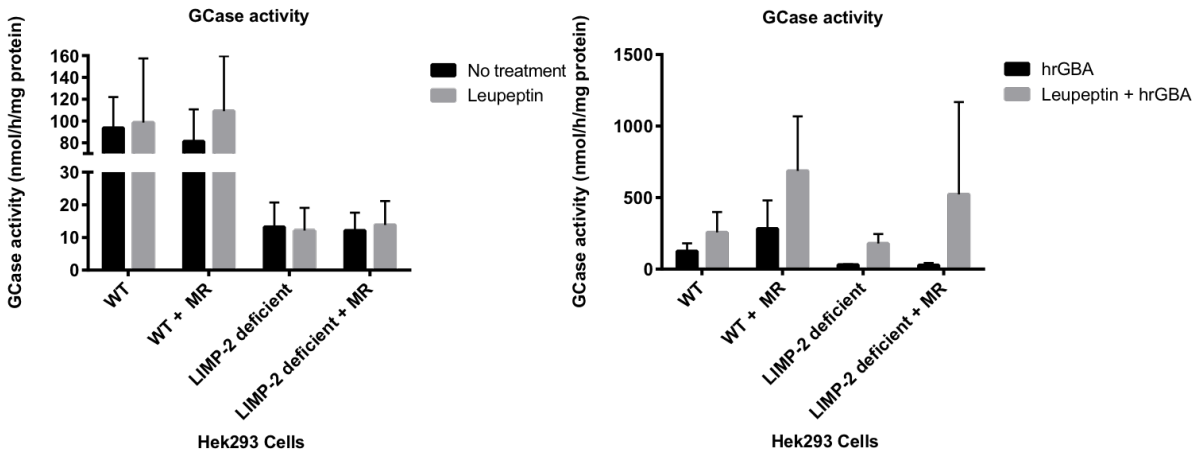

Figure 5.4 – GCase activities in wild type and LIMP-2 deficient HEK293T cells with or without mannose receptor: effect of LIMP-2 and exposure to exogenous GCase. Cellular GCase was measured with the fluorescent substrate 4-MU-β-D-Glc. Left panel - Cells not exposed to exogenous hr*GBA*; Right panel - Cells exposed to exogenous hr*GBA*. "MR" - mannose receptor.

5.3.2.4 Similar uptake of human recombinant glucocerebrosidase by wild type and LIMP-2 deficient HEK293 cells

To evaluate whether the uptake of hr*GBA* differs in LIMP-2 deficient cells, hr*GBA* was added to the various HEK293T cells, with or without expression of the mannose receptor. At several time points up to 30 min, cells were harvested and analyzed for GCase content (Fig. 5.5). Leupeptin was present during the entire experimental procedure. Very similar rates of uptake were observed for wild type and LIMP-2 deficient cells in the absence of mannose receptor, indicating that LIMP-2 plays no major direct role in endocytosis of hr*GBA*. Only the wild type cells expressing mannose receptor showed a slightly faster uptake of hr*GBA* in the experiment depicted.

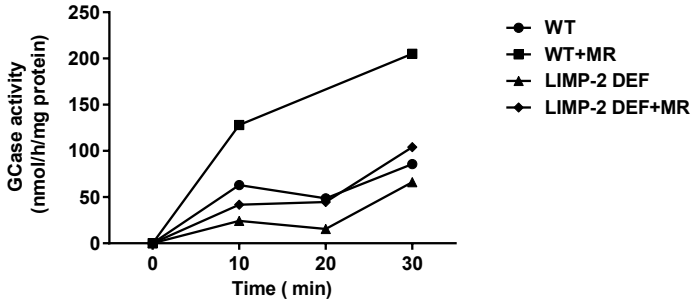

Figure 5.5 – Increment in cellular GCase during exposure to hr*GBA* in different HEK293T cell lines in presence of leupeptin. GCase activities were measured with the fluorescent substrate 4-MU-β-D-Glc. The cellular GCase present prior to uptake was subtracted and the increment in cellular GCase activity over time is shown.

5.3.2.5 Stability of human recombinant glucocerebrosidase in wild type and LIMP-2 deficient lysosomes

Fibroblast from a control subject, an AMRF patient and *GBA* L444P/L444P GD patient were incubated with hr*GBA* for 4 days, and then chased for different time points in the absence of leupeptin (Fig. 5.6). The reduction in cellular GCase activity during the chase was very prominent in AMRF fibroblasts when compared to wild type and GD cells. The half-life of GCase in the AMRF fibroblasts was only about 15 h (Fig. 5.6, right side).

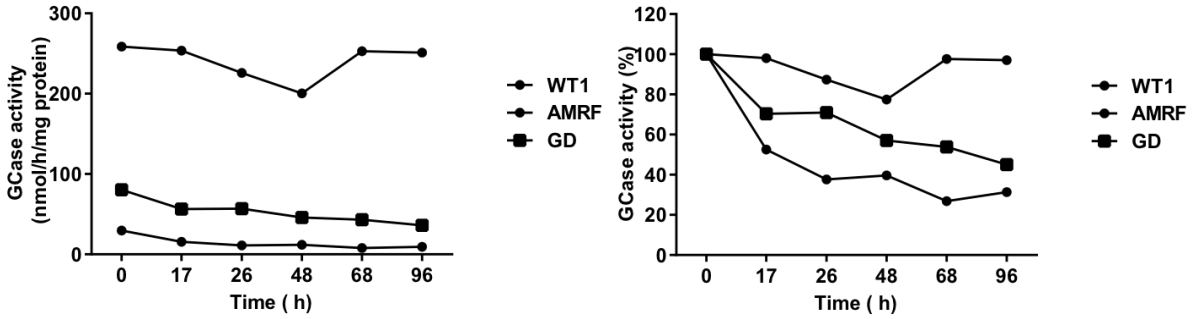

Figure 5.6 – Chase of endocytozed hr*GBA* in different fibroblast cell lines. GCase activities measured with the fluorescent substrate 4-MU-β-D-Glc. Left panel - Absolute GCase activity; Right panel - Relative GCase activity. The activity at the beginning of the experiment (T0) was assumed to be 100%

To assess whether hr*GBA* has a different sensitivity for proteolytic breakdown inside wild type and LIMP-2 deficient lysosomes, a 34 h chase of endocytozed hr*GBA*

was performed in the presence of leupeptin in the differents cell lines (wild type, GD and AMRF fibroblasts) (Fig. 5.7). In the presence of this protease inhibitor the stability of cellular GCase following uptake of hr*GBA* was very similar in wild type, GD and AMRF fibroblasts. This observation, together with the findings obtained in the absence of leupeptin (Fig. 5.6), indicates that proteolytic turnover of endocytozed hr*GBA* occurs faster in AMRF lysosomes compared to LIMP-2 positive lysosomes. Therefore, intralysosomally LIMP-2 may assist in conformational stabilization of GCase and thus reduce its intralysosomal proteolytic degradation.

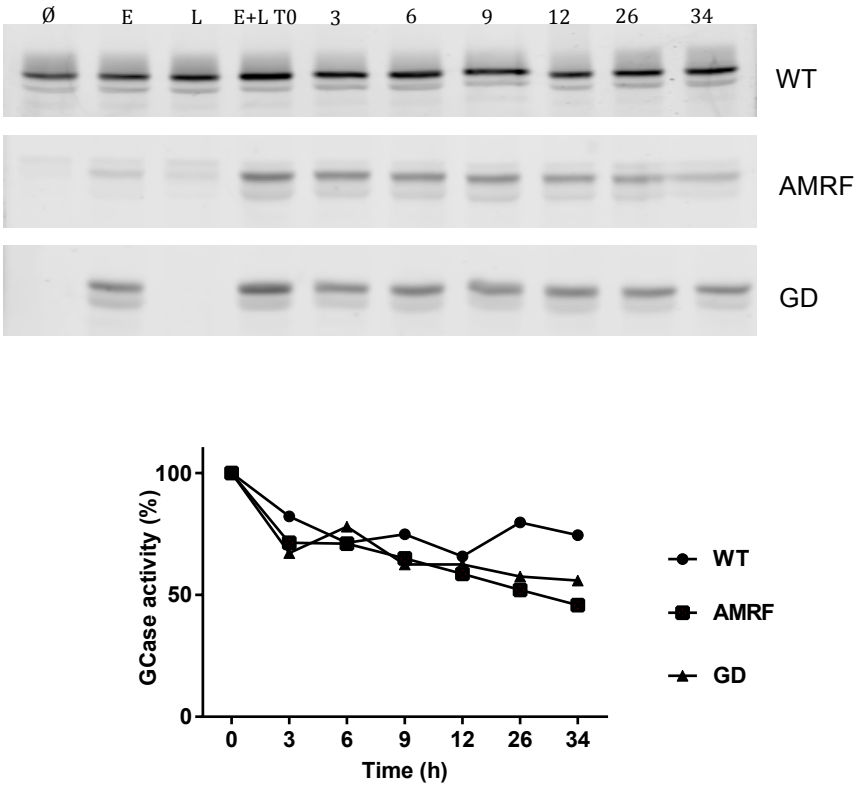

Figure 5.7 – Half-life of hr*GBA* in presence (+) of leupeptin. Activity at T0 was assumed as 100% for each cell line. Upper panel - SDS-PAGE slab-gels with ABP labelling of GCase. Lower panel - GCase activity measured with fluorescent substrate. "Ø" - no treatment; "E" - hr*GBA*; "L" - Leupeptin; "E+L" - Leupeptin plus hr*GBA*.

5.3.3 Discussion

In the present study we investigated the impact of LIMP-2 on GCase beyond it's binding to the receptor protein and subsequent intracellular transport into the lysosome. The key role of LIMP-2 in sorting GCase from the ER to lysosomes has been unequivocally demonstrated. Binding of newly formed GCase to a specific domain in LIMP-2 governs its routing to lysosomes [194]. It has been proposed that at low pH the complex dissociates and GCase is released [58, 202]. However, binding of GCase to LIMP-2 is not completely abolished at pH values below 6.0 [58]. It is therefore conceivable that even inside lysosomes GCase and LIMP-2 may transiently bind with beneficial effects regarding GCase fold and resistance against proteolytic breakdown. To study this possibility we exposed wild type and LIMP-2 deficient HEK293T cells to leupeptin, an inhibitor of the lysosomal cathepsins B, F, L and S, all cysteine proteases. Leupeptin is known for a long time to effectively reduce intralysosomal degradation of GCase [280]. We observed that leupeptin caused a minor increase in GCase levels in fibroblasts obtained from a type 3 GD patient homozygous for *GBA* L444P. It is known that in such individuals, reduced amounts of enzyme reaches the lysosomes due to predominant misfolding in the ER. Consequently, little stabilization by leupeptin treatment can be observed (see also [280]). In contrast, some increase in GCase is induced in wild type fibroblasts by the presence of leupeptin. Striking is the response of AMRF fibroblasts. In this case, the leupeptin mediated increase in cellular GCase is very prominent. This suggests that the little amount of GCase that manages to reach lysosomes during LIMP-2 deficiency is very prone to intralysosomal proteolytic degradation, which is leupeptin inhibitable. A similar observation was obtained from follow-up experiments in which cells were incubated with hrGBA. It was observed that in GD fibroblasts, as in wild type cells, hrGBA was taken up and delivered to lysosomes. Again, in lysosomes of AMRF cells, the hrGBA appeared far more sensitive to proteolytic, leupeptin-inhibitable, degradation when compared to wild type fibroblasts. The half-life of endocytozed hrGBA in AMRF fibroblasts was surprisingly short, being only about 15 h. To exclude if the differences observed between wild type and AMRF fibroblasts

were due to genetic differences beyond the *SCARB2* gene in the two donors, we generated from the same HEK293T cell line by CRISPR technology, LIMP-2 deficient cells. The observations with fibroblasts were fully recapitulated in the HEK293T LIMP-2 deficient cell lines: endogenous or exogenous GCase in LIMP-2 deficient lysosomes appears far more vulnerable to leupeptin-inhibitable proteolytic breakdown. Based on this observation, it can be speculated that indeed transient interactions between LIMP-2 and GCase in lysosomes exert a crucial beneficial effect. Therefore, ERT in AMRF patients may not be a very successful therapeutic approach. Moreover, it may even possible that the effectiveness of ERT is maximized by the endogenous finite presence of LIMP-2 in lysosomes. When ERT with very high doses of hrGBA would result in a far excess of exogenous GCase over endogenous LIMP-2 in lysosomes, the stability of such enzyme could be limited due to restricted availability of LIMP-2. Theoretically, administration of very large amounts of hrGBA to cells may reduce the stability of endogenous GCase due to competition for LIMP-2 stabilization inside lysosomes. It should be noted that a stabilizing effect of LIMP-2 on intralysosomal GCase has important implications. GD patients who concomitantly are carriers for LIMP-2 deficiency may present less lysosomal GCase compared to similar patients with normal LIMP-2. Indeed, it has been reported that carriership for LIMP-2 deficiency acts as modifier and worsens the clinical course of GD [225].

We also investigated whether LIMP-2 may be involved in uptake of GCase, since low amounts of LIMP-2 are likely to be also transiently present at the cell surface. However, no evidence for this was obtained in experiments with wild type and LIMP-2 deficient HEK293T cells. Preliminary experiments regarding the uptake of hrGBA seemed very similar, in contrast to the subsequent stability of the endocytozed enzyme. The use of ERT to treat GCase deficiency in AMRF patients is not an attractive approach. We have earlier demonstrated that GCase is deficient in most cell types during LIMP-2 deficiency (see chapter 3). White blood cells, in particular monocytes-macrophages, do not seem to be implicated in the pathology of AMRF in sharp contrast to the situation in GD. The use of a macrophage targeted, mannose-terminated recombinant GCase, as present in Cerezyme®, Velaglucerase® and Taliglucerase®, would likely not lead to the correction of clinically relevant cell types in

AMRF patients. Other therapeutical approaches such as gene therapy or pharmacological manipulation of the glycosphingolipid metabolism seem to be more attractive to ameliorate abnormalities in AMRF patients. Studies with *LIMP-2 KO* mice, which offer a genuine model for human AMRF, will be decisive to determine in the future, which approach is the most appealing to treat AMRF, a disorder with still unmet clinical needs.

In summary, the interaction of LIMP-2 and GCase takes place in multiple parts of the cell. Immediately after synthesis, GCase is bound to LIMP-2 and routed to lysosomes in a complex. Inside lysosomes, LIMP-2 and GCase transiently dissociate and re-bind. The latter process seems essential for the stability of GCase conformation and its associated resistance against degradation by leupeptin-inhibitable cathepsins. Thus, GCase is heavily dependent on LIMP-2 from its birth to death, from routing from ER to lysosomes and for its intralysosomal survival.

5.4 Pilot study on Substrate Reduction Therapy in LIMP-2 deficiency (Mice and cells)

5.4.1 Methods

5.4.1.1 Animal studies and tissue collection and homogenization

LIMP-2 KO mice, kindly provided by Prof. Paul Saftig (Kiel, Germany), were generated as described in section 4.3.1. A total of 12 animals were used, all male of 3-4 months of age, equally distributed in genotype (wild type and *LIMP-2 KO*). Three wild type and 3 *LIMP-2 KO* mice were treated on a daily basis, for 14 consecutive days with a single dose of the Vehicle (1% DMSO/PBS), while 3 WT and 3 *LIMP-2 KO* mice were treated daily with the GCSi 1307RB20 (1 mg/kg/day). After 14 days, all mice were sacrificed for collection of blood and organs. The collection of the tissues and the homogenization procedure is detailed in section 4.3.2 and 4.3.5, respectively.

5.4.1.2 *SCARB2* gene knock-out in HEK293T cells and transfection of macrophage mannose receptors

SCARB2 gene knock-out and transfection with cDNA encoding mannose receptor is described in section 5.3.1.2 and 5.3.1.3.

5.4.1.3 Culturing of HEK293T cells

HEK293T were cultured in DMEM with high glucose supplemented with 10% FBS (Bodinco) and 100 units/ml Pen/Strep. One day before transfection 4 x 10^5 cells were seeded in a 6 well plate. During 4 days, HEK293T were cultured in DMEM with high glucose (Gibco) supplemented with 10% FBS and 100 units/ml Pen/Strep, with different concentrations (0; 0.1; 1; 10; 50; 100 nM) of the GCSi compound 1307RB20. At the fourth day, the cells were harvested and the homogenization procedure and protein quantification was performed as described in 3.3.4.

5.4.1.4 Neutral glycosphingolipids, glucosylsphingosine and cholesterol-glucoside measurements

Neutral glycosphingolipids, GlcSph and GlcChol were determined in the homogenates as described in section 4.3.11.

5.4.2 Results

5.4.2.1 Substrate reduction therapy and *LIMP-2 KO* mice

A new generation of GCS inhibitors has been recently generated, with increased specificity [167]. These ido-deoxynojirimycin-type compounds strongly inhibit GCS and non-lysosomal β-glucosidase, GBA2, but very poorly GCase. From these new compounds available, it was selected the 1307RB20, which has an IC_{50} for GCS of 2.5 nM, for *GBA2* of 0.6 nM and for GCase of 6 μM [167]. In order to decrease the levels of GlcCer, *LIMP-2 KO* mice were treated for 14 consecutive days with 1307RB20, which was administered daily at 1 mg/kg. The animals were sacrificed and the levels of ceramide, GlcCer, GlcSph and GlcChol in liver, kidney, spleen, eye, duodenum and ileum were analyzed (Fig. 5.8 to 5.11).

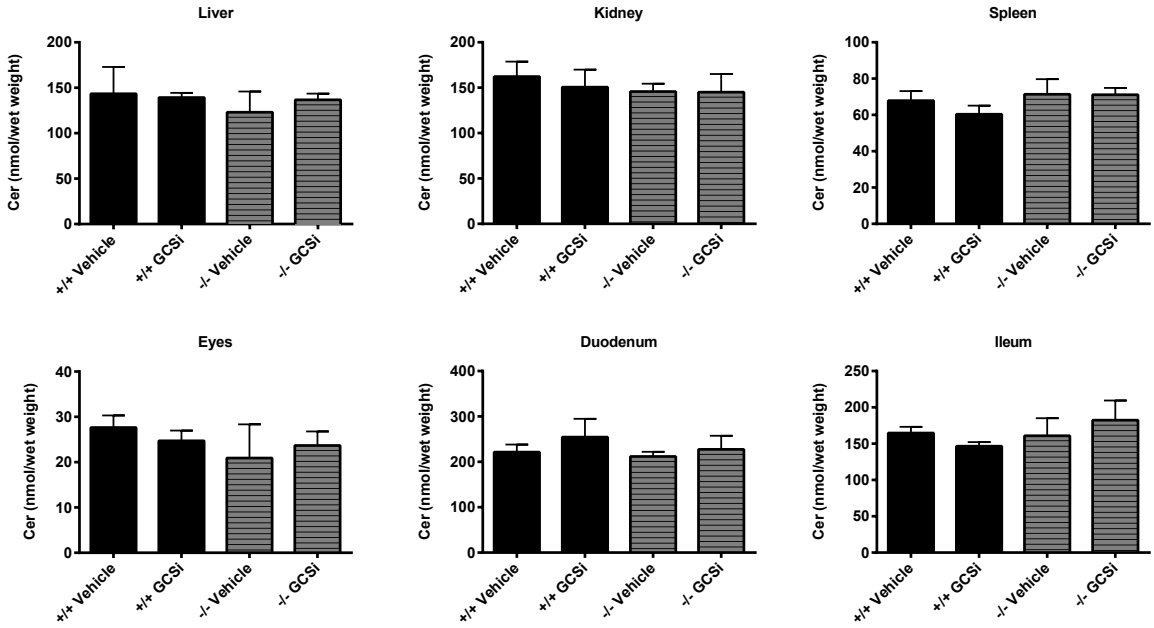

Figure 5.8 – Ceramide levels in wild type (+/+) and *LIMP-2 KO* (-/-) mice treated with vehicle or GCSi.

Untreated wild type and *LIMP-2 KO* mice have similar levels of ceramide in the analyzed organs. The conducted treatment with the GCS inhibitor did not change the ceramide content of these organs (Fig. 5.8). Regarding GlcCer, no marked

differences exist between control and *LIMP-2 KO* mice in the liver, eye, duodenum and ileum (Fig. 5.9). Only the kidney of *LIMP-2 KO* mice presents a two-fold higher amount of GlcCer, when compared to wild type mice. The treatment with GCSi did not result in a clear reduction in the levels of this glycosphingolipid as expected (Fig. 5.9). Only in the case of the duodenum a slight decrease in the levels of GlcCer was observed in control and *LIMP-2 KO* mice subjected to treatment. In the eye, and more clearly in the spleen, the GCS inhibithor treatment led to an increase of GlcCer levels which can only be ascribed to *GBA2* inhibition without concomitant major inhibition of GCS. Next, the deacylated form of GlcCer, GlcSph was measured (Fig. 5.10).

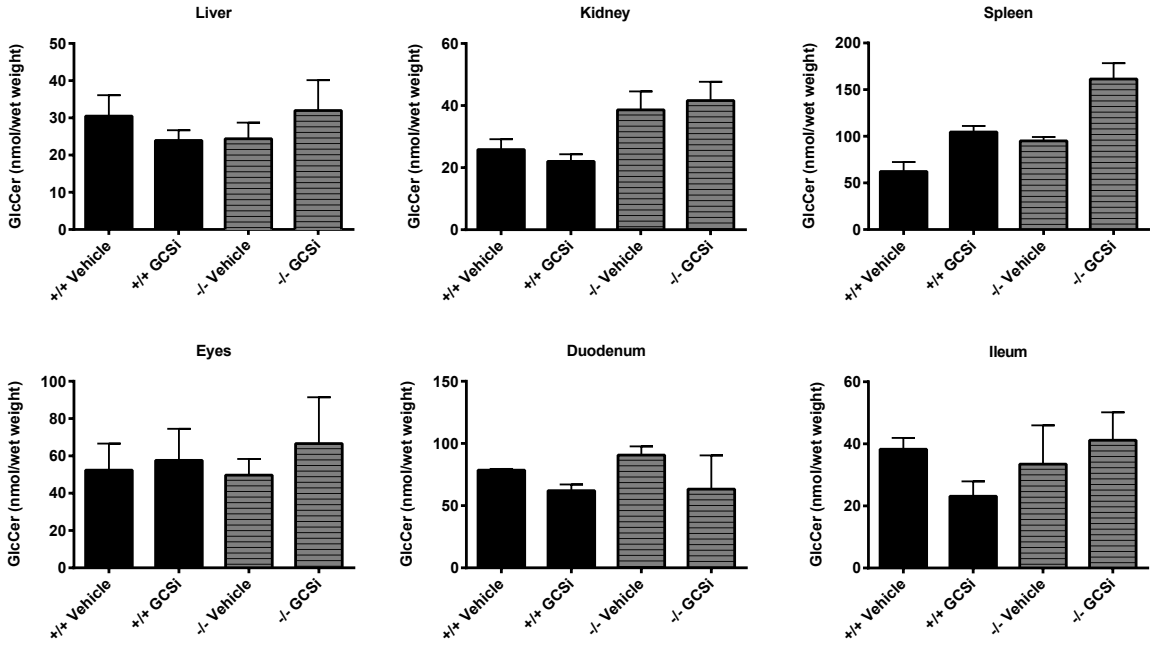

Figure 4.9 – GlcCer levels in wild type (+/+) and *LIMP-2 KO* (-/-) mice treated with vehicle or GCSi.

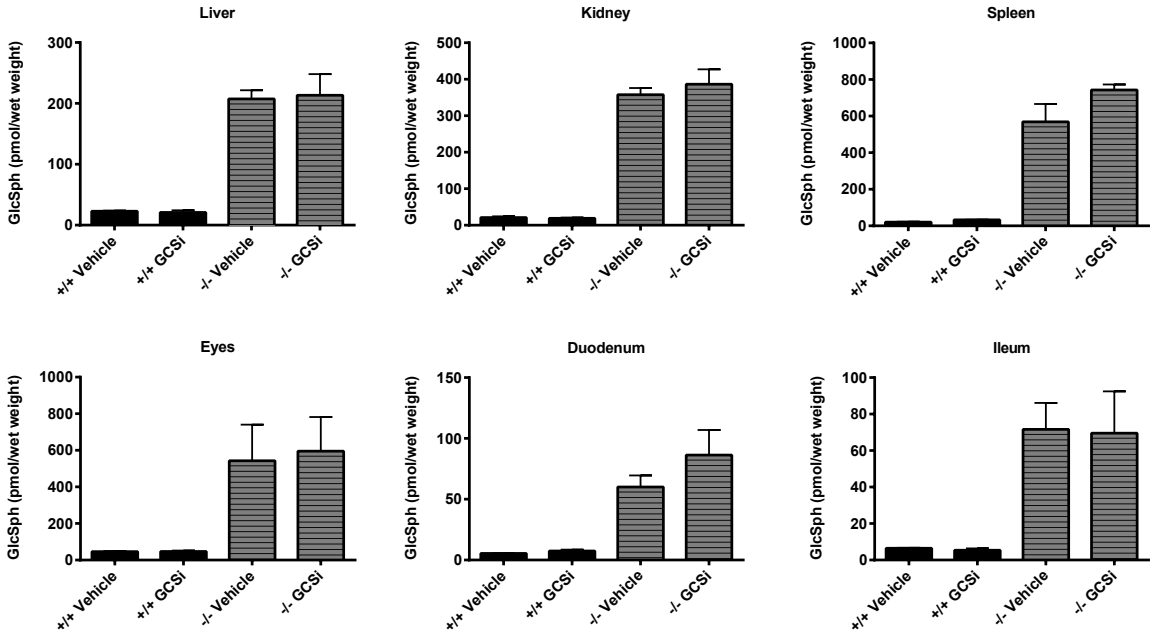

Figure 5.10 – GlcSph levels in wild type (+/+) and *LIMP-2 KO* (-/-) mice treated with vehicle or GCSi.

LIMP-2 KO mice show increased GlcSph levels in all tissues when compared to control mice. The abnormality is particularly evident in the spleen and eye (Fig. 5.10). The treatment with the GCS inhibitor failed to decrease GlcSph levels as it was expected (Fig. 5.10).

Since 1307RB20 is a more potent inhibitor of *GBA2* as compared to GCS [167], and *GBA2* forms by transglucosylation GlcChol [252, 281] (Marques *et al.*, unpublished results), the concentration of this lipid was also determined in untreated and treated mice (Fig. 5.11).

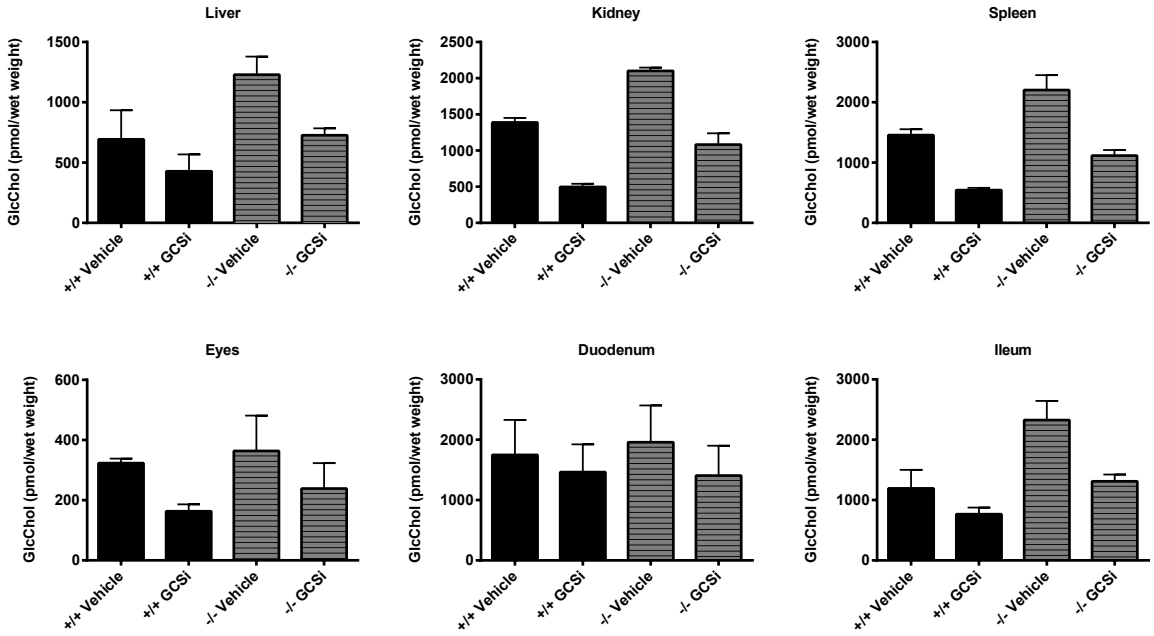

Figure 5.11 – GlcChol levels in wild type (+/+) and *LIMP-2 KO* (-/-) mice treated with vehicle or GCSi.

LIMP-2 KO mice show higher tissue levels of GlcChol than wild type (Fig. 5.11). Treatment with 1307RB20 reduced GlcChol levels in *LIMP-2 KO* mice as well as in the control group in all organs examined. This finding suggests that the concentration of 1307RB20 used was sufficient to inhibit *GBA2*. Apparently, however the concentration was not high enough to cause a major inhibition of glucosphingolipid *de novo* synthesis via GCS.

5.4.2.2 Substrate reduction therapy and LIMP-2 deficient cells

In order to understand if the administered dose of 1307RB20 was sufficiently high, a cell-based experiment was carried out. Wild type HEK293T cells and HEK293T cells, with the *SCARB2* gene depleted by CRISPR technology, were used to test the *in vivo* inhibitory activity of 1307RB20. Cells were treated with different concentrations of 1307RB20, ranging from 0-100 nM, for 3 days. The cells were collected and ceramide, GlcCer, GlcSph and GlcChol levels were measured (Fig. 5.12).

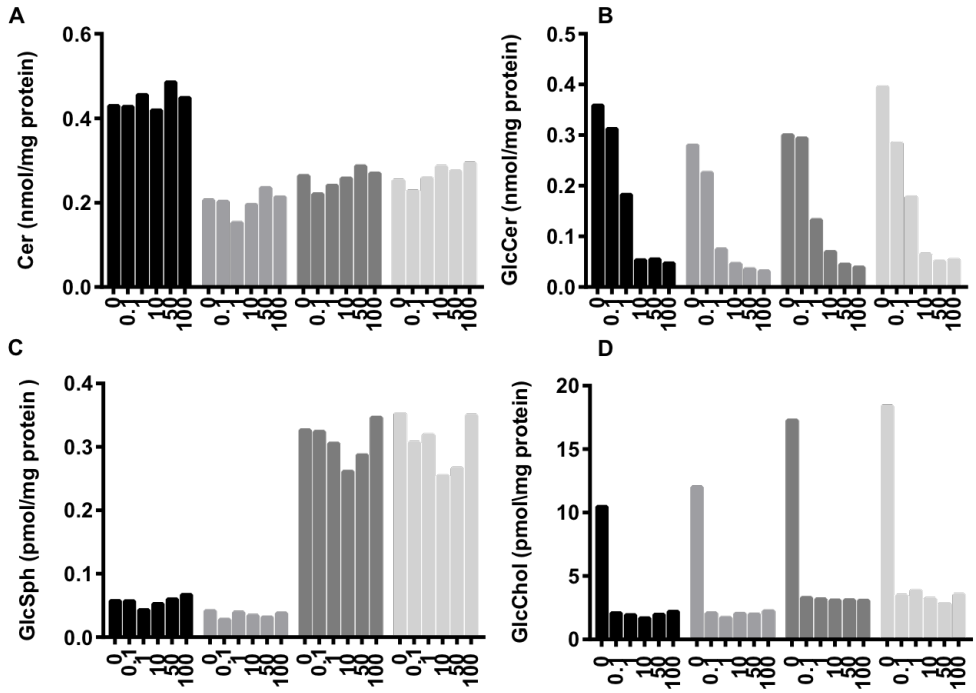

Figure 5.12 – Levels of Ceramide, GlcCer, GlcSph, GlcChol in wild type and LIMP-2 deficient HEK293T cells treated with 1307RB20. WT WT+MR LIMP-2 deficient LIMP-2 deficient + MR

No significant changes were observed in ceramide levels in the HEK293T cell lines treated with different concentrations of 1307RB20 (Fig. 5.12A). In the case of the GlcCer, wild type and LIMP-2 deficient cells showed similar levels when not treated. GlcCer levels started to decrease with increasing 1307RB20 concentration in the medium, being reduced to half at the concentration of 1 nM (Fig 5.12B). HEK293T LIMP-2 deficient cells present a massive storage of GlcSph, when compared to wild type cell lines. Surprisingly, again with 1307RB20 treatment rendered minor reductions in GlcSph. At higher concentrations of 1307RB20, GlcSph levels even started to increase again (Fig 5.12C). In sharp contrast, GlcChol already at the lowest concentration tested, 0.1 nM, showed a drastic reduction in both wild type and LIMP-2 deficient HEK293T cells (Fig 5.12D).

5.4.3 Discussion

Substrate reduction offers an alternative therapy to ERT for type 1 GD patients, especially for those patients who do not tolerate ERT well because of immunoreactivity, hypersensitivity, or poor venous access. SRT aims to inhibit the first step in the glycosphingolipid biosynthesis, catalyzed by GCS, and thus generate a better balance between biosynthesis and catabolism of glycosphingolipids [158, 274, 282, 283]. In LIMP-2 deficiency, causing AMRF due to the lack of GCase, the levels of GlcCer and especially its deacylated form, GlcSph, are increased. Likewise, in GD and AMRF, accumulating GlcCer is actively converted to GlcSph by the lysosomal enzyme acid ceramidase [284]. Since in LIMP-2 deficiency, the monocyte lineage presents relatively high residual GCase activity, avoiding the formation of lipid-laden macrophages, ERT with a macrophage-targeted enzyme does not seem an ideal therapeutic approach [201, 218, 271, 285]. On the other hand, SRT seems to be an attractive option for treatment of lipid abnormalities caused by LIMP-2 deficiency, due to the induced reduction in GlcCer. Wild type and *LIMP-2 KO* mice were treated daily, during 14 days, with 1 mg/kg of 1307RB20. Whilst the lack of effect of the inhibitor treatment on ceramide levels was expected, the fact that no reductions were seen in the levels of GlcCer or GlcSph in the treated animals was surprising. Only in the case of the duodenum, a slight reduction of GlcCer was observed for the treated mice. Given the lack of response to the inhibitor 1307RB20 in GlcCer and GlcSph tissue concentrations in *LIMP-2 KO* mice, it suggests that the administered dose and/or the time period of drug treatment were insufficient to generate the desired response.

The enzyme *GBA2* is also inhibited by 1307RB20 and the reduction in tissues of treated mice of GlcChol, a lipid formed by *GBA2* activity, suggest that the applied concentration was sufficient to significantly inhibit this enzyme in the animals. The IC_{50} of *GBA2* for 1307RB20 (0.6 nM) is about 4-fold lower than that of GCS (2.5 nM). Therefore, it seems that treatment of animals with a 10-fold higher dose would have most likely resulted in a detectable reduction of GlcCer. Indeed, experiments with HEK293T cells indicated that 1307RB20 is able to lower GlcCer significantly at

concentration ranging from 1 – 10 nM. The findings obtained with HEK293T cells are consistent with earlier determined inhibitory parameters using different *in vitro* determinations [167]. The finding with LIMP-2 deficient HEK293T cells treated with 1307RB20, which at concentrations of 10 nM leads to a reduction in GlcCer but without concomitant major reduction in GlcSph, remains puzzling. It is generally assumed that GlcSph is predominantly generated in GCase deficient lysosomes by deacylation of accumulating GlcCer through the action of acid ceramidase (*ASAH1*). The present findings on GlcSph in the LIMP-2 deficient cells are difficult to reconcile with this observation. Further investigations with LIMP-2 deficient HEK293T cells fed with $^{13}C_5$ isotope-labelled GlcCer and GlcSph, which have recently become available by synthesis (Wisse, Ferraz, unpublished), will certainly shed some light on the observed phenomenon.

It is of great importance to determine whether GlcSph abnormalities during LIMP-2 deficiency are responsive to SRT based on pharmacological GCS inhibition. Of note, treatment of type 1 GD patients with the latest generation GCS inhibitor, Eliglustat, did result in marked reduction of GlcSph in plasma (Ferraz, Smid, unpublished results). A comparison of the effects of Eliglustat and 1307RB20 on GlcSph metabolism in LIMP-2 deficient cells will be extremely informative to assess the potential of SRT for treatment of AMRF.

Due to the lack of established treatments for AMRF, it seems mandatory to include LIMP-2 deficient cells in screenings for candidate drugs aiming to modify glycosphingolipid metabolism and ameliorate the symptomatology of AMRF patients.

6. CONCLUSION

CONCLUSION

The work here presented describes laboratory investigations on the consequences of lysosomal membrane protein LIMP-2 deficiency, focusing in to the impact on the lysosomal hydrolase GCase that degrades intralysosomally GlcCer.

At the start of the thesis work, it was already known that LIMP-2 acts as a transporter of newly formed GCase to lysosomes [57]. It was also recognized that the rare inherited disease AMRF is caused by inherited defects in the *SCARB2* gene encoding LIMP-2 [210]. Surprisingly, the clinical manifestation of AMRF differs completely from GD, which is caused by mutations in the *GBA* gene encoding GCase [218]. There were also already indications that LIMP-2 deficiency causes a cell-type specific reduction in GCase levels, with the decrease being particularly small in white blood cells [201]. The high residual GCase activity in white blood cells, including monocytes/macrophages, could explain the absence of lipid-laden macrophages in AMRF patients. In sharp contrast to this, lipid-laden macrophages, the “Gaucher cells”, are the hallmark of GD and are thought to underlie various clinical manifestations ranging from splenomegaly, hepatomegaly, pancytopenia, anemia, thrombocytopenia to skeletal deterioration [113]. None of these symptoms occur in AMRF patients [218]. Characteristic features of AMRF are neurological manifestations with prominent epileptic attacks and ataxia. Only severely affected type 2 and 3 GD patients develop neurological complications at infantile and juvenile age, respectively. Most GD patients however develop a non-neuronopathic (type 1) course of disease with variable severity and age of onset of visceral symptoms [87].

The aims of the thesis investigation were the following: establishment of an improved procedure for laboratory diagnosis of AMRF, obtain insight in the cell-type specificity of GCase deficiency during LIMP-2 deficiency and to examine potential therapeutic avenues for AMRF.

A. Improved laboratory diagnosis of AMRF.

The initial studies focused on the features of GCase in leukocytes and cultured fibroblasts as well as plasma specimens of AMRF patients, GD patients and normal

subjects [248]. These studies were largely conducted by the newly developed research tools for visualization of GCase enzyme [131, 133]. It was confirmed that GCase levels are extremely low in AMRF fibroblasts, even lower than in type 1 GD fibroblasts. The detection of GCase with this very sensitive method allowed the demonstration of partial secretion of residual GCase from AMRF fibroblasts, contrary to the situation observed for GD and wild type fibroblasts.

Subsequent examination of plasma of an AMRF patient revealed increased amounts of GCase. Since GCase is unstable at neutral pH, enzyme activity is rapidly lost when plasma samples are not immediately frozen. Diagnosis of AMRF patients based on elevated GCase activity is therefore not reliable since false negatives may occur.

Given the noted very low levels of GCase in AMRF fibroblasts and the earlier finding that GCase deficient Gaucher fibroblasts show markedly increased levels of GlcSph formed from accumulating GlcCer [117], the sphingoid base was studied in AMRF cells. Clear increases of GlcSph were noted for AMRF fibroblasts and subsequent analysis of plasma specimens of AMRF patients showed elevated GlcSph levels far above normal values. This finding was confirmed by investigation of plasma specimens of *LIMP-2 KO* and normal mice. Plasma GlcSph is also increased in symptomatic GD patients, which also typically show elevated plasma biomarkers derived from Gaucher cells like chitotriosidase [89]. Such lipid-laden macrophages are not present in AMRF patients [201] and consequently plasma chitotriosidase is in the normal range. Combining all the findings, a differential laboratory diagnosis of AMRF and GD can be made. The workflow for convenient laboratory diagnosis of AMRF, prior to sequencing of the *SCARB2* gene, is as follows. If in an individual a markedly increased plasma GlcSph is detected in the absence of elevated chitotriosidase this is an indication for AMRF. Measurement of GCase activity in fibroblasts should show a reduced enzymatic activity to consider further the diagnosis AMRF. Such diagnosis can be further substantiated with the sequencing of the *SCARB2* gene.

In conclusion, demonstration of functional GCase deficiency by detection of abnormal high GlcSph in plasma is an important step in identification of individuals suffering from deficiency in LIMP-2 [248].

B. Tissue and cell-type dependent impact of LIMP-2 deficiency on secondary GCase reduction and lipid abnormalities.

Mutations in the *SCARB2* gene cause defects in the integral membrane protein LIMP-2 and subsequent impaired transport of newly formed GCase to lysosomes of cells of AMRF patients. The marked phenotypic difference between GD and AMRF prompted a detailed investigation on abnormalities in GCase and functionally related lipid abnormalities. The number of identified AMRF patients is still small, limiting investigations with human material. Fortunately, a genuine animal model for AMRF was generated by Saftig and co-workers some years ago when generating a knock-out of the *SCARB2* gene. The disease symptoms of these *LIMP-2 KO* mice phenotypically resemble in many aspects AMRF in man [190]. As part of the thesis work, GCase and its lipid metabolites were examined in several tissues of *LIMP-2 KO* mice. First, it was examined whether LIMP-2 deficiency also affects other lysosomal matrix enzymes than GCase. For this purpose, the proteome of isolated lysosomes from hepatocytes of wild type and *LIMP-2 KO* mice was examined by LC-MS^{e}. No significant differences were noted in lysosomal matrix proteins, except a major deficiency in GCase. Next, the level of active GCase molecules in various tissues of *LIMP-2 KO* mice was analyzed. Comparable results were obtained either by using conventional enzymatic assay or ABP, revealing a gradient in deficiency of functional GCase along LIMP-2 deficient tissues. Next, lipid levels were determined in the various tissues. Importantly, the concentrations of GlcCer did not correlate with the extent of GCase deficiency. For example, GlcCer was normal in liver despite an extremely low GCase level. In sharp contrast to the findings for GlcCer, GlcSph was markedly increased in tissues, which correlate with GCase deficiency. The amount of sphingoid base was the highest in those tissues with lowest GCase content. The maximal increase in tissue GlcSph occurred already in very young (2 months old) *LIMP-2 KO* mice. Apparently, in most cell types of LIMP-2 mice, storage of GlcCer is

prevented by active deacylation of the lipid to GlcSph. This deacylation seems to be catalyzed by the lysosomal acid ceramidase (*ASAH1*) [89] (Ferraz et al ,unpublished results).

At the Department of Medical Biochemistry, The Netherlands, another lipid abnormality in GD patients was recently identified (Marques *et al.* to be published). The hitherto unknown lipid GlcChol (GlcChol) is elevated in GD patients. Analysis of tissues of *LIMP-2 KO* mice also revealed elevated levels of GlcChol. This indicates that GCase normally degrades the glucosylated sterol.

The marked differences in clinical symptoms of AMRF patients and GD patients are likely due to the absence of Gaucher cells in AMRF patients. The cause for this prominent difference was further investigated. Considerable residual GCase activity is present in LIMP-2 deficient white blood cells, sharply contrasting with the low residual GCase in AMRF fibroblasts. The cause for this striking difference was experimentally studied. It was observed a considerable uptake through (dynamin-dependent) endocytosis of GCase from the medium by AMRF lymphoblasts, but not fibroblasts. Based on this observation, it seems likely that in AMRF patients the re-uptake by leukocytes and macrophages of GCase secreted by tissue in plasma, renders sufficient residual GCase activity in these cells to prevent formation of Gaucher cells.

In conclusion, investigations with *LIMP-2 KO* mice revealed that marked differences occur among tissues and cell types in the amount of residual GCase. White blood cells show high residual GCase levels, likely due to uptake from plasma of secreted enzyme from tissues. This may explain the absence of lipid-laden macrophages in the animals. Most LIMP-2 deficient tissues seem to compensate very efficiently for their lack in GCase very efficiently by de-acylating GlcCer to GlcSph.

C. LIMP-2 deficiency: therapeutic approaches and intralysosomal interaction of LIMP-2 and GCase.

Although deficiency of GCase occurs both in GD and AMRF patients, no treatment is presently available for AMRF. For non-neuronopathic type 1 GD, however two

different kinds of therapies are registered: macrophage-targeted ERT and glycosphingolipid SRT. ERT aims to directly supplement macrophages in GD patients with GCase by chronic infusions with a macrophage-targeted recombinant GCase [145]. Since GCase is the prominent biochemical abnormality in AMRF patients we studied the feasibility of supplementing LIMP-2 deficient cells with recombinant GCase. For this purpose, we exposed cells to recombinant hrGCase (Cerezyme®) presently used in ERT of type 1 GD patients. Experiments were performed with normal and AMRF fibroblasts as well as with normal and LIMP-2 deficient HEK293T cells expressing mannose receptors to promote uptake of mannose-terminated Cerezyme®. In all cell types it was observed the endocytotic uptake and delivery to lysosomes, however GCase is rapidly degraded in LIMP-2 deficient lysosomes. The half-life of the enzyme in LIMP-2 lysosomes is far shorter than in corresponding normal lysosomes. Apparently, transient interactions of GCase with LIMP-2, in the lysosome, contribute to stabilization of the compact conformation of the enzyme and thus prevent its proteolytic breakdown. This notion is of great importance since it has important implications (see Fig. 6.1). It suggests that the amount of LIMP-2 in lysosomes installs an intrinsic limit for the efficacy with which lysosomal GCase activity can be increased by ERT. When too much enzyme is taken up, lack of interaction with the limited amount of LIMP-2 will promote rapid proteolytic breakdown. Based on this experimental findings, ERT for AMRF seems not a wise approach. The present enzyme used in ERT of type 1 GD is neither attractive as drug for neurologically affected AMRF patients since it is targeted to visceral macrophages and does not pass the BBB.

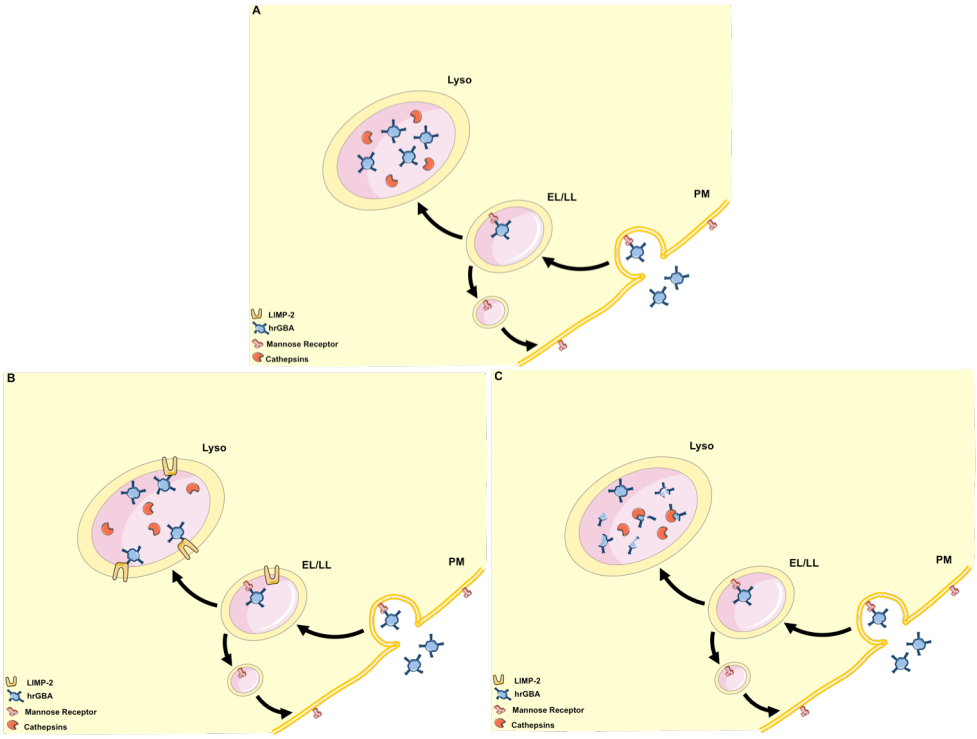

Figure 6.1 – Schematic model for uptake and stability of hrGBA. Presently accepted view (A); Proposed model for LIMP-2 positive wild type cells (B); Model for LIMP-2 deficient cells (C).

Given the drawbacks of ERT with GCase as treatment of AMRF, SRT may offer a more attractive therapy approach. SRT aims to reduce glycosphingolipid substrate levels for GCase by inhibiting GCS. A new generation of brain-permeable, potent GCS inhibitors, the so-called biphenyl-pentoxy-ido-deoxynojirimycins, has recently been developed by Aerts, Overkleeft and colleagues [167]. For this purpose *LIMP-2 KO* mice were orally treated with a brain-permeable GCS inhibitor at a nanomolar concentration. The dose used proved however to be too small to render sufficient inhibition of glycosphingolipid synthesis. Higher doses will be needed to establish the therapeutic efficacy in *LIMP-2 KO* mice.

In conclusion, a treatment is not yet available to ameliorate symptoms in AMRF. There is still an unmet need for this rare inherited disease. ERT with available (macrophage-targeted) GCase is not an attractive approach for treatment of AMRF. More promising is substrate reduction therapy using oral inhibitors of GlcCer synthesis. Further investigations on such approach in *LIMP-2 KO* mice are warranted.

Another important conclusion is that LIMP-2 seems to influence GCase at various stages of its life cycle. Firstly, LIMP-2 through binding in the endoplasmic reticulum and Golgi apparatus transports newly formed GCase to lysosomes, and secondly, by transient interactions in the lysosome it stabilizes the fold of GCase, and consequently protects it against proteolytic breakdown. Thus, LIMP-2 has a dual action as transporter and as chaperone of GCase.

7. REFERENCES

1. De Duve C, Pressman BC, Gianetto R, Wattiaux R, Appelmans F: **Tissue fractionation studies. 6. Intracellular distribution patterns of enzymes in rat-liver tissue.** *Biochem J* 1955, **60**:604–17.

2. Kornfeld S: **Structure and function of the mannose 6-phosphate/insulinlike growth factor II receptors.** *Annu Rev Biochem* 1992, **61**:307–30.

3. Eskelinen E-L: **Roles of LAMP-1 and LAMP-2 in lysosome biogenesis and autophagy**. *Mol Aspects Med* 2006, **27**:495–502.

4. Kornfeld S, Mellman I: **The Biogenesis of Lysosomes**. 1989.

5. Kolter T, Sandhoff K: **Sphingolipid metabolism diseases.** *Biochim Biophys Acta* 2006, **1758**:2057–79.

6. Luzio JP, Poupon V, Lindsay MR, Mullock BM, Piper RC, Pryor PR: **Membrane dynamics and the biogenesis of lysosomes (Review)**. *Mol Membr Biol* 2003, **20**:141–154.

7. Van Meel E, Klumperman J: **Imaging and imagination: understanding the endo-lysosomal system.** *Histochem Cell Biol* 2008, **129**:253–66.

8. Matteoni R, Kreis TE: **Translocation and clustering of endosomes and lysosomes depends on microtubules.** *J Cell Biol* 1987, **105**:1253–65.

9. Cohn ZA, Benson B: **The in vitro differentiation of mononuclear phagocytes. 3. The reversibility of granule and hydrolytic enzyme formation and the turnover of granule constituents.** *J Exp Med* 1965, **122**:455–66.

10. De Duve: **[Cellular pathology].** *J Sci Med Lille* 1959, **77**:437–43.

11. Glaumann H, Ericsson JL, Marzella L: **Mechanisms of intralysosomal degradation with special reference to autophagocytosis and heterophagocytosis of cell organelles.** *Int Rev Cytol* 1981, **73**:149–82.

12. Ohkuma S, Moriyama Y, Takano T: **Identification and characterization of a proton pump on lysosomes by fluorescein-isothiocyanate-dextran fluorescence.** *Proc Natl Acad Sci U S A* 1982, **79**:2758–62.

13. Arai K, Shimaya A, Hiratani N, Ohkuma S: **Purification and characterization of lysosomal H(+)-ATPase. An anion-sensitive v-type H(+)-ATPase from rat liver lysosomes.** *J Biol Chem* 1993, **268**:5649–60.

14. Mellman I, Fuchs R, Helenius A: **Acidification of the endocytic and exocytic pathways.** *Annu Rev Biochem* 1986, **55**:663–700.

15. Braulke T, Bonifacino JS: **Sorting of lysosomal proteins.** *Biochim Biophys Acta* 2009, **1793**:605–14.

16. Fukuda M: **Lysosomal membrane glycoproteins. Structure, biosynthesis, and intracellular trafficking.** *J Biol Chem* 1991, **266**:21327–30.

17. Winchester BG: **Lysosomal membrane proteins.** *Eur J Paediatr Neurol* 2001, **5 Suppl A**:11–9.

18. Neufeld EF: **Lysosomal Storage Diseases**. 1991, **60**:257–280.

19. Swetha MG, Sriram V, Krishnan KS, Oorschot VMJ, ten Brink C, Klumperman J, Mayor S: **Lysosomal membrane protein composition, acidic pH and sterol content are regulated via a light-dependent pathway in metazoan cells.** *Traffic* 2011, **12**:1037–55.

20. Jäättelä M: **Multiple cell death pathways as regulators of tumour initiation and progression.** *Oncogene* 2004, **23**:2746–56.

21. Reddy A, Caler E V, Andrews NW: **Plasma membrane repair is mediated by Ca(2+)-regulated exocytosis of lysosomes.** *Cell* 2001, **106**:157–69.

22. Efeyan A, Zoncu R, Sabatini DM: **Amino acids and mTORC1: from lysosomes to disease.** *Trends Mol Med* 2012, **18**:524–33.

23. Settembre C, Fraldi A, Medina DL, Ballabio A: **Signals from the lysosome: a control centre for cellular clearance and energy metabolism.** *Nat Rev Mol Cell Biol* 2013, **14**:283–96.

24. Venkatachalam K, Wong C-O, Zhu MX: **The role of TRPMLs in endolysosomal trafficking and function.** *Cell Calcium* 2014.

25. Hamer I, Van Beersel G, Arnould T, Jadot M: **Lipids and lysosomes.** *Curr Drug Metab* 2012, **13**:1371–87.

26. Peters C, von Figura K: **Biogenesis of lysosomal membranes**. *FEBS Lett* 1994, **346**:108–114.

27. Rapoport TA: **Protein translocation across and integration into membranes.** *CRC Crit Rev Biochem* 1986, **20**:73–137.

28. Arnsburg K, Kirstein-Miles J: **Interrelation between protein synthesis, proteostasis and life span.** *Curr Genomics* 2014, **15**:66–75.

29. Hammond C, Helenius A: **Quality control in the secretory pathway**. *Curr Opin Cell Biol* 1995, **7**:523–529.

30. Meusser B, Hirsch C, Jarosch E, Sommer T: **ERAD: the long road to destruction.** *Nat Cell Biol* 2005, **7**:766–72.

31. Helenius A, Aebi M: **Roles of N-linked glycans in the endoplasmic reticulum.** *Annu Rev Biochem* 2004, **73**:1019–49.

32. Lenertz LY, Wang Z, Guadarrama A, Hill LM, Gavala ML, Bertics PJ: **Mutation of putative N-linked glycosylation sites on the human nucleotide receptor P2X7 reveals a key residue important for receptor function.** *Biochemistry* 2010, **49**:4611–9.

33. Saftig P, Klumperman J: **Lysosome biogenesis and lysosomal membrane proteins: trafficking meets function.** *Nat Rev Mol Cell Biol* 2009, **10**:623–35.

34. Varki A, Kornfeld S: **Identification of a rat liver alpha-N-acetylglucosaminyl phosphodiesterase capable of removing "blocking" alpha-N-acetylglucosamine residues from phosphorylated high mannose oligosaccharides of lysosomal enzymes.** *J Biol Chem* 1980, **255**:8398–401.

35. Varki A, Kornfeld S: **Structural studies of phosphorylated high mannose-type oligosaccharides.** *J Biol Chem* 1980, **255**:10847–58.

36. Waheed A, Pohlmann R, Hasilik A, von Figura K: **Subcellular location of two enzymes involved in the synthesis of phosphorylated recognition markers in lysosomal enzymes.** *J Biol Chem* 1981, **256**:4150–2.

37. Sly WS: **Receptor-mediated transport of acid hydrolases to lysosomes.** *Curr Top Cell Regul* 1985, **26**:27–38.

38. Campbell CH, Rome LH: **Coated vesicles from rat liver and calf brain contain lysosomal enzymes bound to mannose 6-phosphate receptors.** *J Biol Chem* 1983, **258**:13347–52.

39. Von Figura K, Hasilik A: **Lysosomal enzymes and their receptors.** *Annu Rev Biochem* 1986, **55**:167–93.

40. Hoflack B, Kornfeld S: **Purification and characterization of a cation-dependent mannose 6-phosphate receptor from murine P388D1 macrophages and bovine liver.** *J Biol Chem* 1985, **260**:12008–14.

41. Hunziker W, Geuze HJ: **Intracellular trafficking of lysosomal membrane proteins.** *Bioessays* 1996, **18**:379–89.

42. Gonzalez-Noriega A, Grubb JH, Talkad V, Sly WS: **Chloroquine inhibits lysosomal enzyme pinocytosis and enhances lysosomal enzyme secretion by impairing receptor recycling.** *J Cell Biol* 1980, **85**:839–52.

43. Makrypidi G, Damme M, Müller-Loennies S, Trusch M, Schmidt B, Schlüter H, Heeren J, Lübke T, Saftig P, Braulke T: **Mannose 6 dephosphorylation of lysosomal proteins mediated by acid phosphatases Acp2 and Acp5.** *Mol Cell Biol* 2012, **32**:774–82.

44. Doray B, Bruns K, Ghosh P, Kornfeld S: **Interaction of the cation-dependent mannose 6-phosphate receptor with GGA proteins.** *J Biol Chem* 2002, **277**:18477–82.

45. Yoneyama Y, Matsuo M, Take K, Kabuta T, Chida K, Hakuno F, Takahashi S-I: **The AP-1 complex regulates intracellular localization of insulin receptor substrate 1, which is required for insulin-like growth factor I-dependent cell proliferation.** *Mol Cell Biol* 2013, **33**:1991–2003.

46. Stahlschmidt W, Robertson MJ, Robinson PJ, McCluskey A, Haucke V: **Clathrin terminal domain-ligand interactions regulate sorting of mannose 6-phosphate receptors mediated by AP-1 and GGA adaptors.** *J Biol Chem* 2014, **289**:4906–18.

47. Ghosh P, Kornfeld S: **The cytoplasmic tail of the cation-independent mannose 6-phosphate receptor contains four binding sites for AP-1.** *Arch Biochem Biophys* 2004, **426**:225–30.

48. Markmann S, Thelen M, Cornils K, Schweizer M, Brocke-Ahmadinejad N, Willnow T, Heeren J, Gieselmann V, Braulke T, Kollmann K: **Lrp1/LDL receptor play critical roles in mannose 6-phosphate-independent lysosomal enzyme targeting.** *Traffic* 2015.

49. Leroy JG, Demars RI: **Mutant enzymatic and cytological phenotypes in cultured human fibroblasts.** *Science* 1967, **157**:804–6.

50. Hasilik A, Waheed A, von Figura K: **Enzymatic phosphorylation of lysosomal enzymes in the presence of UDP-N-acetylglucosamine. Absence of the activity in I-cell fibroblasts.** *Biochem Biophys Res Commun* 1981, **98**:761–7.

51. Reitman ML, Varki A, Kornfeld S: **Fibroblasts from patients with I-cell disease and pseudo-Hurler polydystrophy are deficient in uridine 5'-diphosphate-N-acetylglucosamine: glycoprotein N-acetylglucosaminylphosphotransferase activity.** *J Clin Invest* 1981, **67**:1574–9.

52. Van Dongen JM, Willemsen R, Ginns EI, Sips HJ, Tager JM, Barranger JA, Reuser AJ: **The subcellular localization of soluble and membrane-bound lysosomal enzymes in I-cell fibroblasts: a comparative immunocytochemical study.** *Eur J Cell Biol* 1985, **39**:179–89.

53. Leroy JG, Spranger JW: **I-cell disease.** *N Engl J Med* 1970, **283**:598–9.

54. Gelfman CM, Vogel P, Issa TM, Turner CA, Lee W-S, Kornfeld S, Rice DS: **Mice lacking alpha/beta subunits of GlcNAc-1-phosphotransferase exhibit growth retardation, retinal degeneration, and secretory cell lesions.** *Invest Ophthalmol Vis Sci* 2007, **48**:5221–8.

55. Peters C, Braun M, Weber B, Wendland M, Schmidt B, Pohlmann R, Waheed A, von Figura K: **Targeting of a lysosomal membrane protein: a tyrosine-containing endocytosis signal in the cytoplasmic tail of lysosomal acid phosphatase is necessary and sufficient for targeting to lysosomes.** *EMBO J* 1990, **9**:3497–506.

56. Aerts JM, Schram AW, Strijland A, van Weely S, Jonsson LM, Tager JM, Sorrell SH, Ginns EI, Barranger JA, Murray GJ: **Glucocerebrosidase, a lysosomal enzyme that does not undergo oligosaccharide phosphorylation.** *Biochim Biophys Acta* 1988, **964**:303–8.

57. Reczek D, Schwake M, Schröder J, Hughes H, Blanz J, Jin X, Brondyk W, Van Patten S, Edmunds T, Saftig P: **LIMP-2 is a receptor for lysosomal mannose-6-phosphate-independent targeting of beta-glucocerebrosidase.** *Cell* 2007, **131**:770–83.

58. Zachos C, Blanz J, Saftig P, Schwake M: **A critical histidine residue within LIMP-2 mediates pH sensitive binding to its ligand β-glucocerebrosidase.** *Traffic* 2012, **13**:1113–23.

59. Ni X, Morales CR: **The lysosomal trafficking of acid sphingomyelinase is mediated by sortilin and mannose 6-phosphate receptor.** *Traffic* 2006, **7**:889–902.

60. Canuel M, Korkidakis A, Konnyu K, Morales CR: **Sortilin mediates the lysosomal targeting of cathepsins D and H.** *Biochem Biophys Res Commun* 2008, **373**:292–7.

61. Lefrancois S, Zeng J, Hassan AJ, Canuel M, Morales CR: **The lysosomal trafficking of sphingolipid activator proteins (SAPs) is mediated by sortilin.** *EMBO J* 2003, **22**:6430–7.

62. Sandhoff K, Kolter T: **Processing of sphingolipid activator proteins and the topology of lysosomal digestion.** *Acta Biochim Pol* 1998, **45**:373–84.

63. Kolter T, Sandhoff K: **Principles of lysosomal membrane digestion: stimulation of sphingolipid degradation by sphingolipid activator proteins and anionic lysosomal lipids.** *Annu Rev Cell Dev Biol* 2005, **21**:81–103.

64. Vaccaro AM, Salvioli R, Tatti M, Ciaffoni F: **Saposins and their interaction with lipids.** *Neurochem Res* 1999, **24**:307–14.

65. Chang MHY, Bindloss CA, Grabowski GA, Qi X, Winchester B, Hopwood JJ, Meikle PJ: **Saposins A, B, C, and D in Plasma of Patients with Lysosomal Storage Disorders**. *Clin Chem* 2000, **46**:167–174.

66. Tylki-Szymańska A, Czartoryska B, Vanier M-T, Poorthuis BJMH, Groener JAE, Ługowska A, Millat G, Vaccaro AM, Jurkiewicz E: **Non-neuronopathic Gaucher disease due to saposin C deficiency.** *Clin Genet* 2007, **72**:538–42.

67. Meikle PJ: **Prevalence of Lysosomal Storage Disorders**. *JAMA* 1999, **281**:249.

68. Pinto R, Caseiro C, Lemos M, Lopes L, Fontes A, Ribeiro H, Pinto E, Silva E, Rocha S, Marcão A, Ribeiro I, Lacerda L, Ribeiro G, Amaral O, Sá Miranda MC: **Prevalence of lysosomal storage diseases in Portugal.** *Eur J Hum Genet* 2004, **12**:87–92.

69. Platt FM, Boland B, van der Spoel AC: **The cell biology of disease: lysosomal storage disorders: the cellular impact of lysosomal dysfunction.** *J Cell Biol* 2012, **199**:723–34.

70. Eskelinen E-L, Tanaka Y, Saftig P: **At the acidic edge: emerging functions for lysosomal membrane proteins**. *Trends Cell Biol* 2003, **13**:137–145.

71. Corrotte M, Castro-Gomes T, Koushik AB, Andrews NW: **Approaches for plasma membrane wounding and assessment of lysosome-mediated repair responses.** *Methods Cell Biol* 2015, **126**:139–58.

72. Futerman AH, van Meer G: **The cell biology of lysosomal storage disorders.** *Nat Rev Mol Cell Biol* 2004, **5**:554–65.

73. Wilcox WR: **Lysosomal storage disorders: the need for better pediatric recognition and comprehensive care.** *J Pediatr* 2004, **144**(5 Suppl):S3–14.

74. Gupta N, Oppenheim IM, Kauvar EF, Tayebi N, Sidransky E: **Type 2 Gaucher disease: phenotypic variation and genotypic heterogeneity.** *Blood Cells Mol Dis* 2011, **46**:75–84.

75. Mistry P: **Phenotype variations in Gaucher disease**. *La Rev Médecine Interne* 2006, **27**:S3–S6.

76. Sidransky E: **Gaucher disease: complexity in a "simple" disorder**. *Mol Genet Metab* 2004, **83**:6–15.

77. Lo SM, Choi M, Liu J, Jain D, Boot RG, Kallemeijn WW, Aerts JMFG, Pashankar F, Kupfer GM, Mane S, Lifton RP, Mistry PK: **Phenotype diversity in type 1 Gaucher disease: discovering the genetic basis of Gaucher**

disease/hematologic malignancy phenotype by individual genome analysis. *Blood* 2012, **119**:4731–40.

78. Goker-Alpan O, Hruska KS, Orvisky E, Kishnani PS, Stubblefield BK, Schiffmann R, Sidransky E: **Divergent phenotypes in Gaucher disease implicate the role of modifiers.** *J Med Genet* 2005, **42**:e37.

79. Degroote S, Wolthoorn J, van Meer G: **The cell biology of glycosphingolipids.** *Semin Cell Dev Biol* 2004, **15**:375–87.

80. Sandhoff K: **Metabolic and cellular bases of sphingolipidoses.** *Biochem Soc Trans* 2013, **41**:1562–8.

81. Xu Y-H, Barnes S, Sun Y, Grabowski GA: **Multi-system disorders of glycosphingolipid and ganglioside metabolism.** *J Lipid Res* 2010, **51**:1643–75.

82. Schulze H, Kolter T, Sandhoff K: **Principles of lysosomal membrane degradation: Cellular topology and biochemistry of lysosomal lipid degradation.** *Biochim Biophys Acta* 2009, **1793**:674–83.

83. Ichikawa S, Sakiyama H, Suzuki G, Hidari KI, Hirabayashi Y: **Expression cloning of a cDNA for human ceramide glucosyltransferase that catalyzes the first glycosylation step of glycosphingolipid synthesis.** *Proc Natl Acad Sci U S A* 1996, **93**:12654.

84. Kolter T, Sandhoff K: **Lysosomal degradation of membrane lipids.** *FEBS Lett* 2010, **584**:1700–12.

85. Van Meer G, Wolthoorn J, Degroote S: **The fate and function of glycosphingolipid glucosylceramide.** *Philos Trans R Soc Lond B Biol Sci* 2003, **358**:869–73.

86. Brady RO, Kanfer JN, Shapiro D: **METABOLISM OF GLUCOCEREBROSIDES. II. EVIDENCE OF AN ENZYMATIC DEFICIENCY IN GAUCHER'S DISEASE.** *Biochem Biophys Res Commun* 1965, **18**:221–5.

87. Beutler E, Grabowski GA: **Gaucher disease.** In *The Metabolic and Molecular Bases of Inherited Disease. 7th ed. New York, NY: McGraw-Hill;* 7th ed. Edited by McGraw-Hill. New York, NY; 1995:2641–2670.

88. Brady RO, Gal AE, Bradley RM, Martensson E, Warshaw AL, Laster L: **Enzymatic defect in Fabry's disease. Ceramidetrihexosidase deficiency.** *N Engl J Med* 1967, **276**:1163–7.

89. Ferraz MJ, Kallemeijn WW, Mirzaian M, Herrera Moro D, Marques A, Wisse P, Boot RG, Willems LI, Overkleeft HS, Aerts JM: **Gaucher disease and Fabry**

disease: new markers and insights in pathophysiology for two distinct glycosphingolipidoses. *Biochim Biophys Acta* 2014, **1841**:811–25.

90. Vanier MT: **Complex lipid trafficking in Niemann-Pick disease type C.** *J Inherit Metab Dis* 2014, **38**:187–99.

91. Barneveld RA, Keijzer W, Tegelaers FP, Ginns EI, Geurts van Kessel A, Brady RO, Barranger JA, Tager JM, Galjaard H, Westerveld A, Reuser AJ: **Assignment of the gene coding for human beta-glucocerebrosidase to the region q21-q31 of chromosome 1 using monoclonal antibodies.** *Hum Genet* 1983, **64**:227–31.

92. Ginns EI, Choudary P V, Tsuji S, Martin B, Stubblefield B, Sawyer J, Hozier J, Barranger JA: **Gene mapping and leader polypeptide sequence of human glucocerebrosidase: implications for Gaucher disease.** *Proc Natl Acad Sci U S A* 1985, **82**:7101–5.

93. Horowitz M, Wilder S, Horowitz Z, Reiner O, Gelbart T, Beutler E: **The human glucocerebrosidase gene and pseudogene: Structure and evolution**. *Genomics* 1989, **4**:87–96.

94. Aerts JM, Donker-Koopman WE, Murray GJ, Barranger JA, Tager JM, Schram AW: **A procedure for the rapid purification in high yield of human glucocerebrosidase using immunoaffinity chromatography with monoclonal antibodies.** *Anal Biochem* 1986, **154**:655–63.

95. Hruska KS, LaMarca ME, Scott CR, Sidransky E: **Gaucher disease: mutation and polymorphism spectrum in the glucocerebrosidase gene (GBA).** *Hum Mutat* 2008, **29**:567–83.

96. Beutler E: **Gaucher disease: multiple lessons from a single gene disorder**. *Acta Paediatr* 2006, **95**:103–109.

97. Ohashi T, Hong CM, Weiler S, Tomich JM, Aerts JM, Tager JM, Barranger JA: **Characterization of human glucocerebrosidase from different mutant alleles.** *J Biol Chem* 1991, **266**:3661–7.

98. Alfonso Palacín P, Pocoví M: **[Genetics of Gaucher's disease. Genotype-phenotype correlation].** *Med Clin (Barc)* 2011, **137 Suppl** :17–22.

99. Boot RG, Hollak CE, Verhoek M, Sloof P, Poorthuis BJ, Kleijer WJ, Wevers RA, van Oers MH, Mannens MM, Aerts JM, van Weely S: **Glucocerebrosidase genotype of Gaucher patients in The Netherlands: limitations in prognostic value.** *Hum Mutat* 1997, **10**:348–58.

100. Grace ME, Ashton-Prolla P, Pastores GM, Soni A, Desnick RJ: **Non-pseudogene-derived complex acid beta-glucosidase mutations causing mild type 1 and severe type 2 gaucher disease.** *J Clin Invest* 1999, **103**:817–23.

101. Inzelberg R, Hassin-Baer S, Jankovic J: **Genetic movement disorders in patients of Jewish ancestry.** *JAMA Neurol* 2014, **71**:1567–72.

102. Guggenbuhl P, Grosbois B, Chalès G: **Gaucher disease.** *Joint Bone Spine* 2008, **75**:116–24.

103. Lui K, Commens C, Choong R, Jaworski R: **Collodion babies with Gaucher's disease.** *Arch Dis Child* 1988, **63**:854–6.

104. Stone DL, Carey WF, Christodoulou J, Sillence D, Nelson P, Callahan M, Tayebi N, Sidransky E: **Type 2 Gaucher disease: the collodion baby phenotype revisited.** *Arch Dis Child Fetal Neonatal Ed* 2000, **82**:F163–6.

105. Baris HN, Cohen IJ, Mistry PK: **Gaucher disease: the metabolic defect, pathophysiology, phenotypes and natural history.** *Pediatr Endocrinol Rev* 2014, **12 Suppl 1**:72–81.

106. Mehta A: **Epidemiology and natural history of Gaucher's disease**. *Eur J Intern Med* 2006, **17**:S2–S5.

107. Tybulewicz VL, Tremblay ML, LaMarca ME, Willemsen R, Stubblefield BK, Winfield S, Zablocka B, Sidransky E, Martin BM, Huang SP: **Animal model of Gaucher's disease from targeted disruption of the mouse glucocerebrosidase gene.** *Nature* 1992, **357**:407–10.

108. Sibille A, Eng CM, Kim SJ, Pastores G, Grabowski GA: **Phenotype/genotype correlations in Gaucher disease type I: clinical and therapeutic implications.** *Am J Hum Genet* 1993, **52**:1094–101.

109. Holleran WM, Takagi Y, Menon GK, Jackson SM, Lee JM, Feingold KR, Elias PM: **Permeability barrier requirements regulate epidermal beta-glucocerebrosidase.** *J Lipid Res* 1994, **35**:905–12.

110. Liu Y, Suzuki K, Reed JD, Grinberg A, Westphal H, Hoffmann A, Döring T, Sandhoff K, Proia RL: **Mice with type 2 and 3 Gaucher disease point mutations generated by a single insertion mutagenesis procedure.** *Proc Natl Acad Sci U S A* 1998, **95**:2503–8.

111. Enquist IB, Nilsson E, Månsson J-E, Ehinger M, Richter J, Karlsson S: **Successful Low-Risk Hematopoietic Cell Therapy in a Mouse Model of Type 1 Gaucher Disease**. *Stem Cells* 2009, **27**:744–752.

112. Mistry PK, Liu J, Yang M, Nottoli T, McGrath J, Jain D, Zhang K, Keutzer J, Chuang W-L, Mehal WZ, Zhao H, Lin A, Mane S, Liu X, Peng YZ, Li JH, Agrawal M, Zhu L-L, Blair HC, Robinson LJ, Iqbal J, Sun L, Zaidi M: **Glucocerebrosidase gene-deficient mouse recapitulates Gaucher disease displaying cellular and molecular dysregulation beyond the macrophage.** *Proc Natl Acad Sci U S A* 2010, **107**:19473–8.

113. Boven LA, van Meurs M, Boot RG, Mehta A, Boon L, Aerts JM, Laman JD: **Gaucher cells demonstrate a distinct macrophage phenotype and resemble alternatively activated macrophages.** *Am J Clin Pathol* 2004, **122**:359–69.

114. Bussink AP, van Eijk M, Renkema GH, Aerts JM, Boot RG: **The biology of the Gaucher cell: the cradle of human chitinases.** *Int Rev Cytol* 2006, **252**:71–128.

115. Hollak CE, van Weely S, van Oers MH, Aerts JM: **Marked elevation of plasma chitotriosidase activity. A novel hallmark of Gaucher disease.** *J Clin Invest* 1994, **93**:1288–92.

116. Rolfs A, Giese A-K, Grittner U, Mascher D, Elstein D, Zimran A, Böttcher T, Lukas J, Hübner R, Gölnitz U, Röhle A, Dudesek A, Meyer W, Wittstock M, Mascher H: **Glucosylsphingosine is a highly sensitive and specific biomarker for primary diagnostic and follow-up monitoring in Gaucher disease in a non-Jewish, Caucasian cohort of Gaucher disease patients.** *PLoS One* 2013, **8**:e79732.

117. Dekker N, van Dussen L, Hollak CEM, Overkleeft H, Scheij S, Ghauharali K, van Breemen MJ, Ferraz MJ, Groener JEM, Maas M, Wijburg FA, Speijer D, Tylki-Szymanska A, Mistry PK, Boot RG, Aerts JM: **Elevated plasma glucosylsphingosine in Gaucher disease: relation to phenotype, storage cell markers, and therapeutic response**. *Blood* 2011, **118**:e118–e127.

118. Nilsson O, Svennerholm L: **Accumulation of glucosylceramide and glucosylsphingosine (psychosine) in cerebrum and cerebellum in infantile and juvenile Gaucher disease.** *J Neurochem* 1982, **39**:709–18.

119. Orvisky E, Sidransky E, McKinney CE, Lamarca ME, Samimi R, Krasnewich D, Martin BM, Ginns EI: **Glucosylsphingosine accumulation in mice and patients with type 2 Gaucher disease begins early in gestation.** *Pediatr Res* 2000, **48**:233–7.

120. Tamargo RJ, Velayati A, Goldin E, Sidransky E: **The role of saposin C in Gaucher disease.** *Mol Genet Metab* 2012, **106**:257–63.

121. Ayto R, Hughes DA: **Gaucher Disease and Myeloma**. *Crit Rev Oncog* 2013, **18**:247–268.

122. De Fost M, Out TA, de Wilde FA, Tjin EPM, Pals ST, van Oers MHJ, Boot RG, Aerts JFMG, Maas M, Vom Dahl S, Hollak CEM: **Immunoglobulin and free light chain abnormalities in Gaucher disease type I: data from an adult cohort of 63 patients and review of the literature.** *Ann Hematol* 2008, **87**:439–49.

123. Schapira AH V: **Glucocerebrosidase and Parkinson disease: Recent advances.** *Mol Cell Neurosci* 2015.

124. Siebert M, Sidransky E, Westbroek W: **Glucocerebrosidase is shaking up the synucleinopathies.** *Brain* 2014, **137**(Pt 5):1304–22.

125. Bae E-J, Yang NY, Lee C, Lee H-J, Kim S, Sardi SP, Lee S-J: **Loss of glucocerebrosidase 1 activity causes lysosomal dysfunction and α-synuclein aggregation.** *Exp Mol Med* 2015, **47**:e153.

126. Mazzulli JR, Xu Y-H, Sun Y, Knight AL, McLean PJ, Caldwell GA, Sidransky E, Grabowski GA, Krainc D: **Gaucher disease glucocerebrosidase and α-synuclein form a bidirectional pathogenic loop in synucleinopathies.** *Cell* 2011, **146**:37–52.

127. Sardi SP, Cheng SH, Shihabuddin LS: **Gaucher-related synucleinopathies: The examination of sporadic neurodegeneration from a rare (disease) angle.** *Prog Neurobiol* 2015.

128. Sardi SP, Clarke J, Viel C, Chan M, Tamsett TJ, Treleaven CM, Bu J, Sweet L, Passini MA, Dodge JC, Yu WH, Sidman RL, Cheng SH, Shihabuddin LS: **Augmenting CNS glucocerebrosidase activity as a therapeutic strategy for parkinsonism and other Gaucher-related synucleinopathies.** *Proc Natl Acad Sci U S A* 2013, **110**:3537–42.

129. Sardi SP, Singh P, Cheng SH, Shihabuddin LS, Schlossmacher MG: **Mutant GBA1 expression and synucleinopathy risk: first insights from cellular and mouse models.** *Neurodegener Dis* 2012, **10**:195–202.

130. Aerts JMFG, Kallemeijn WW, Wegdam W, Joao Ferraz M, van Breemen MJ, Dekker N, Kramer G, Poorthuis BJ, Groener JEM, Cox-Brinkman J, Rombach SM, Hollak CEM, Linthorst GE, Witte MD, Gold H, van der Marel GA, Overkleeft HS, Boot RG: **Biomarkers in the diagnosis of lysosomal storage disorders: proteins, lipids, and inhibodies.** *J Inherit Metab Dis* 2011, **34**:605–19.

131. Witte MD, Kallemeijn WW, Aten J, Li K-Y, Strijland A, Donker-Koopman WE, van den Nieuwendijk AMCH, Bleijlevens B, Kramer G, Florea BI, Hooibrink B, Hollak CEM, Ottenhoff R, Boot RG, van der Marel GA, Overkleeft HS, Aerts JMFG: **Ultrasensitive in situ visualization of active glucocerebrosidase molecules.** *Nat Chem Biol* 2010, **6**:907–13.

132. Witte MD, Walvoort MTC, Li K-Y, Kallemeijn WW, Donker-Koopman WE, Boot RG, Aerts JMFG, Codée JDC, van der Marel GA, Overkleeft HS: **Activity-based profiling of retaining β-glucosidases: a comparative study.** *Chembiochem* 2011, **12**:1263–9.

133. Kallemeijn WW, Li K-Y, Witte MD, Marques ARA, Aten J, Scheij S, Jiang J, Willems LI, Voorn-Brouwer TM, van Roomen CPAA, Ottenhoff R, Boot RG, van den Elst H, Walvoort MTC, Florea BI, Codée JDC, van der Marel GA, Aerts JMFG, Overkleeft HS: **Novel activity-based probes for broad-spectrum profiling of retaining β-exoglucosidases in situ and in vivo.** *Angew Chem Int Ed Engl* 2012, **51**:12529–33.

134. Li K-Y, Jiang J, Witte MD, Kallemeijn WW, Donker-Koopman WE, Boot RG, Aerts JMFG, Codée JDC, van der Marel GA, Overkleeft HS: **Exploring functional cyclophellitol analogues as human retaining beta-glucosidase inhibitors.** *Org Biomol Chem* 2014, **12**:7786–91.

135. Boot RG, Verhoek M, Donker-Koopman W, Strijland A, van Marle J, Overkleeft HS, Wennekes T, Aerts JMFG: **Identification of the non-lysosomal glucosylceramidase as beta-glucosidase 2.** *J Biol Chem* 2007, **282**:1305–12.

136. Yildiz Y, Matern H, Thompson B, Allegood JC, Warren RL, Ramirez DMO, Hammer RE, Hamra FK, Matern S, Russell DW: **Mutation of beta-glucosidase 2 causes glycolipid storage disease and impaired male fertility.** *J Clin Invest* 2006, **116**:2985–94.

137. Van Weely S, Brandsma M, Strijland A, Tager JM, Aerts JM: **Demonstration of the existence of a second, non-lysosomal glucocerebrosidase that is not deficient in Gaucher disease.** *Biochim Biophys Acta* 1993, **1181**:55–62.

138. Körschen HG, Yildiz Y, Raju DN, Schonauer S, Bönigk W, Jansen V, Kremmer E, Kaupp UB, Wachten D: **The non-lysosomal β-glucosidase GBA2 is a non-integral membrane-associated protein at the endoplasmic reticulum (ER) and Golgi.** *J Biol Chem* 2013, **288**:3381–93.

139. Burke DG, Rahim AA, Waddington SN, Karlsson S, Enquist I, Bhatia K, Mehta A, Vellodi A, Heales S: **Increased glucocerebrosidase (GBA) 2 activity in GBA1 deficient mice brains and in Gaucher leucocytes.** *J Inherit Metab Dis* 2013, **36**:869–72.

140. Pentchev PG: **Niemann-Pick C research from mouse to gene.** *Biochim Biophys Acta* 2004, **1685**:3–7.

141. Salvioli R, Scarpa S, Ciaffoni F, Tatti M, Ramoni C, Vanier MT, Vaccaro AM: **Glucosylceramidase mass and subcellular localization are modulated by cholesterol in Niemann-Pick disease type C.** *J Biol Chem* 2004, **279**:17674–80.

142. Aerts JM, Hollak C, Boot R, Groener A: **Biochemistry of glycosphingolipid storage disorders: implications for therapeutic intervention.** *Philos Trans R Soc Lond B Biol Sci* 2003, **358**:905–14.

143. Mistry PK, Liu J, Sun L, Chuang W-L, Yuen T, Yang R, Lu P, Zhang K, Li J, Keutzer J, Stachnik A, Mennone A, Boyer JL, Jain D, Brady RO, New MI, Zaidi M: **Glucocerebrosidase 2 gene deletion rescues type 1 Gaucher disease.** *Proc Natl Acad Sci U S A* 2014, **111**:4934–9.

144. Erikson A: **Remaining problems in the management of patients with Gaucher disease.** *J Inherit Metab Dis* 2001, **24 Suppl 2**:122–6; discussion 87–8.

145. Barton NW, Brady RO, Dambrosia JM, Di Bisceglie AM, Doppelt SH, Hill SC, Mankin HJ, Murray GJ, Parker RI, Argoff CE: **Replacement therapy for inherited enzyme deficiency--macrophage-targeted glucocerebrosidase for Gaucher's disease.** *N Engl J Med* 1991, **324**:1464–70.

146. Bijsterbosch MK, Donker W, van de Bilt H, van Weely S, van Berkel TJ, Aerts JMFG, Bilt H, Weely S, Berkel TJC: **Quantitative Analysis of the Targeting of Mannose-Terminal Glucocerebrosidase. Predominant Uptake by Liver Endothelial Cells**. *Eur J Biochem* 1996, **237**:344–349.

147. Grabowski GA, Barton NW, Pastores G, Dambrosia JM, Banerjee TK, McKee MA, Parker C, Schiffmann R, Hill SC, Brady RO: **Enzyme therapy in type 1 Gaucher disease: comparative efficacy of mannose-terminated glucocerebrosidase from natural and recombinant sources.** *Ann Intern Med* 1995, **122**:33.

148. Barton NW, Furbish FS, Murray GJ, Garfield M, Brady RO: **Therapeutic response to intravenous infusions of glucocerebrosidase in a patient with Gaucher disease.** *Proc Natl Acad Sci U S A* 1990, **87**:1913–6.

149. Hughes DA, Gonzalez DE, Lukina EA, Mehta A, Kabra M, Elstein D, Kisinovsky I, Giraldo P, Bavdekar A, Hangartner TN, Wang N, Crombez E, Zimran A: **Velaglucerase alfa (VPRIV) enzyme replacement therapy in patients with Gaucher disease: Long-term data from phase III clinical trials.** *Am J Hematol* 2015.

150. Chung YK, Sohn YB, Sohn JM, Lee J, Chang MS, Kwun Y, Kim CH, Lee JY, Yook YJ, Ko A-R, Jin D-K: **A biochemical and physicochemical comparison of two recombinant enzymes used for enzyme replacement therapies of hunter syndrome.** *Glycoconj J* 2014, **31**:309–15.

151. Shaaltiel Y, Gingis-Velitski S, Tzaban S, Fiks N, Tekoah Y, Aviezer D: **Plant-based oral delivery of β-glucocerebrosidase as an enzyme replacement therapy for Gaucher's disease.** *Plant Biotechnol J* 2015.

152. Eng CM, Guffon N, Wilcox WR, Germain DP, Lee P, Waldek S, Caplan L, Linthorst GE, Desnick RJ: **Safety and efficacy of recombinant human alpha-galactosidase A--replacement therapy in Fabry's disease.** *N Engl J Med* 2001, **345**:9–16.

153. Amalfitano A, Bengur AR, Morse RP, Majure JM, Case LE, Veerling DL, Mackey J, Kishnani P, Smith W, McVie-Wylie A, Sullivan JA, Hoganson GE, Phillips JA, Schaefer GB, Charrow J, Ware RE, Bossen EH, Chen YT: **Recombinant human acid alpha-glucosidase enzyme therapy for infantile glycogen storage disease type II: results of a phase I/II clinical trial.** *Genet Med* , **3**:132–8.

154. Kakkis ED, Muenzer J, Tiller GE, Waber L, Belmont J, Passage M, Izykowski B, Phillips J, Doroshow R, Walot I, Hoft R, Neufeld EF: **Enzyme-replacement therapy in mucopolysaccharidosis I.** *N Engl J Med* 2001, **344**:182–8.

155. Muenzer J, Lamsa JC, Garcia A, Dacosta J, Garcia J, Treco DA: **Enzyme replacement therapy in mucopolysaccharidosis type II (Hunter syndrome): a preliminary report.** *Acta Paediatr Suppl* 2002, **91**:98–9.

156. Harmatz P, Whitley CB, Waber L, Pais R, Steiner R, Plecko B, Kaplan P, Simon J, Butensky E, Hopwood JJ: **Enzyme replacement therapy in mucopolysaccharidosis VI (Maroteaux-Lamy syndrome).** *J Pediatr* 2004, **144**:574–80.

157. Haddley K: **Elosulfase alfa.** *Drugs Today (Barc)* 2014, **50**:475–83.

158. Aerts JMFG, Hollak CEM, Boot RG, Groener JEM, Maas M: **Substrate reduction therapy of glycosphingolipid storage disorders.** *J Inherit Metab Dis* 2006, **29**:449–56.

159. Platt FM, Jeyakumar M, Andersson U, Priestman DA, Dwek RA, Butters TD, Cox TM, Lachmann RH, Hollak C, Aerts JM, Van Weely S, Hrebícek M, Moyses C, Gow I, Elstein D, Zimran A: **Inhibition of substrate synthesis as a strategy for glycolipid lysosomal storage disease therapy.** *J Inherit Metab Dis* 2001, **24**:275–90.

160. Cox T, Lachmann R, Hollak C, Aerts J, van Weely S, Hrebícek M, Platt F, Butters T, Dwek R, Moyses C, Gow I, Elstein D, Zimran A: **Novel oral treatment of Gaucher's disease with N-butyldeoxynojirimycin (OGT 918) to decrease substrate biosynthesis.** *Lancet* 2000, **355**:1481–5.

161. Elstein D, Hollak C, Aerts JMFG, van Weely S, Maas M, Cox TM, Lachmann RH, Hrebicek M, Platt FM, Butters TD, Dwek RA, Zimran A: **Sustained therapeutic effects of oral miglustat (Zavesca, N-butyldeoxynojirimycin, OGT 918) in type I Gaucher disease.** *J Inherit Metab Dis* 2004, **27**:757–66.

162. Cox TM: **Substrate reduction therapy for lysosomal storage diseases.** *Acta Paediatr Suppl* 2005, **94**:69–75; discussion 57.

163. Hughes DA, Pastores GM: **Eliglustat for Gaucher's disease: trippingly on the tongue.** *Lancet* 2015.

164. Poole RM: **Eliglustat: first global approval.** *Drugs* 2014, **74**:1829–36.

165. Cox TM, Drelichman G, Cravo R, Balwani M, Burrow TA, Martins AM, Lukina E, Rosenbloom B, Ross L, Angell J, Puga AC: **Eliglustat compared with imiglucerase in patients with Gaucher's disease type 1 stabilised on enzyme replacement therapy: a phase 3, randomised, open-label, non-inferiority trial.** *Lancet* 2015.

166. Mistry PK, Lukina E, Ben Turkia H, Amato D, Baris H, Dasouki M, Ghosn M, Mehta A, Packman S, Pastores G, Petakov M, Assouline S, Balwani M, Danda S, Hadjiev E, Ortega A, Shankar S, Solano MH, Ross L, Angell J, Peterschmitt MJ: **Effect of oral eliglustat on splenomegaly in patients with Gaucher disease type 1: the ENGAGE randomized clinical trial.** *JAMA* 2015, **313**:695–706.

167. Ghisaidoobe AT, van den Berg RJBHN, Butt SS, Strijland A, Donker-Koopman WE, Scheij S, van den Nieuwendijk AMCH, Koomen G-J, van Loevezijn A, Leemhuis M, Wennekes T, van der Stelt M, van der Marel GA, van Boeckel CAA, Aerts JMFG, Overkleeft HS: **Identification and development of biphenyl substituted iminosugars as improved dual glucosylceramide synthase/neutral glucosylceramidase inhibitors.** *J Med Chem* 2014, **57**:9096–104.

168. Boyd RE, Lee G, Rybczynski P, Benjamin ER, Khanna R, Wustman BA, Valenzano KJ: **Pharmacological chaperones as therapeutics for lysosomal storage diseases.** *J Med Chem* 2013, **56**:2705–25.

169. Dahl M, Doyle A, Olsson K, Månsson J-E, Marques ARA, Mirzaian M, Aerts JM, Ehinger M, Rothe M, Modlich U, Schambach A, Karlsson S: **Lentiviral gene therapy using cellular promoters cures type 1 Gaucher disease in mice.** *Mol Ther* 2015.

170. Bleistein J, Heidrich HG, Debuch H: **The phospholipids of liver lysosomes from untreated rats.** *Hoppe Seylers Z Physiol Chem* 1980, **361**:595–7.

171. Forster S, Scarlett L, Lloyd JB: **The effect of lysosomotropic detergents on the permeability properties of the lysosome membrane.** *Biochim Biophys Acta* 1987, **924**:452–7.

172. Lübke T, Lobel P, Sleat DE: **Proteomics of the lysosome.** *Biochim Biophys Acta* 2009, **1793**:625–35.

173. Schröder B, Wrocklage C, Pan C, Jäger R, Kösters B, Schäfer H, Elsässer H-P, Mann M, Hasilik A: **Integral and associated lysosomal membrane proteins.** *Traffic* 2007, **8**:1676–86.

174. Schröder BA, Wrocklage C, Hasilik A, Saftig P: **The proteome of lysosomes**. *Proteomics* 2010, **10**:4053–4076.

175. Pols MS, van Meel E, Oorschot V, ten Brink C, Fukuda M, Swetha MG, Mayor S, Klumperman J: **hVps41 and VAMP7 function in direct TGN to late endosome transport of lysosomal membrane proteins.** *Nat Commun* 2013, **4**:1361.

176. Lewis V, Green SA, Marsh M, Vihko P, Helenius A, Mellman I: **Glycoproteins of the lysosomal membrane.** *J Cell Biol* 1985, **100**:1839–47.

177. Bonifacino JS, Traub LM: **Signals for sorting of transmembrane proteins to endosomes and lysosomes.** *Annu Rev Biochem* 2003, **72**:395–447.

178. Ogata S, Fukuda M: **Lysosomal targeting of Limp II membrane glycoprotein requires a novel Leu-Ile motif at a particular position in its cytoplasmic tail.** *J Biol Chem* 1994, **269**:5210–7.

179. Bonifacino JS, Dell'Angelica EC: **Molecular bases for the recognition of tyrosine-based sorting signals.** *J Cell Biol* 1999, **145**:923–6.

180. Tabuchi N, Akasaki K, Sasaki T, Kanda N, Tsuji H: **Identification and characterization of a major lysosomal membrane glycoprotein, LGP85/LIMP II in mouse liver.** *J Biochem* 1997, **122**:756–63.

181. Lupas AN, Gruber M: **The structure of alpha-helical coiled coils.** *Adv Protein Chem* 2005, **70**:37–78.

182. Yu YB: **Coiled-coils: stability, specificity, and drug delivery potential.** *Adv Drug Deliv Rev* 2002, **54**:1113–29.

183. Tao N, Wagner SJ, Lublin DM: **CD36 is palmitoylated on both N- and C-terminal cytoplasmic tails.** *J Biol Chem* 1996, **271**:22315–20.

184. Calvo D, Dopazo J, Vega MA: **The CD36, CLA-1 (CD36L1), and LIMPII (CD36L2) gene family: cellular distribution, chromosomal location, and genetic evolution**. *Genomics* 1995, **25**:100–106.

185. Kuronita T: **A role for the lysosomal membrane protein LGP85 in the biogenesis and maintenance of endosomal and lysosomal morphology**. *J Cell Sci* 2002, **115**:4117–4131.

186. Silverstein RL, Febbraio M: **CD36, a scavenger receptor involved in immunity, metabolism, angiogenesis, and behavior.** *Sci Signal* 2009, **2**:re3.

187. Park YM: **CD36, a scavenger receptor implicated in atherosclerosis.** *Exp Mol Med* 2014, **46**:e99.

188. Mulcahy J V, Riddell DR, Owen JS: **Human scavenger receptor class B type II (SR-BII) and cellular cholesterol efflux.** *Biochem J* 2004, **377**(Pt 3):741–7.

189. Neculai D, Schwake M, Ravichandran M, Zunke F, Collins RF, Peters J, Neculai M, Plumb J, Loppnau P, Pizarro JC, Seitova A, Trimble WS, Saftig P, Grinstein S, Dhe-Paganon S: **Structure of LIMP-2 provides functional insights with implications for SR-BI and CD36.** *Nature* 2013, **504**:172–6.

190. Gamp A-C, Tanaka Y, Lullmann-Rauch R, Wittke D, D'Hooge R, De Deyn PP, Moser T, Maier H, Hartmann D, Reiss K, Illert A-L, von Figura K, Saftig P: **LIMP-2/LGP85 deficiency causes ureteric pelvic junction obstruction, deafness and peripheral neuropathy in mice**. *Hum Mol Genet* 2003, **12**:631–646.

191. Fujita H, Takata Y, Kono A, Tanaka Y, Takahashi T, Himeno M, Kato K: **Isolation and sequencing of a cDNA clone encoding the 85 kDa human lysosomal sialoglycoprotein (hLGP85) in human metastatic pancreas islet tumor cells**. *Biochem Biophys Res Commun* 1992, **184**:604–611.

192. Okazaki I, Himeno M, Ezaki J, Ishikawa T, Kato K: **Purification and characterization of an 85 kDa sialoglycoprotein in rat liver lysosomal membranes.** *J Biochem* 1992, **111**:763–9.

193. Fujita H, Ezaki J, Noguchi Y, Kono A, Himeno M, Kato K: **Isolation and sequencing of a cDNA clone encoding 85kDa sialoglycoprotein in rat liver lysosomal membranes**. *Biochem Biophys Res Commun* 1991, **178**:444–452.

194. Blanz J, Groth J, Zachos C, Wehling C, Saftig P, Schwake M: **Disease-causing mutations within the lysosomal integral membrane protein type 2 (LIMP-2) reveal the nature of binding to its ligand beta-glucocerebrosidase.** *Hum Mol Genet* 2010, **19**:563–72.

195. Sandoval I V, Arredondo JJ, Alcalde J, Gonzalez Noriega A, Vandekerckhove J, Jimenez MA, Rico M: **The residues Leu(Ile)475-Ile(Leu, Val, Ala)476, contained in the extended carboxyl cytoplasmic tail, are critical for targeting of the resident lysosomal membrane protein LIMP II to lysosomes.** *J Biol Chem* 1994, **269**:6622–31.

196. Le Borgne R, Alconada A, Bauer U, Hoflack B: **The mammalian AP-3 adaptor-like complex mediates the intracellular transport of lysosomal membrane glycoproteins.** *J Biol Chem* 1998, **273**:29451–61.

197. Fujita H, Saeki M, Yasunaga K, Ueda T, Imoto T, Himeno M: **In vitro binding study of adaptor protein complex (AP-1) to lysosomal targeting motif (LI-motif).** *Biochem Biophys Res Commun* 1999, **255**:54–8.

198. Höning S, Sandoval I V, von Figura K: **A di-leucine-based motif in the cytoplasmic tail of LIMP-II and tyrosinase mediates selective binding of AP-3.** *EMBO J* 1998, **17**:1304–14.

199. Tabuchi N, Akasaki K, Tsuji H: **Ile (476), a constituent of di-leucine-based motif of a major lysosomal membrane protein, LGP85/LIMP II, is important for its proper distribution in late endosomes and lysosomes**. *Biochem Biophys Res Commun* 2002, **295**:149–156.

200. Tabuchi N, Akasaki K, Tsuji H: **Distribution of a major lysosomal membrane glycoprotein, LGP85/LIMP II, in rat tissues.** *Biol Pharm Bull* 2000, **23**:394–6.

201. Balreira A, Gaspar P, Caiola D, Chaves J, Beirão I, Lima JL, Azevedo JE, Miranda MCS: **A nonsense mutation in the LIMP-2 gene associated with progressive myoclonic epilepsy and nephrotic syndrome.** *Hum Mol Genet* 2008, **17**:2238–43.

202. Zhao Y, Ren J, Padilla-Parra S, Fry EE, Stuart DI: **Lysosome sorting of β-glucocerebrosidase by LIMP-2 is targeted by the mannose 6-phosphate receptor.** *Nat Commun* 2014, **5**:4321.

203. Rijnboutt S, Kal AJ, Geuze HJ, Aerts H, Strous GJ: **Mannose 6-phosphate-independent targeting of cathepsin D to lysosomes in HepG2 cells.** *J Biol Chem* 1991, **266**:23586–92.

204. Rijnboutt S, Aerts HM, Geuze HJ, Tager JM, Strous GJ: **Mannose 6-phosphate-independent membrane association of cathepsin D, glucocerebrosidase, and sphingolipid-activating protein in HepG2 cells.** *J Biol Chem* 1991, **266**:4862–8.

205. Jović M, Kean MJ, Szentpetery Z, Polevoy G, Gingras A-C, Brill JA, Balla T: **Two phosphatidylinositol 4-kinases control lysosomal delivery of the Gaucher disease enzyme, β-glucocerebrosidase.** *Mol Biol Cell* 2012, **23**:1533–45.

206. Waugh MG: **PIPs in Neurological Diseases**. *Biochim Biophys Acta - Mol Cell Biol Lipids* 2015.

207. Knipper M, Claussen C, Rüttiger L, Zimmermann U, Lüllmann-Rauch R, Eskelinen E-L, Schröder J, Schwake M, Saftig P: **Deafness in LIMP2-deficient mice due to early loss of the potassium channel KCNQ1/KCNE1 in marginal cells of the stria vascularis.** *J Physiol* 2006, **576**(Pt 1):73–86.

208. Young P, Suter U: **The causes of Charcot-Marie-Tooth disease.** *Cell Mol Life Sci* 2003, **60**:2547–60.

209. Suter U, Scherer SS: **Disease mechanisms in inherited neuropathies.** *Nat Rev Neurosci* 2003, **4**:714–26.

210. Berkovic SF, Dibbens LM, Oshlack A, Silver JD, Katerelos M, Vears DF, Lüllmann-Rauch R, Blanz J, Zhang KW, Stankovich J, Kalnins RM, Dowling JP, Andermann E, Andermann F, Faldini E, D'Hooge R, Vadlamudi L, Macdonell RA, Hodgson BL, Bayly MA, Savige J, Mulley JC, Smyth GK, Power DA, Saftig P, Bahlo M: **Array-based gene discovery with three unrelated subjects shows SCARB2/LIMP-2 deficiency causes myoclonus epilepsy and glomerulosclerosis.** *Am J Hum Genet* 2008, **82**:673–84.

211. Fu Y-J, Aida I, Tada M, Tada M, Toyoshima Y, Takeda S, Nakajima T, Naito H, Nishizawa M, Onodera O, Kakita A, Takahashi H: **Progressive myoclonus epilepsy: extraneuronal brown pigment deposition and system neurodegeneration in the brains of Japanese patients with novel SCARB2 mutations.** *Neuropathol Appl Neurobiol* 2014, **40**:551–63.

212. Badhwar A, Berkovic SF, Dowling JP, Gonzales M, Narayanan S, Brodtmann A, Berzen L, Caviness J, Trenkwalder C, Winkelmann J, Rivest J, Lambert M, Hernandez-Cossio O, Carpenter S, Andermann F, Andermann E: **Action myoclonus-renal failure syndrome: characterization of a unique cerebro-renal disorder.** *Brain* 2004, **127**(Pt 10):2173–82.

213. Dibbens LM, Michelucci R, Gambardella A, Andermann F, Rubboli G, Bayly MA, Joensuu T, Vears DF, Franceschetti S, Canafoglia L, Wallace R, Bassuk AG, Power DA, Tassinari CA, Andermann E, Lehesjoki AE, Berkovic SF: **SCARB2 mutations in progressive myoclonus epilepsy (PME) without renal failure.** *Ann Neurol* 2009, **66**:532–6.

214. Andermann E, Andermann F, Carpenter S, Wolfe LS, Nelson R, Patry G, Boileau J: **Action myoclonus-renal failure syndrome: a previously unrecognized neurological disorder unmasked by advances in nephrology.** *Adv Neurol* 1986, **43**:87–103.

215. Hopfner F, Schormair B, Knauf F, Berthele A, Tölle TR, Baron R, Maier C, Treede R-D, Binder A, Sommer C, Maihöfner C, Kunz W, Zimprich F, Heemann U, Pfeufer A, Näbauer M, Kääb S, Nowak B, Gieger C, Lichtner P, Trenkwalder C, Oexle K, Winkelmann J: **Novel SCARB2 mutation in action myoclonus-renal failure syndrome and evaluation of SCARB2 mutations in isolated AMRF features.** *BMC Neurol* 2011, **11**:134.

216. Zeigler M, Meiner V, Newman JP, Steiner-Birmanns B, Bargal R, Sury V, Mengistu G, Kakhlon O, Leykin I, Argov Z, Abramsky O, Lossos A: **A novel SCARB2**

mutation in progressive myoclonus epilepsy indicated by reduced β-glucocerebrosidase activity. *J Neurol Sci* 2014, **339**:210–3.

217. Rubboli G, Franceschetti S, Berkovic SF, Canafoglia L, Gambardella A, Dibbens LM, Riguzzi P, Campieri C, Magaudda A, Tassinari CA, Michelucci R: **Clinical and neurophysiologic features of progressive myoclonus epilepsy without renal failure caused by SCARB2 mutations.** *Epilepsia* 2011, **52**:2356–63.

218. Chaves J, Beirão I, Balreira A, Gaspar P, Caiola D, Sá-Miranda MC, Lima JL: **Progressive myoclonus epilepsy with nephropathy C1q due to SCARB2/LIMP-2 deficiency: clinical report of two siblings.** *Seizure* 2011, **20**:738–40.

219. Gleich K, Desmond MJ, Lee D, Berkovic SF, Dibbens LM, Katerelos M, Bayly MA, Fraser SA, Martinello P, Vears DF, Mount P, Power DA: **Abnormal Processing of Autophagosomes in Transformed B Lymphocytes from SCARB2-Deficient Subjects.** *Biores Open Access* 2013, **2**:40–6.

220. Gonzalez A, Valeiras M, Sidransky E, Tayebi N: **Lysosomal integral membrane protein-2: a new player in lysosome-related pathology.** *Mol Genet Metab* 2014, **111**:84–91.

221. Dibbens LM, Karakis I, Bayly MA, Costello DJ, Cole AJ, Berkovic SF: **Mutation of SCARB2 in a patient with progressive myoclonus epilepsy and demyelinating peripheral neuropathy.** *Arch Neurol* 2011, **68**:812–3.

222. Perandones C, Pellene LA, Micheli F: **A new SCARB2 mutation in a patient with progressive myoclonus ataxia without renal failure.** *Mov Disord* 2014, **29**:158–9.

223. Guerrero-López R, García-Ruiz PJ, Giráldez BG, Durán-Herrera C, Querol-Pascual MR, Ramírez-Moreno JM, Más S, Serratosa JM: **A new SCARB2 mutation in a patient with progressive myoclonus ataxia without renal failure.** *Mov Disord* 2012, **27**:1826–7.

224. Lee DHK, Gan P-Y, Katerelos M, Fraser SA, Gleich K, Holdsworth SR, Power DA: **Absence of the lysosomal protein Limp-2 attenuates renal injury in crescentic glomerulonephritis.** *Immunol Cell Biol* 2014, **92**:400–8.

225. Velayati A, DePaolo J, Gupta N, Choi JH, Moaven N, Westbroek W, Goker-Alpan O, Goldin E, Stubblefield BK, Kolodny E, Tayebi N, Sidransky E: **A mutation in SCARB2 is a modifier in Gaucher disease.** *Hum Mutat* 2011, **32**:1232–8.

226. Yamayoshi S, Iizuka S, Yamashita T, Minagawa H, Mizuta K, Okamoto M, Nishimura H, Sanjoh K, Katsushima N, Itagaki T, Nagai Y, Fujii K, Koike S: **Human SCARB2-dependent infection by coxsackievirus A7, A14, and A16 and enterovirus 71.** *J Virol* 2012, **86**:5686–96.

227. Li X, Fan P, Jin J, Su W, An D, Xu L, Sun S, Zhang Y, Meng X, Gao F, Kong W, Jiang C: **Establishment of cell lines with increased susceptibility to EV71/CA16 by stable overexpression of SCARB2.** *Virol J* 2013, **10**:250.

228. Lin Y-W, Lin H-Y, Tsou Y-L, Chitra E, Hsiao K-N, Shao H-Y, Liu C-C, Sia C, Chong P, Chow Y-H: **Human SCARB2-mediated entry and endocytosis of EV71.** *PLoS One* 2012, **7**:e30507.

229. Yamayoshi S, Yamashita Y, Li J, Hanagata N, Minowa T, Takemura T, Koike S: **Scavenger receptor B2 is a cellular receptor for enterovirus 71.** *Nat Med* 2009, **15**:798–801.

230. Yamayoshi S, Fujii K, Koike S: **Scavenger receptor b2 as a receptor for hand, foot, and mouth disease and severe neurological diseases.** *Front Microbiol* 2012, **3**:32.

231. Yamayoshi S, Koike S: **Identification of a human SCARB2 region that is important for enterovirus 71 binding and infection.** *J Virol* 2011, **85**:4937–46.

232. Carrasco-Marín E, Fernández-Prieto L, Rodriguez-Del Rio E, Madrazo-Toca F, Reinheckel T, Saftig P, Alvarez-Dominguez C: **LIMP-2 links late phagosomal trafficking with the onset of the innate immune response to Listeria monocytogenes: a role in macrophage activation.** *J Biol Chem* 2011, **286**:3332–41.

233. Schroen B, Leenders JJ, van Erk A, Bertrand AT, van Loon M, van Leeuwen RE, Kubben N, Duisters RF, Schellings MW, Janssen BJ, Debets JJ, Schwake M, Høydal MA, Heymans S, Saftig P, Pinto YM: **Lysosomal integral membrane protein 2 is a novel component of the cardiac intercalated disc and vital for load-induced cardiac myocyte hypertrophy.** *J Exp Med* 2007, **204**:1227–35.

234. Roet KCD, Franssen EHP, de Bree FM, Essing AHW, Zijlstra S-JJ, Fagoe ND, Eggink HM, Eggers R, Smit AB, van Kesteren RE, Verhaagen J: **A multilevel screening strategy defines a molecular fingerprint of proregenerative olfactory ensheathing cells and identifies SCARB2, a protein that improves regenerative sprouting of injured sensory spinal axons.** *J Neurosci* 2013, **33**:11116–35.

235. Michelakakis H, Xiromerisiou G, Dardiotis E, Bozi M, Vassilatis D, Kountra P-M, Patramani G, Moraitou M, Papadimitriou D, Stamboulis E, Stefanis L, Zintzaras E, Hadjigeorgiou GM: **Evidence of an association between the scavenger receptor class B member 2 gene and Parkinson's disease.** *Mov Disord* 2012, **27**:400–5.

236. Rothaug M, Zunke F, Mazzulli JR, Schweizer M, Altmeppen H, Lüllmann-Rauch R, Kallemeijn WW, Gaspar P, Aerts JM, Glatzel M, Saftig P, Krainc D, Schwake M, Blanz J: **LIMP-2 expression is critical for β-glucocerebrosidase activity and α-synuclein clearance.** *Proc Natl Acad Sci U S A* 2014, **111**:15573–8.

237. Gan-Or Z, Girard SL, Noreau A, Leblond CS, Gagnon JF, Arnulf I, Mirarchi C, Dauvilliers Y, Desautels A, Mitterling T, Cochen De Cock V, Frauscher B, Monaca C, Hogl B, Dion PA, Postuma RB, Montplaisir JY, Rouleau GA: **Parkinson's Disease Genetic Loci in Rapid Eye Movement Sleep Behavior Disorder.** *J Mol Neurosci* 2015.

238. Dardis A, Filocamo M, Grossi S, Ciana G, Franceschetti S, Dominissini S, Rubboli G, Di Rocco M, Bembi B: **Biochemical and molecular findings in a patient with myoclonic epilepsy due to a mistarget of the beta-glucosidase enzyme.** *Mol Genet Metab* 2009, **97**:309–11.

239. Aerts JM, Hollak CE: **Plasma and metabolic abnormalities in Gaucher's disease.** *Baillieres Clin Haematol* 1997, **10**:691–709.

240. Aerts JMFG, Brul S, Donker-Koopman WE, van Weely S, Murray GJ, Barranger JA, Tager JM, Schram AW: **Efficient routing of glucocerebrosidase to lysosomes requires complex oligosaccharide chain formation**. *Biochem Biophys Res Commun* 1986, **141**:452–458.

241. Groener JEM, Poorthuis BJHM, Kuiper S, Helmond MTJ, Hollak CEM, Aerts JMFG: **HPLC for simultaneous quantification of total ceramide, glucosylceramide, and ceramide trihexoside concentrations in plasma.** *Clin Chem* 2007, **53**:742–7.

242. Aerts JM, Donker-Koopman WE, van der Vliet MK, Jonsson LM, Ginns EI, Murray GJ, Barranger JA, Tager JM, Schram AW: **The occurrence of two immunologically distinguishable beta-glucocerebrosidases in human spleen.** *Eur J Biochem* 1985, **150**:565–74.

243. Desmond MJ, Lee D, Fraser SA, Katerelos M, Gleich K, Martinello P, Li YQ, Thomas MC, Michelucci R, Cole AJ, Saftig P, Schwake M, Stapleton D, Berkovic SF, Power DA: **Tubular proteinuria in mice and humans lacking the intrinsic lysosomal protein SCARB2/Limp-2.** *Am J Physiol Renal Physiol* 2011, **300**:F1437–47.

244. Higashiyama Y, Doi H, Wakabayashi M, Tsurusaki Y, Miyake N, Saitsu H, Ohba C, Fukai R, Miyatake S, Joki H, Koyano S, Suzuki Y, Tanaka F, Kuroiwa Y, Matsumoto N: **A novel SCARB2 mutation causing late-onset progressive myoclonus epilepsy.** *Mov Disord* 2013, **28**:552–3.

245. Perandones C, Micheli FE, Pellene LA, Bayly MA, Berkovic SF, Dibbens LM: **A case of severe hearing loss in action myoclonus renal failure syndrome resulting from mutation in SCARB2.** *Mov Disord* 2012, **27**:1200–1.

246. Armesilla AL, Vega MA: **Structural organization of the gene for human CD36 glycoprotein.** *J Biol Chem* 1994, **269**:18985–91.

247. Vega MA, Rodriguez F, Seguí B, Calés C, Alcalde J, Sandoval I V: **Targeting of lysosomal integral membrane protein LIMP II. The tyrosine-lacking carboxyl cytoplasmic tail of LIMP II is sufficient for direct targeting to lysosomes.** *J Biol Chem* 1991, **266**:16269–72.

248. Gaspar P, Kallemeijn WW, Strijland A, Scheij S, Van Eijk M, Aten J, Overkleeft HS, Balreira A, Zunke F, Schwake M, Sá Miranda C, Aerts JMFG: **Action myoclonus-renal failure syndrome: diagnostic applications of activity-based probes and lipid analysis.** *J Lipid Res* 2014, **55**:138–45.

249. Liou B, Haffey WD, Greis KD, Grabowski GA: **The LIMP-2/SCARB2 binding motif on acid β-glucosidase: basic and applied implications for Gaucher disease and associated neurodegenerative diseases.** *J Biol Chem* 2014, **289**:30063–74.

250. Lee D, Gleich K, Fraser SA, Katerelos M, Mount PF, Power DA: **Limited capacity of proximal tubular proteolysis in mice with proteinuria.** *Am J Physiol Renal Physiol* 2013, **304**:F1009–19.

251. Schmid J, Oelbe M, Saftig P, Schwake M, Schweda F: **Parallel regulation of renin and lysosomal integral membrane protein 2 in renin-producing cells: further evidence for a lysosomal nature of renin secretory vesicles.** *Pflugers Arch* 2013, **465**:895–905.

252. Akiyama H, Kobayashi S, Hirabayashi Y, Murakami-Murofushi K: **Cholesterol glucosylation is catalyzed by transglucosylation reaction of β-glucosidase 1.** *Biochem Biophys Res Commun* 2013, **441**:838–43.

253. Kallemeijn WW, Witte MD, Voorn-Brouwer TM, Walvoort MTC, Li K-Y, Codée JDC, van der Marel GA, Boot RG, Overkleeft HS, Aerts JMFG: **A sensitive gel-based method combining distinct cyclophellitol-based probes for the identification of acid/base residues in human retaining β-glucosidases.** *J Biol Chem* 2014, **289**:35351–62.

254. Damme M, Morelle W, Schmidt B, Andersson C, Fogh J, Michalski J-C, Lübke T: **Impaired lysosomal trimming of N-linked oligosaccharides leads to hyperglycosylation of native lysosomal proteins in mice with alpha-mannosidosis.** *Mol Cell Biol* 2010, **30**:273–83.

255. Wattiaux R, Wibo M, Baudhuin P: **[Effect of the injection of Triton WR 1339 on the hepatic lysosomes of the rat].** *Arch Int Physiol Biochim* 1963, **71**:140–2.

256. Vissers JPC, Langridge JI, Aerts JMFG: **Analysis and quantification of diagnostic serum markers and protein signatures for Gaucher disease.** *Mol Cell Proteomics* 2007, **6**:755–66.

257. Aerts JM, Groener JE, Kuiper S, Donker-Koopman WE, Strijland A, Ottenhoff R, van Roomen C, Mirzaian M, Wijburg FA, Linthorst GE, Vedder AC, Rombach SM, Cox-Brinkman J, Somerharju P, Boot RG, Hollak CE, Brady RO, Poorthuis BJ: **Elevated globotriaosylsphingosine is a hallmark of Fabry disease.** *Proc Natl Acad Sci U S A* 2008, **105**:2812–7.

258. Mirzaian M, Wisse P, Ferraz MJ, Gold H, Donker-Koopman WE, Verhoek M, Overkleeft HS, Boot RG, Kramer G, Dekker N, Aerts JMFGFG, Kramer G, Dekker N: **Mass spectrometric quantification of glucosylsphingosine in plasma and urine of type 1 Gaucher patients using an isotope standard**. *Blood Cells, Mol Dis* 2015, **54**:307–14.

259. Folch J, Lees M, SLoane Stanley GH: **A simple method for the isolation and purification of total lipides from animal tissues.** *J Biol Chem* 1957, **226**:497–509.

260. Tosato G, Cohen JI: **Generation of Epstein-Barr Virus (EBV)-immortalized B cell lines.** *Curr Protoc Immunol* 2007, **Chapter 7**:Unit 7.22.

261. Bonta PI, van Tiel CM, Vos M, Pols TWH, van Thienen J V, Ferreira V, Arkenbout EK, Seppen J, Spek CA, van der Poll T, Pannekoek H, de Vries CJM: **Nuclear receptors Nur77, Nurr1, and NOR-1 expressed in atherosclerotic lesion macrophages reduce lipid loading and inflammatory responses.** *Arterioscler Thromb Vasc Biol* 2006, **26**:2288–94.

262. Arribas JCD, Herrero AG, Martín-Lomas M, Cañada FJ, He S, Withers SG: **Differential mechanism-based labeling and unequivocal activity assignment of the two active sites of intestinal lactase/phlorizin hydrolase**. *Eur J Biochem* 2000, **267**:6996–7005.

263. Buller HA, Van Wassenaer AG, Raghavan S, Montgomery RK, Sybicki MA, Grand RJ: **New insights into lactase and glycosylceramidase activities of rat lactase-phlorizin hydrolase**. *Am J Physiol Gastrointest Liver Physiol* 1989, **257**:G616–623.

264. Kirchhausen T, Macia E, Pelish HE: **Use of dynasore, the small molecule inhibitor of dynamin, in the regulation of endocytosis.** *Methods Enzymol* 2008, **438**:77–93.

265. Ellen S, Gupta N, Velayati A, Choi J, Stubblefield B, Sidransky E, Tayebi Na: **45. Are mutations in LIMP-2 associated with myoclonic epilepsy in patients with Gaucher disease?** *Mol Genet Metab* 2010, **99**:S17.

266. Scholz SW, Jeon BS: **GBA mutations and Parkinson disease: When genotype meets phenotype.** *Neurology* 2015, **84**:866–7.

267. Lee J-Y, Lee BH, Kim G-H, Jung C-W, Lee J, Choi J-H, Yoo H-W: **Clinical and genetic characteristics of Gaucher disease according to phenotypic subgroups.** *Korean J Pediatr* 2012, **55**:48–53.

268. Hopfner F, Schulte EC, Mollenhauer B, Bereznai B, Knauf F, Lichtner P, Zimprich A, Haubenberger D, Pirker W, Brücke T, Peters A, Gieger C, Kuhlenbäumer G, Trenkwalder C, Winkelmann J: **The role of SCARB2 as susceptibility factor in Parkinson's disease.** *Mov Disord* 2013, **28**:538–40.

269. Maniwang E, Tayebi N, Sidransky E: **Is Parkinson disease associated with lysosomal integral membrane protein type-2?: challenges in interpreting association data.** *Mol Genet Metab* 2013, **108**:269–71.

270. Manning-Boğ AB, Schüle B, Langston JW: **Alpha-synuclein-glucocerebrosidase interactions in pharmacological Gaucher models: a biological link between Gaucher disease and parkinsonism.** *Neurotoxicology* 2009, **30**:1127–32.

271. Zimran A, Elstein D: **Management of Gaucher disease: enzyme replacement therapy.** *Pediatr Endocrinol Rev* 2014, **12 Suppl 1**:82–7.

272. Haddley K: **Taliglucerase alfa for the treatment of Gaucher's disease.** *Drugs Today (Barc)* 2012, **48**:525–32.

273. Traynor K: **Taliglucerase alfa approved for Gaucher disease.** *Am J Health Syst Pharm* 2012, **69**:1009.

274. Moyses C: **Substrate reduction therapy: clinical evaluation in type 1 Gaucher disease**. *Philos Trans R Soc B Biol Sci* 2003, **358**:955–960.

275. Alobaidy H: **Recent advances in the diagnosis and treatment of niemann-pick disease type C in children: a guide to early diagnosis for the general pediatrician.** *Int J Pediatr* 2015, **2015**:816593.

276. Lachmann RH: **Miglustat: Substrate reduction therapy for glycosphingolipid lysisomal storage disorders**. *Drugs of Today* 2006, **42**:29.

277. Overkleeft HS, Renkema GH, Neele J, Vianello P, Hung IO, Strijland A, van der Burg AM, Koomen GJ, Pandit UK, Aerts JM: **Generation of specific deoxynojirimycin-type inhibitors of the non-lysosomal glucosylceramidase.** *J Biol Chem* 1998, **273**:26522–7.

278. Benito JM, García Fernández JM, Ortiz Mellet C: **Pharmacological chaperone therapy for Gaucher disease: a patent review.** *Expert Opin Ther Pat* 2011, **21**:885–903.

279. Ran FA, Hsu PD, Wright J, Agarwala V, Scott DA, Zhang F: **Genome engineering using the CRISPR-Cas9 system.** *Nat Protoc* 2013, **8**:2281–308.

280. Jonsson LM V., Murray GJ, Sorrel SH, Strijland A, Aerts JFGM, Ginns EI, Barranger JA, Tager JM, Schram AW: **Biosynthesis and maturation of glucocerebrosidase in Gaucher fibroblasts**. *Eur J Biochem* 1987, **164**:171–179.

281. Maslov MA, Morozova NG, Chizhik EI, Rapoport DA, Ryabchikova EI, Zenkova MA, Serebrennikova GA: **Synthesis and delivery activity of new cationic cholesteryl glucosides.** *Carbohydr Res* 2010, **345**:2438–49.

282. Butters TD, Mellor HR, Narita K, Dwek RA, Platt FM: **Small-molecule therapeutics for the treatment of glycolipid lysosomal storage disorders.** *Philos Trans R Soc Lond B Biol Sci* 2003, **358**:927–45.

283. Lachmann RH, Platt FM: **Substrate reduction therapy for glycosphingolipid storage disorders**. *Expert Opin Investig Drugs* 2001, **10**:455–466.

284. Yamaguchi Y, Sasagasako N, Goto I, Kobayashi T: **The synthetic pathway for glucosylsphingosine in cultured fibroblasts.** *J Biochem* 1994, **116**:704–10.

285. Van Dussen L, Hendriks EJ, Groener JEM, Boot RG, Hollak CEM, Aerts JMFG: **Value of plasma chitotriosidase to assess non-neuronopathic Gaucher disease severity and progression in the era of enzyme replacement therapy.** *J Inherit Metab Dis* 2014, **37**:991–1001.

8.PUBLICATIONS